STEADY LAMINAR COMPRESSIBLE MAGNETO-FLUID-DYNAMIC GAS FLOWS IN CHANNELS

Thesis by

Kenneth Gunder Harstad

In Partial Fulfillment of the Requirements

For the Degree of

Doctor of Philosophy

California Institute of Technology

Pasadena, California

1967

(Submitted December 13, 1966)

ACKNOWLEDGMENTS

The author wishes to express his sincere and deep appreciation to Professor Julian Cole for his assistance and advice given during the course of this study.

Thanks are also given to the National Science Foundation, under whose support the author studied for three years; to the Jet Propulsion Laboratory, where the author developed much of the material used in Appendices A and B; to Mr. Gary Russell of the Jet Propulsion Laboratory; and to Mrs. Robert Duffy for her assistance in the preparation of this manuscript.

ABSTRACT

Numerical computations are carried out for the core flow of subsonic MFD generator channels with a large length-to-height ratio and fine electrode segmentation. The working fluid is taken as potassium seeded argon. Variable transport properties and radiation effects are considered. It is shown that transverse variations in fluid properties are very important in Faraday generators; a one-dimensional analysis of the flow is not adequate. Axial currents in non-equilibrium flows can be kept low if the right value of the Hall parameter can be obtained; this also depends critically on the Mach number and load parameter. Mach numbers much less than one and high load parameters are to be avoided. Attainment of very large Hall parameters and fields cannot be expected.

TABLE OF CONTENTS

LIST OF SYMBOLS

$\overline{\overline{A}}$ – a matrix operator, see page 61

$A^*_{ij}, B^*_{ij}, C^*_{ij}$ cross-section ratios

$\vec{B}$ – total magnetic field

$\vec{\mathcal{B}}$ – applied magnetic field

$\vec{b}$ – induced magnetic field

B_ν – Planck function

C_p – specific heat at constant pressure

c – speed of light

$\vec{C}_T$ – function defining a stream transformation, see page 20

$\vec{D}_e$ – an electron thermal diffusion force, see page 61

d – degree of ionization

$\vec{E}$ – electric field

e – electron charge (absolute value)

$\vec{F}$ – magnetic force

f – function defining the channel cross-sectional area

$\vec{g}$ – acceleration due to gravity

g – Gaunt factor; degeneracy of an energy level

$\underline{G}$ – electron heat conduction parameter, see page 6

$G = \underline{G}/\epsilon$

Ha – Hartmann number

H_c – length defining cut-off frequencies ν_c , see page 47

H – channel height

h – enthalpy

I_H – ionization energy of hydrogen

$\overline{\overline{I}}$ – unit matrix

I_ν - specific radiation intensity

ΔI - lowering of ionization potential

i_e - internal energy of the electron

I_s - ionization energy of the seed

I - magnet current

$\vec{j}$ - current density

J - transverse current density, see page 49

J_s - Jacobian of the stream transformation, page 19

$J_{ss'}$ - Jacobian of a modified stream transformation, page 23

J_{sE} - Jacobian of the stream transformation in the electrode boundary layer

J_{sI} - Jacobian of the stream transformation in the insulator boundary layer

j_ν - source function

K - load parameter

k_ν - absorption cross-section per unit mass

k - Boltzmann's constant

$\mathcal{K}$ - thermal conductivity

L - channel length

$\vec{\ell}$ - vector of direction cosines

$\mathcal{L}$ - velocity potential, page 41

$\vec{\mathcal{L}}$ - vector defined on page 19

M - Mach number; weighting factor (with subscript)

m_j - atomic mass

N - interaction parameter; number of streamlines (page 84); quantum number

n_j - number density

O_i – operators defined on page 24

p – pressure

$\bar{\bar{P}}_e$ – electron stress tensor

Pr – Prandtl number

Q_{el_j} – elastic energy exchange during collision

Q_{inel_j} – inelastic energy exchange during collision

q_c – net charge density

$\vec{q}_e$ – electron heat flux

$\vec{q}_R$ – radiative heat flux

$\vec{q}$ – total heat flux

q – a form of the Hall parameter, page 31

Q_R – radiative loss

R – gas constant; winding resistance; Rydberg constant; function defined on page 19

R_m – magnetic Reynolds number

$[R]$ – matrix defined on page 87

$\vec{R}_e$ – portion of the electron heat flux, see page 61

S – channel wall slope

T_s – indicates stream transformation

$T_{ss'}$ – indicates modified stream transformation

T_{sE} – indicates stream transformation in the electrode boundary layer

T_{sI} – indicates stream transformation in the insulator boundary layer

τ_{bl} – a characteristic boundary layer thickness defined on page 88

τ_B – a characteristic induction transition thickness defined on page 88

T_e – electron temperature

T – gas temperature

$\vec{u}$ – gas velocity

$\vec{V}$ – vector of velocities and enthalpies defined on page 86

$\vec{W}$ – vector of forces and dissipation defined on page 87

W – channel width

w – emission line half half-width in angular frequency units

w_λ – line half half-width in A^o

$w_\nu = w/2\pi$

$\vec{w_j}$ – diffusion velocity

X – axial coordinate

y – transverse coordinate

z – transverse coordinate

α – channel height to length ratio

$\bar{\alpha}$ – ionization ratio

α_p – Planck mean absorption coefficient

α_R – Rosseland mean absorption coefficient

α_T – thermal diffusion ratio

α_ν – absorption cross-section per unit volume

β – channel width to height ratio

γ – ratio of specific heats

γ_s – seed ratio

Δ – conductivity ratio, see page 18

Δ_o – parameter defined on page 61

δ_o – parameter defined on page 61

δ_T – thermal sub-layer thickness defined on page 18

$\epsilon = (Ha)^{-1}$

$\mathcal{E}$ - electric permittivity

$\bar{\mathcal{E}}$ - parameter defined on page 61

ζ - stream coordinate

ζ_{ij} - parameter defined on page 61

η - electrode boundary-layer coordinate

c' - square of ratio of characteristic fluid velocity to speed of light

λ - wave length of photon

λ_D - Debye length

Λ_{ij} - parameter defined on page 62

λ_e - heat conductivity for electrons

μ - magnetic permeability

μ_v - dynamic viscosity

μ_{ik} - reduced mass

ν - insulator boundary layer coordinate; circular frequency

ν_o - parameter defined on page 61; circular frequency of line center

ν_c - cut-off frequency, see page 47

ξ - stream coordinate

ρ - mass density

σ - electrical conductivity

σ_{SB} - Stefan-Boltzmann constant

$\bar{\bar{\tau}}$ - viscous stress tensor

τ_{ij} - collision time

τ_o - net collision time defined on page 60

τ_e – net collision time defined on page 61

τ_ν – optical depth

ϕ – magnetic field potential

Φ – viscous dissipation

ψ – electric field potential

$\vec{\omega\tau}$ – Hall parameter

Ω – solid angle

ω – angular frequency

$\overline{\omega\tau}$ – characteristic value of the Hall parameter

INTRODUCTION

This thesis is concerned with the solution of the equations of motion for a MFD (magneto-fluid-dynamic) gas flowing in a rectangular channel and subjected to crossed electric and magnetic fields. Emphasis is placed on channels used as electric power generators; some slight differences in the approach to the problem are required for accelerators. The gas is assumed to consist of an inert parent gas (such as argon) and an alkali seed material (such as potassium). The equations to be solved are essentially the Navier-Stokes equations with terms added to account for electromagnetic effects. Appendix A gives the forms of these additional terms and also discusses implicit approximations in the set of equations used.

There have been many papers written on MFD channel flows. In many, a one-dimensional analysis of the problem is employed. Detailed study of the transport properties is usually lacking. Even in the cases of analysis in more than one dimension, there are simplifying assumptions made such as the flow is incompressible or fully developed, or some fluid property is constant, etc. It is the purpose of this study to develop a sufficiently general set of equations allowing all major effects to be examined without unduly restrictive assumptions and yet to have the equations tractable to numerical calculations. In particular, it is desired to know the effects of compressibility, variable transport properties (including the Hall effect), and transverse variations in fluid properties. A somewhat qualitative study of the effects of radiation and an elevated electron temperature is also

included. This will be discussed in a following section. Asymptotic expansions in small parameters inherent to the problem are employed to simplify the equations of motion.

A list of the equations to be solved is given below. In this section, dimensional quantities will have a dagger (†). Superscript numbers in brackets denote reference numbers. The symbols are conventional. Unless otherwise noted, the MKS system of units is used for dimensional quantities.

Continuity equation: $$\nabla^\dagger \cdot \rho^\dagger \vec{u}^\dagger = 0$$

Momentum equations: $$\rho^\dagger \vec{u}^\dagger \cdot \nabla^\dagger \vec{u}^\dagger + \nabla^\dagger p^\dagger = \nabla^\dagger \cdot \bar{\bar{\tau}}^\dagger + (\vec{j}^\dagger + q_c^\dagger \vec{u}^\dagger) \times \vec{B}^\dagger + q_c^\dagger \vec{E}^\dagger$$

where $$\bar{\bar{\tau}}^\dagger = \lambda^\dagger \nabla^\dagger \cdot \vec{u}^\dagger \bar{\bar{I}} + \mu_v^\dagger \, def^\dagger \vec{u}^\dagger$$

$\lambda^\dagger$ = bulk viscosity

$\mu_v^\dagger$ = shear viscosity

$\bar{\bar{I}}$ = identity tensor

$def^\dagger \vec{u}^\dagger = \nabla^\dagger \vec{u}^\dagger + (\nabla^\dagger \vec{u}^\dagger)^{transpose}$

$q_c^\dagger$ = net charge density

Energy equation: $$\rho^\dagger \vec{u}^\dagger \cdot \nabla^\dagger h^\dagger = \vec{u}^\dagger \cdot \nabla^\dagger p^\dagger + \frac{1}{\sigma^\dagger} (j^\dagger)^2 + \Phi^\dagger - \nabla^\dagger \cdot \vec{q}^\dagger$$

where $$\Phi^\dagger = \bar{\bar{\tau}}^\dagger : \nabla^\dagger \vec{u}^\dagger$$

$$\vec{q}^\dagger = -\kappa^\dagger \nabla^\dagger T^\dagger + \vec{q}_e^\dagger + \vec{q}_R^\dagger$$

$\mathcal{K}^+$ = thermal conductivity of the parent gas

$\vec{q}_e^{\,+}$ = electron heat flux (Appendix A), not to be confused with the electronic charge density

$\vec{q}_R^{\,+}$ = radiation heat flux

σ^+ = electrical conductivity (Appendix A)

State equations: $p^+ = p^+(\rho^+, h^+)$, $h^+ = h^+(\rho^+, T^+)$

Ohm's law: $\vec{j}^+ + \vec{j}^+ \times \vec{\omega\tau} = \sigma^+(\vec{E}^+ + \vec{u}^+ \times \vec{B}^+)$

($\vec{\omega\tau}$ is the Hall parameter, see Appendix A)

Maxwell's equations: $\mu^+(\vec{j}^+ + q_c^+ \vec{u}^+) = \nabla^+ \times \vec{B}^+$

$$q_c^+ = \varepsilon^+ \nabla^+ \cdot \vec{E}^+$$

$$\nabla^+ \cdot \vec{B}^+ = \nabla^+ \times \vec{E}^+ = 0$$

It is to be noted that the above equations are based on a single fluid model. Effects of pressure diffusion and thermal diffusion are neglected; this is quite reasonable for low ionization ratios* and not too great an electron temperature. See Appendix A for a further discussion of this point.

From the entrance conditions, a characteristic velocity u^*, characteristic enthalpy h^*, and characteristic density ρ^* are known. Also known are the magnitude of the applied induction B^*, channel length L, channel height H, and channel width W. Other reference quantities will be defined later.

* Defined as the ion mass density divided by the total mass density.

I. FLOWS IN LOCAL EQUILIBRIUM

Nondimensional Equations

Let M denote a characteristic Mach number for the flow, K a characteristic load parameter, and $\overline{\omega\tau}$ a characteristic value of the Hall parameter. $M^2 = \rho^* u^{*2}/(\gamma p^\dagger(\rho^*, h^*))$, where γ = specific heat ratio; $K \approx E^*/(u^* B^*)$ for some E^*. Then if $\overline{\omega\tau}^2 M^2 (1-K)^2 < O(1)$, the flow can be said to be in local equilibrium, i.e., $T_e^\dagger = T^\dagger$ [18, 20] (see also Appendix A). For this type of flow, the single fluid model is especially applicable. A study is made of the flow with the following assumptions:

1) To insure maximum efficiency, both the gas kinetic and thermal energies are to be converted to electrical energy. If these conversions are done more of less simultaneously, the Mach number will not vary drastically. However, sufficient thermal energy is required to keep the level of ionization high enough to insure high electrical conductivity. This suggests the Mach number is not large and will be decreasing with axial distance. It is assumed that the flow is entirely subsonic with a Mach number of order unity. (This includes nearly incompressible conditions, say M = 0.3.) Thus, a shock is avoided along with the attendant total pressure loss and other complications.

2) The load factor, K, always less than unity for the generator mode, does not vary drastically. A more precise statement of this assumption will be given later.

3) The channel cross-sectional area will be constant or monotonically increasing.

4) Except possibly at the channel entrance and exit, the applied induction varies weakly.

5) The gas is thermally perfect.

6) The Prandtl number, $Pr = \mu_v^\dagger C_p^\dagger / \kappa^\dagger$, is constant.

7) The parameters $\mu^\dagger$ and $\epsilon^\dagger$ are constant and equal to their values in free space.

8) The usual 'quasi-neutrality' approximation is made and any net charge effects are neglected.

9) The flow is stable.

10) The electrodes are finely segmented.

Assumption 1) means $h^* = u^{*2}$ and a reference pressure can be defined as $p^* = \rho^* u^{*2}$. Assumption 2) means $E^* = u^* B^*$. Thus, $\overline{\omega\tau} \leq O(1)$ for equilibrium flows. From Ohm's law, a reference current can be defined: $j^* = \sigma^* E^*$ where $\sigma^* = \sigma^\dagger(\rho^*, h^*)$. Also, $\mu_v^* = \mu_v^\dagger(h^*)$. In correspondence with Faraday's law, $q_c^* = \epsilon_o^\dagger u^* B^* / (\frac{H_o}{2})$ where $H_o = H_{entrance}$. From Appendix A, $q_e^* = \sigma^* u^* B^* h^* k^\dagger / (R^\dagger e^\dagger)$. It can be shown by one-dimensional analysis[1] that the conditions of assumptions 1) and 3) are consistent. For accelerators, of course, assumptions 1) and 2) must be modified. As an analytical simplification, the cross-sectional area will be characterized by a single function of the axial variable.

The state equations are: $p^\dagger = \rho^\dagger R^\dagger T^\dagger$,

$$h^\dagger(T^\dagger) = \int_{T^\dagger} C_p^\dagger(T^\dagger)\, dT^\dagger .$$

The equations will now be written in nondimensional form.

Let the axial distance be given by X^+, the electrode walls by $Y^+ = \pm \frac{H_o}{2} f(X^+)$, and the insulator walls by $Z^+ = \pm \frac{W_o}{2} f(X^+)$, $f(0) = 1$, $f'(X^+) \geq 0$ (see Figure 1, next page). Nondimensional variables and parameters are defined as follows:

$$X \equiv X^+/L, \quad Y \equiv Y^+/(\tfrac{H_o}{2}), \quad Z \equiv Z^+/(\tfrac{H_o}{2}),$$

$$\lambda \equiv \lambda^+/\mu_r^*, \quad T \equiv \frac{R^+T^+}{h^*}, \quad \vec{u} \equiv \vec{u}^+/u^*, \quad h \equiv h^+/h^*, \text{ etc.},$$

$$\alpha \equiv H_o/2L,$$

$$\beta \equiv W_o/H_o.$$

Interaction parameter, $N \equiv \dfrac{\sigma^* L B^{*2}}{\rho^* u^*}$.

Hartmann number, $Ha \equiv \epsilon^{-1} \equiv \dfrac{H_o B^*}{2}\sqrt{\dfrac{\sigma^*}{\mu_r^*}}$.

Magnetic Reynolds number, $Rm \equiv \mu_o^+ \sigma^* u^* \dfrac{H_o}{2}$.

Electron heat conduction parameter, $G \equiv \dfrac{k^+ \sigma^* B^*}{\rho^* e^+ R^+}$.

Since N can be interpreted as indicative of the degree of

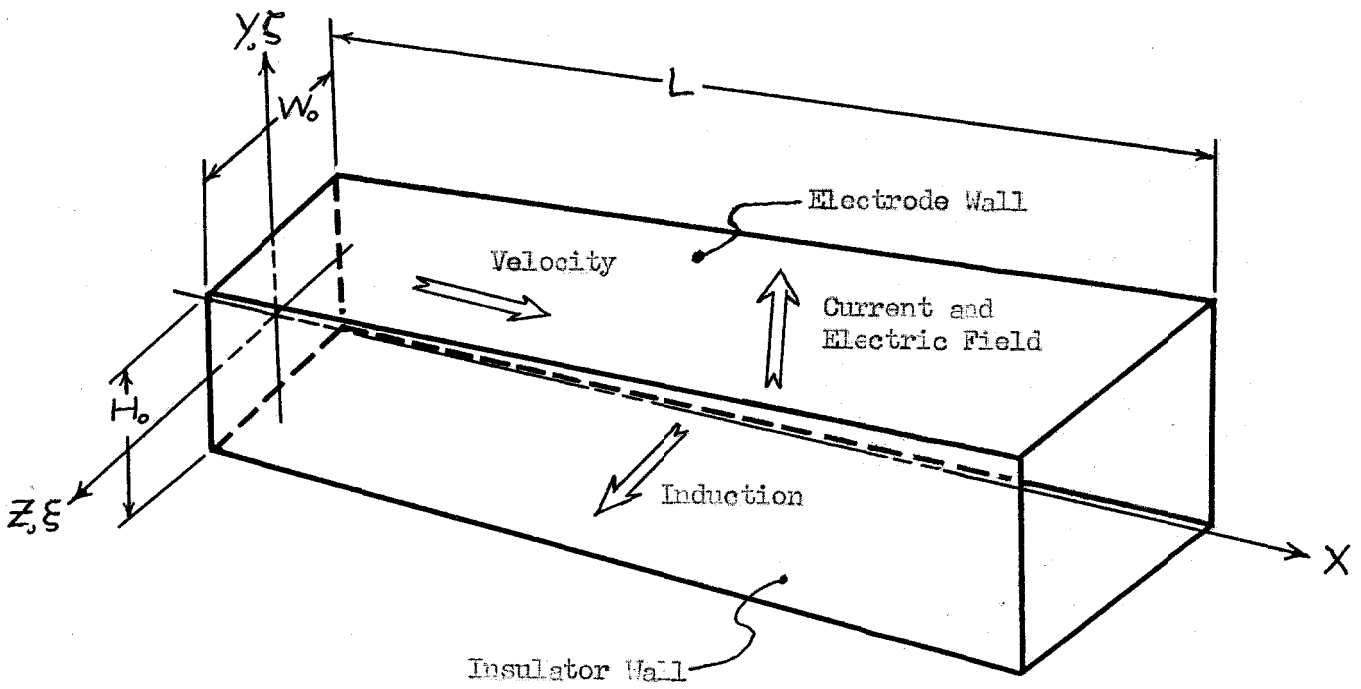

Figure 1. Co-ordinates.

completion of energy exchange between the fluid and the electromagnetic fields in length L , let $N = 1$. This parameter in effect 'defines' the generator length L .

When stated in suitable nondimensional variables, assumption 8) simply means that the problem is nonrelativistic:

the electromagnetic force, $\vec{F}_{em} \approx \vec{j} \times \vec{B} + \frac{c}{R_m} q_c (\vec{E} + \vec{u} \times \vec{B})$,

and the total current, $\vec{j}_{total} = \vec{j} + \vec{j}_{convection} = \vec{j} + \frac{c}{R_m} q_c \vec{u}$

where $c \equiv \varepsilon_0^+ \mu_0^+ u^{*2} = \left(\frac{u^*}{c^+}\right)^2$, $c \ll\ll R_m$,

hence, the electrostatic force and convection current are ignored.

The dimensionless equations are:

Continuity: $$\nabla_\alpha \cdot \rho \vec{u} = 0$$

where $$\nabla_\alpha \equiv \left(\alpha \frac{\partial}{\partial x}, \frac{\partial}{\partial y}, \frac{\partial}{\partial z}\right)$$

Momentum: $$\rho \vec{u} \cdot \nabla_\alpha \vec{u} + \nabla_\alpha p = \alpha (\vec{j} \times \vec{B} + \epsilon^2 \nabla_\alpha \cdot \overline{\overline{\tau}})$$

where $$\overline{\overline{\tau}} = \lambda \nabla_\alpha \cdot \vec{u} \, \overline{\overline{I}} + \mu_r \, \overrightarrow{def}_\alpha \vec{u},$$

$$\overrightarrow{def}_\alpha \vec{u} = \nabla_\alpha \vec{u} + (\nabla_\alpha \vec{u})^{\text{transpose}}$$

Energy: $$\rho \vec{u} \cdot \nabla_\alpha h = \vec{u} \cdot \nabla_\alpha p + \alpha \left(j^2/\sigma + \epsilon^2 \Phi_\alpha + \frac{\epsilon^2}{P_r} \nabla_\alpha \cdot \mu_r \nabla_\alpha h\right) +$$

$$-\underline{\underline{\mathcal{G}}}\,\nabla_\alpha \cdot \vec{q}_e$$

where $\Phi_\alpha = \underline{\underline{\tau}} : \nabla_\alpha \vec{u}$.

(For equilibrium flows, of course, the radiation term is not included.)

State: $p = \rho\, T(h)$

($T(h) = \frac{\gamma-1}{\gamma} h$ for a calorically perfect gas, γ = constant.)

Ohm's law: $\vec{j} + \vec{j} \times \omega\vec{\tau} = \sigma(\vec{E} + \vec{u} \times \vec{B})$

Maxwell's equations: $R_m \vec{j} = \nabla_\alpha \times \vec{B}$,

$$\nabla_\alpha \cdot \vec{B} = \nabla_\alpha \times \vec{E} = 0$$

Values of the Parameters

Physically, the following are reasonable values for some of the variables in the problem[2-13]:

$\sigma^* \approx$ 10 to 100 mho/m ,

$u^* \approx$ 300 to 2000 m/sec,

$L \approx$ 1 m , $\qquad H_o \approx$ 0.1 m,

$B^* \approx$ 1 to 3 web/m^2 ,

$\rho^* \approx$ 0.1 kg/m^3 ,

$\mu_v^* \approx$ 10^{-4} kg/m-sec .

These values, derived from the references cited, correspond to $N \leq O(1)$. From them, it is found $R_m \approx 10^{-4}$ to 10^{-2} and $H_a \approx 10^2$.

It is assumed that the channel is long, that is, $\alpha << 1$. Therefore, asymptotic expansions in the small parameters Rm, ϵ, and α will be considered.

The expansion in the parameter α is the weakest in the sense that it is the largest parameter. Only zeroth order terms in the expansions in Rm and ϵ need be considered, while it may be desirable to give attention to first order terms in the expansion in α. Note that $\alpha/Rm \approx 10^{-10}$ to 10^{-6}.

If m_a^+ is the atomic mass, then $k^+ = R^+ m_a^+$. Thus, $\underline{G}$ is given by $m_a^+ \sigma^* B^*/(e^+ \rho^*)$. Also, if n_e^+ and n_a^+ are the electron and neutral atom number densities,

$$\sigma^+ \approx \frac{e^+ n_e^+}{B^+} |\vec{\omega\tau}|$$

and

$$\rho^+ \approx m_a^+ n_a^+ \approx \rho^*,$$

hence

$$\underline{G} \approx \frac{n_e^+}{n_a^+} |\vec{\omega\tau}|,$$

that is, $\underline{G}$ is proportional to the Hall parameter and the ionization ratio and can be expected to be quite small. Using the values given on the previous page, with $m_a^+ = O(10^{-25})$ kg and $e^+ = 1.6 \times 10^{-19}$ coul, $\underline{G} \approx 10^{-4}$ to 10^{-2}. It is expected that the electron heat conduction will have importance only in the electrode boundary layer where the temperature gradient is large and aligned with the current density vector. (The electron heat conduction vector behaves roughly as the product of the electron temperature and current density; see Appendix A.) Let $\underline{G} \equiv \epsilon G$ where $G \leq O(1)$.

Expansion in the Parameter Rm

A small value of R_m implies that the induction differs only slightly from the applied magnetic field; this means that it may be regarded as known. The magnetic Reynolds number is one of the smaller parameters, if not the smallest. Only one equation need be considered: $R_m \vec{j} = \nabla_\alpha \times \vec{B}$.

Let $\vec{B} = \vec{\mathcal{B}} + R_m \vec{b}$ + higher order terms. Then $\vec{j} = \nabla_\alpha \times \vec{b}$ + higher order terms, or $\nabla_\alpha \cdot \vec{j} = 0$; also $\nabla_\alpha \cdot \vec{\mathcal{B}} = \nabla_\alpha \times \vec{\mathcal{B}} = 0$. The applied induction is given by $\vec{\mathcal{B}} = \nabla_\alpha \phi$ where ϕ is a known harmonic potential. Vector $\vec{B}$ is replaced by $\vec{\mathcal{B}}$ in Ohm's law and the momentum equations.

Expansion in the Parameter ϵ : Boundary Layers

The fact that the Hartmann number is large means that the flow field can be split into two parts; an inviscid core region and viscous boundary layer regions. This division is carried out next.

The zeroth order equations for the inviscid core flow are formed by applying the limit $\epsilon \to 0$. If $\vec{n}$ is the normal vector to the channel wall, then the boundary condition on $\vec{u}$ is $\vec{u} \cdot \vec{n} = 0$. Formulation of the proper entrance conditions will be given later. The walls are given by: $y = \pm f(x)$ and $z = \pm \beta f(x)$ where $f(0) = 1$, $0 \le f'(x) \le O(1)$. Segmented electrodes are located at $y = \pm f(x)$, insulator walls at $z = \pm \beta f(x)$. The applied induction is assumed to be oriented mainly along the z-axis.

Next, consider the electrode boundary layer. Corresponding

to $y = \pm f$, the boundary layer variable $\eta \equiv (f \mp y)/\epsilon$ is introduced, along with:

$$u_x \equiv \bar{u}_x, \quad u_y \equiv \mp (\epsilon \bar{u}_y - \alpha f' \bar{u}_x), \quad u_z \equiv \bar{u}_z,$$

$$\bar{\nabla}_\alpha \equiv \left(\alpha \frac{\partial}{\partial x}, \frac{\partial}{\partial \eta}, \frac{\partial}{\partial z}\right).$$

Consider the transformation $(x, y, z) \xrightarrow[T_\epsilon]{} (x, \eta, z)$. Derivatives transform as follows:

$$\frac{\partial}{\partial x} \xrightarrow[T_\epsilon]{} \frac{\partial}{\partial x} + \frac{f'}{\epsilon} \frac{\partial}{\partial \eta},$$

$$\frac{\partial}{\partial y} \xrightarrow[T_\epsilon]{} \mp \epsilon^{-1} \frac{\partial}{\partial \eta},$$

$$\vec{u} \cdot \nabla_\alpha \xrightarrow[T_\epsilon]{} \vec{u} \cdot \bar{\nabla}_\alpha.$$

The matching of the boundary layer to the core flow is given by the usual limits:

As $\eta \to \infty$ $(\epsilon \to 0)$,

$$\bar{u}_x \to u_{x\,core}\big|_{y=\pm f}, \qquad \frac{\partial \bar{u}_x}{\partial \eta} \to 0,$$

$$\bar{u}_z \to u_{z\,core}\big|_{y=\pm f}, \qquad etc.$$

The transformed fluid equations are:

Continuity: $$\bar{\nabla}_\alpha \cdot \rho \vec{u} = 0$$

Momentum: $$\rho \vec{u} \cdot \bar{\nabla}_\alpha \bar{u}_x + \alpha \frac{\partial p}{\partial x} = \alpha (\vec{j} \times \vec{B})_x +$$

$$+ \alpha [1 + \alpha^2 (f')^2]^2 \frac{\partial}{\partial \eta} \mu_y \frac{\partial \bar{u}_x}{\partial \eta} + \alpha^2 f' [\pm (\vec{j} \times \vec{B})_y +$$

$$- \rho \vec{u} \cdot \bar{\nabla}_\alpha (f' \bar{u}_x)] + \epsilon \alpha f' \rho \vec{u} \cdot \bar{\nabla}_\alpha \bar{u}_y + O(\alpha \epsilon^2, \alpha^2 f' \epsilon),$$

$$\frac{\partial p}{\partial \eta} = O(\alpha\epsilon, \epsilon^2),$$

and $$\rho \vec{u}\cdot\vec{\nabla}_\alpha \bar{u}_z + \frac{\partial p}{\partial z} = \alpha (\vec{j}\times\vec{B})_z + \alpha[1+\alpha^2(f')^2]\frac{\partial}{\partial\eta}\mu_r \frac{\partial \bar{u}_z}{\partial\eta} +$$

$$+ O(\alpha\epsilon^2, \alpha^2 f'\epsilon)$$

Energy: $$\rho \vec{u}\cdot\vec{\nabla}_\alpha h = \vec{u}\cdot\vec{\nabla}_\alpha p + \alpha j^2/\sigma - G(\alpha f' \frac{\partial q_{ex}}{\partial\eta} \mp \frac{\partial q_{ey}}{\partial\eta}) +$$

$$+ \alpha[1+\alpha^2(f')^2]\mu_r \left\{[1+\alpha^2(f')^2]\left(\frac{\partial \bar{u}_x}{\partial\eta}\right)^2 + \left(\frac{\partial \bar{u}_z}{\partial\eta}\right)^2\right\} +$$

$$+ \frac{\alpha}{P_r}[1+\alpha^2(f')^2]\frac{\partial}{\partial\eta}\mu_r \frac{\partial h}{\partial\eta} + O(\alpha\epsilon^2, \alpha^2 f'\epsilon)$$

The state equation and Ohm's law remain the same. The boundary conditions for the fluid equations are: $h = h_{electrode} = h(T_{electrode})$, $\vec{u} = 0 \quad @ \quad \eta = 0.$

Finally, Maxwell's equations are examined under the transformation:

$$\nabla_\alpha \times \vec{E} = 0 \xrightarrow[T_E]{}$$

$$\begin{pmatrix} \mp\frac{1}{\epsilon}\frac{\partial E_z}{\partial\eta} - \frac{\partial E_y}{\partial z} \\ \frac{\partial E_x}{\partial z} - \alpha\frac{\partial E_z}{\partial x} - \frac{\alpha f'}{\epsilon}\frac{\partial E_z}{\partial\eta} \\ \alpha\frac{\partial E_y}{\partial x} + \frac{\alpha f'}{\epsilon}\frac{\partial E_y}{\partial\eta} \pm \frac{1}{\epsilon}\frac{\partial E_x}{\partial\eta} \end{pmatrix} = 0.$$

Therefore, $E_z = E_{z\,core}\big|_{y=\pm f} + O(\epsilon)$

and $\alpha f' E_y \pm E_x = (\alpha f' E_y \pm E_x)_{core}\big|_{y=\pm f} + O(\epsilon)$,

i.e., the electric field tangential to the boundary layer is given by the core value, independent of η . The same holds for the induction.

$$\nabla_\alpha \cdot \vec{B} = 0 \xrightarrow[T_E]{}$$

$$\alpha \frac{\partial B_x}{\partial x} + \frac{\partial B_z}{\partial z} + \frac{1}{\epsilon}\frac{\partial}{\partial \eta}(\alpha f' B_x \mp B_y) = 0,$$

or $\alpha f' B_x \mp B_y = (\alpha f' B_x \mp B_y)_{core}\big|_{y=\pm f} + O(\epsilon)$.

The normal induction is also that given by the core and is also independent of η . Similarly, the normal current density is the core value. Hence, the normal electric field must adjust through the boundary layer to make up for the loss of effective field $(\vec{u}\times\vec{B})_n$ as $\vec{u}\to 0$ $(\eta\to 0)$.

The same procedure is used for the insulator boundary layer. The boundary layer variable is $\nu = (\beta f \mp z)/\epsilon$. Let

$$u_x \equiv \tilde{u}_x,\quad u_y \equiv \tilde{u}_y,\quad u_z \equiv \mp(\epsilon\tilde{u}_z - \alpha\beta f'\tilde{u}_x),$$

$$\tilde{\nabla}_\alpha \equiv \left(\alpha\frac{\partial}{\partial x}, \frac{\partial}{\partial y}, \frac{\partial}{\partial \nu}\right).$$

Consider $(x, y, z) \xrightarrow[T_I]{} (x, y, \nu)$. The expressions from transformation T_I are the same as those from T_E except that

a) a 'bar' is replaced by a 'tilda' wherever it occurs;

b) the symbol η is replaced by ν ;

c) the symbols y and z are interchanged;

d) the function f' is multiplied by β wherever it occurs.

Matching, boundary conditions, and results from Maxwell's equations are similar to those obtained previously. Due to boundary conditions, the normal current is zero.

A combination of T_E and T_I is necessary for the channel corners. The resulting equations are relevant only if no large cross-flows exist in the boundary layers. The corners occupy only a very small portion of the flow field; they are neglected and the equations for the corner flows will not be given. The zeroth order boundary layer equations are obtained by the limit $\epsilon \to 0$. Higher order approximations can be formed by use of the appropriate asymptotic series. They will not be discussed.

Discussion of the Equations

Before proceeding, an examination of the consequences of the equations developed so far is in order. The main induction component is B_z, main velocity is u_x, and main electric field and current are E_y and j_y. Thus, $j_y \approx \sigma (E_y - u_x B_z) \approx -\sigma u_x B_z (1 - K_\ell)$

where K_ℓ is the local load parameter. It has been implicitly assumed that both K_ℓ and $(1-K_\ell)$ are of $O(1)$. If K_ℓ is near unity, large effects can be noticed. Let $\delta \equiv (1-K_\ell) \ll 1$. Then the local interaction parameter per unit length, $N_\ell = O(\delta)$, also $j_y = O(\delta)$. In the insulator boundary layer $u_x \to 0$, $E_y = E_{y\,core}$; therefore, $j_y = O(1)$. Since the boundary layer thickness is of $O(\epsilon)$, the total boundary layer current $\int j_y dy = O(\epsilon)$ while the total current in the

core $\int j_y \, dz = O(\delta)$.

Thus, if $\delta \leq O(\epsilon)$, a significant part of the current can be shorted through the boundary layers[14, 15]. It is even possible for almost complete shorting to occur, in which case the channel no longer acts as a generator. Due to the fact that the current density becomes nearly aligned with the induction in the electrode boundary layer, the $\vec{j} \times \vec{B}$ force in this boundary layer drops off, resulting in a thickening of the boundary layer (to $O(\sqrt{\epsilon})$ for incompressible, fully developed flow[14]). Of course, operation in this mode is undesirable and would result from operating a channel of length greater than that given by the interaction parameter and with nearly constant voltage drops between electrodes. Then, near the exit, the interaction would be weak; little power would be available (operation would be near open circuit); and the flow would approach being fully developed. (It is easy to show this implies the flow becomes nearly incompressible.) A longer than necessary magnet would result in greater excitation power losses. This possibility need not be considered. It is assumed that the electrode voltage drops decrease as the velocity in such a manner that $1 - K_\ell >> \epsilon$, i.e., $1 - K_\ell = O(1)$ and also $K_\ell = O(1)$, $N_\ell = O(1)$. This gives the true meaning of assumption 2). Losses due to boundary layer shorting are thus assumed small.

One may ask if it is reasonable to consider the parameter α small. A short channel would give lower heat losses and would possibly require less excitation power. For H_0, u^*, ρ^* fixed,

then since $N = 1$, $B^* \sim \sqrt{\alpha}$ and $L \sim \alpha^{-1}$. The excitation power $\sim I^2 R$ where I is the excitation current and R is the winding resistance; it is reasonable to expect $B \sim I$ and $R \sim L$. Therefore, $I^2 R \sim B^2 L \sim N$. A decrease in length is compensated by an increase in the induction necessary to give a complete interaction; the excitation power should vary weakly with α. Since boundary layer shorting is small, only heat transfer losses are significantly reduced by having α not small. For practical (not experimental) operation, the device would be large to produce high power. (It is assumed that although the values of quantities given on page 9 are for contemporary experimental facilities, the parameters R_m and H_a will be qualitatively the same for large devices.) As the total power output varies as the volume and the total heat loss as the area, the relative heat loss decreases with size and is of less importance. It is expected also that the best temperature-resistant materials will be used, providing lowest possible heat loss. On the other hand, end losses due to end shorting and induction drop-off are more important for short channels. The electromagnetic force is also larger (that is, the interaction parameter based on channel height); this probably tends to make the flow unstable. There will be no attempt to make an analytical justification of this in this study; the reader is referred to papers on stability in channel flows[16-18]. In any case, many experimental facilities have a small height-to-length ratio; hence, consideration of small α is of some importance.

In considering boundary layers on cold walls, it is possible that the electrical conductivity, which is in general strongly tempera-

ture dependent, may have a value near the wall much smaller than the core value. This can cause charge buildup in the electrode boundary layer to such an extent that charge effects become important[19]. Faraday's and Ohm's laws give (neglecting the Hall effect):

$$q_c = \nabla_\alpha \cdot \vec{E} = \vec{j} \cdot \nabla_\alpha (1/\sigma) + (\nabla_\alpha \times \vec{u}) \times \vec{B}.$$

Even considering large velocity gradients in the boundary layer, the second term gives charge effects of $O(\frac{\epsilon}{\epsilon R_m}) \leq O(10^{-4})$; charge effects due to this term can be neglected. However, suppose $\sigma^+_{\text{boundary layer}} << \sigma^+_{\text{core}}$. Then a reference quantity σ^*_{BL} based on the wall temperature needs to be introduced; let $\Delta \equiv \sigma^*_{BL}/\sigma^* << 1$. A thermal sub-layer forms; let the thickness be δ_T (in units of $H_0/2$). It is given by reference 19:

$$\delta_T = \left[\frac{\Delta}{(\gamma-1)M^2 P_r}\right]^{1/2} \epsilon,$$

thus, charge effects (= $O(\frac{\epsilon}{\delta_T \Delta R_m})$ from above) are of $O(1)$ if $\Delta \leq O\left((\frac{\epsilon}{\epsilon R_m})^{2/3}\right)$. The charge buildup can also cause changes in the tangential electric field across the boundary layer of $O(\alpha\epsilon/\Delta)$. It can be seen that for the model flow discussed here, these effects are important if and only if $\Delta \leq O(10^{-3})$. Since, from a heat loss standpoint, cold walls are not desirable, it will be assumed that this effect can be neglected.

It is to be noted that supersonic flow can be had in an equilibrium situation only if $B^* \leq O(10^{-1})$ web/m^2. This means L would be very large or the efficiency would be low; this situation can not be considered practical.

Transformation to Stream Coordinates

1. Core flow. It is more convenient for computation not to use the rectangular Cartesian coordinate system, but rather stream coordinates. The boundary condition on the velocity vector for the core flow can be incorporated into the stream coordinates and the resulting fluid equations in the limit $\alpha \to 0$ have a simpler form. See Figure 1, page 7. Therefore, consider the transformation $(x,y,z) \xrightarrow[T_s]{} (x,\xi,\zeta)$ such that $\vec{u}\cdot\nabla_\alpha \xi = \vec{u}\cdot\nabla_\alpha \zeta = 0$. Obviously, the functions ξ and ζ serve as stream functions for the flow. Define a vector $\vec{\mathcal{I}} \equiv \nabla_\alpha \xi \times \nabla_\alpha \zeta = R\rho\vec{u}$, then the Jacobian of the transformation $J_s = \frac{\partial(\xi,\zeta)}{\partial(y,z)} = \mathcal{I}_x$, and $R = J_s/(\rho u_x)$. Now $\nabla_\alpha \cdot \vec{\mathcal{I}} = 0$ and $\nabla_\alpha \cdot \rho\vec{u} = 0$; therefore, $\vec{u}\cdot\nabla_\alpha R = 0$. Thus, $R = R(\xi,\zeta)$ and is given by the entrance conditions. Continuity is satisfied if R, ξ, and ζ are given.

Let $\vec{F} \equiv \vec{j}\times\vec{B}$. T_s gives the following fluid equations for the core flow:

$$\rho u_x \frac{\partial u_x}{\partial x} + \frac{\partial p}{\partial x} + \xi_{,x}\frac{\partial p}{\partial \xi} + \zeta_{,x}\frac{\partial p}{\partial \zeta} = F_x$$

$$\alpha\rho u_x \frac{\partial u_y}{\partial x} + \xi_{,y}\frac{\partial p}{\partial \xi} + \zeta_{,y}\frac{\partial p}{\partial \zeta} = \alpha F_y$$

$$\alpha\rho u_x \frac{\partial u_z}{\partial x} + \xi_{,z}\frac{\partial p}{\partial \xi} + \zeta_{,z}\frac{\partial p}{\partial \zeta} = \alpha F_z$$

$$\rho u_x \frac{\partial h}{\partial x} = u_x \frac{\partial p}{\partial x} + j^2/\sigma$$

The boundary and entrance conditions for the stream functions are:

$$\xi = 0 \quad @ \quad z = -\beta f, \quad \xi = -1 \quad @ \quad z = \beta f,$$

$\zeta = 0$ @ $y = -f$, $\zeta = 1$ @ $y = f$,

$\xi|_{x=0} = -\frac{1}{2}(1 + z/\beta)$,

and $\zeta|_{x=0} = \frac{1}{2}(1 + y)$.

The Pfaffians for dy and dz are:

$$dy = \frac{u_y}{\alpha u_x} dx + \frac{\zeta_{,z}}{J_s} d\xi - \frac{\xi_{,z}}{J_s} d\zeta,$$

$$dz = \frac{u_z}{\alpha u_x} dx - \frac{\zeta_{,y}}{J_s} d\xi + \frac{\xi_{,y}}{J_s} d\zeta.$$

These can be integrated using the wall boundary condition on the velocities, $\vec{u} \cdot \vec{n} = 0$, to give:

$$y = (2\zeta - 1) f(x) + C_y(x, \xi, \zeta),$$

$$z = -\beta(2\xi + 1) f(x) + C_z(x, \xi, \zeta)$$

where $C_y = 0 \quad @ \ \zeta = 0, 1; \quad C_z = 0 \quad @ \ \xi = -1, 0;$

$$\vec{C}_T|_{x=0} = 0;$$

and $$\frac{\partial \vec{C}_T}{\partial x}\Big|_{x=0} = \frac{1}{\alpha} \frac{\vec{u}_T}{u_x}\Big|_{x=0} + f'(0) \begin{pmatrix} 1 - 2\zeta \\ \beta(1 + 2\xi) \end{pmatrix}.$$

(Subscript 'T' indicates 'transverse'.)

2. Boundary layer regions. Now consider T_s near the electrode boundary layer ($y \to \pm f$). There, $\zeta \to 0$ or 1 and $\frac{\partial \zeta}{\partial z} \to 0$, $J_s \to -\zeta_{,y}\, \xi_{,z}$ and $\xi_{,z} \neq 0$. A transformation in the boundary layer is defined: $(x, \eta, z) \xrightarrow[T_{sE}]{} (x, \eta, \xi)$ with the Jacobian $J_{sE} = \xi_{,z}$. The equation $\vec{u} \cdot \nabla_\alpha \xi = 0$ implies $\vec{u} \cdot \bar{\nabla}_\alpha \xi = 0$. Therefore, $\vec{u} \cdot \bar{\nabla}_\alpha \xrightarrow[T_{sE}]{} \alpha \bar{u}_x \frac{\partial}{\partial x} + \bar{u}_y \frac{\partial}{\partial \eta}$ and $\bar{\nabla}_\alpha \cdot \rho \vec{u} = 0 \xrightarrow[T_{sE}]{}$

$$\alpha \frac{\partial \rho \bar{u}_x}{\partial x} + \frac{\partial \rho \bar{u}_y}{\partial \eta} + (\bar{\nabla}_\alpha \xi) \cdot \frac{\partial \rho \vec{u}}{\partial \xi} = 0.$$

It has been assumed that the stream functions ξ , ζ do not vary drastically in the boundary layer region, i.e., $\xi_{,y} = O(1)$ and $\zeta_{,y} = O(1)$. Then $\xi = \xi_{core}|_{y=\pm f} + O(\epsilon)$ as $\xi_{,\eta} = O(\epsilon)$. This assumption of no large cross-flow velocities will be examined later. It is now found that $(\bar{\nabla}_\alpha \xi) \cdot \frac{\partial}{\partial \xi} \rho \vec{u} = (\nabla_\alpha \zeta) \cdot \frac{\partial}{\partial \zeta} \rho \vec{u} =$

$= \alpha \rho u_x \left[\xi_{,y} \frac{\partial}{\partial x}\left(\frac{\zeta_{,z}}{J_s}\right) - \zeta_{,z} \frac{\partial}{\partial x}\left(\frac{\xi_{,y}}{J_s}\right)\right] = -\alpha \rho u_x \frac{\partial}{\partial x} \ln J_{sE} + O(\epsilon)$ near $y = \pm f$.

The boundary layer equations under T_{sE} are:

Continuity: $$\alpha \frac{\partial \rho \bar{u}_x}{\partial x} + \frac{\partial \rho \bar{u}_y}{\partial \eta} = \alpha \rho \bar{u}_x \frac{\partial}{\partial x} \ln J_{sE} + O(\epsilon)$$

where $$J_{sE} = \zeta_{,z}\ core|_{y=\pm f} + O(\epsilon),$$

Momentum: $$\alpha \rho \bar{u}_x \frac{\partial \bar{u}_x}{\partial x} + \rho \bar{u}_y \frac{\partial \bar{u}_x}{\partial \eta} + \alpha \frac{\partial p}{\partial x} = \alpha F_x +$$

$$+ \alpha \left[1 + \alpha^2 (f')^2\right] \frac{\partial}{\partial \eta} \mu_v \frac{\partial \bar{u}_x}{\partial \eta} + \alpha^2 f' \left[\pm F_y - \alpha \rho \bar{u}_x \frac{\partial}{\partial x}(f' \bar{u}_x) + \right.$$

$$\left. - \rho \bar{u}_y \frac{\partial}{\partial \eta}(f' \bar{u}_x)\right] + O(\epsilon),$$

$$\frac{\partial p}{\partial \eta} = O(\epsilon), \quad \therefore \quad p = p_{core} + O(\epsilon),$$

$$\alpha \rho \bar{u}_x \frac{\partial \bar{u}_z}{\partial x} + \rho \bar{u}_y \frac{\partial \bar{u}_z}{\partial \eta} + J_{sE} \frac{\partial p}{\partial \zeta_{core}} = \alpha F_z + \alpha \left[1 + \alpha^2 (f')^2\right] \frac{\partial}{\partial \eta} \mu_v \frac{\partial \bar{u}_z}{\partial \eta} +$$

$$+ O(\epsilon),$$

Energy: $$\alpha \rho \bar{u}_x \frac{\partial h}{\partial x} + \rho \bar{u}_y \frac{\partial h}{\partial \eta} = \alpha \bar{u}_x \frac{\partial p}{\partial x} + \alpha j^2/\sigma + \frac{\alpha}{P_r} \left[1 + \alpha^2 (f')^2\right] \frac{\partial}{\partial \eta} \mu_v \frac{\partial h}{\partial \eta} +$$

$$+ \alpha \left[1 + \alpha^2 (f')^2\right] \mu_v \left\{\left[1 + \alpha^2 (f')^2\right] \left(\frac{\partial \bar{u}_x}{\partial \eta}\right)^2 + \left(\frac{\partial \bar{u}_z}{\partial \eta}\right)^2\right\} - G \left(\alpha f' \frac{\partial g_{ex}}{\partial \eta} + \right.$$

$$\left. \mp \frac{\partial g_{ey}}{\partial \eta}\right) + O(\epsilon).$$

The independent variable ξ_{core} is only a parameter in these equations. Note that T_{sE} provides a source term in the continuity

equation.

A similar procedure is used in the insulator boundary layer region:

$$(x, y, \nu) \xrightarrow[T_{sI}]{} (x, \zeta, \nu),$$

$$J_{sI} = \zeta_{,y}\,\text{core}\,/_{z=\pm\beta f} + O(\epsilon),$$

$$\vec{\tilde{u}} \cdot \tilde{\nabla}_\alpha \xrightarrow[T_{sI}]{} \alpha \tilde{u}_x \frac{\partial}{\partial x} + \tilde{u}_z \frac{\partial}{\partial \nu} \quad \text{as} \quad \vec{\tilde{u}} \cdot \tilde{\nabla}_\alpha \zeta = 0,$$

and $$\tilde{\nabla}_\alpha \cdot \rho \vec{\tilde{u}} = 0 \xrightarrow[T_{sI}]{} \alpha \frac{\partial}{\partial x} \rho \tilde{u}_x + \frac{\partial}{\partial \nu} \rho \tilde{u}_z + (\tilde{\nabla}_\alpha \zeta) \cdot \frac{\partial}{\partial \zeta} \rho \vec{\tilde{u}} = 0$$

where $$(\tilde{\nabla}_\alpha \zeta) \cdot \frac{\partial}{\partial \zeta} \rho \vec{\tilde{u}} = \alpha \rho \tilde{u}_x \left[\zeta_{,z} \frac{\partial}{\partial x} \left(\frac{\zeta_{,y}}{J_s} \right) - \zeta_{,y} \frac{\partial}{\partial x} \left(\frac{\zeta_{,z}}{J_s} \right) \right]$$

$$= -\alpha \rho \tilde{u}_x \frac{\partial}{\partial x} \ln J_{sI} + O(\epsilon).$$

A set of equations analogous to those on the previous page results; ζ_{core} is a parameter in these equations.

Expansion in the Parameter α

1. Core flow. The last group of expansions to be considered is in the parameter α. First, there will be given an examination of the fluid equations in the core.

Let $$u_x \equiv u_{x_0} + \alpha u_{x_1} + \alpha^2 u_{x_2} + \cdots$$

$$u_y \equiv \alpha u_{y_1} + \alpha^2 u_{y_2} + \cdots$$

$$u_z \equiv \alpha u_{z_1} + \alpha^2 u_{z_2} + \cdots$$

$$p \equiv p_0 + \alpha p_1 + \cdots$$

etc.

In rectangular Cartesian coordinates, the zeroth order equations are:

$$\frac{\partial \rho_0 u_{x0}}{\partial x} + \frac{\partial \rho_0 u_{y1}}{\partial y} + \frac{\partial \rho_0 u_{z1}}{\partial z} = 0,$$

$$\rho_0 u_{x0} \frac{\partial u_{x0}}{\partial x} + \rho_0 u_{y1} \frac{\partial u_{x0}}{\partial y} + \rho_0 u_{z1} \frac{\partial u_{x0}}{\partial z} + \frac{dp_0}{dx} = F_{x0},$$

$$p_0 = p_0(x), \quad \nabla_T \times \vec{F}_{T_0} = 0 \quad \text{as} \quad \vec{F}_{T_0} = \nabla_T p_1,$$

$$\rho_0 u_{x0} \frac{\partial h_0}{\partial x} + \rho_0 u_{y1} \frac{\partial h_0}{\partial y} + \rho_0 u_{z1} \frac{\partial h_0}{\partial z} = u_{x0} \frac{dp_0}{dx} + j_0^2/\sigma_0$$

where $\sigma_0 = \sigma(p_0, h_0)$

and $p_0 = \rho_0 T(h_0)$.

The higher order equations are linear in the higher order terms. Note that a constraint on $\vec{F}_{T_0}$ results. The next step is to look at the equations in stream coordinates.

The stream functions are written as an asymptotic series:

$$\xi = \xi_0 + \alpha \xi_1 + \alpha^2 \xi_2 + \cdots = \xi_0 + \Delta\xi,$$

$$\zeta = \zeta_0 + \alpha \zeta_1 + \cdots = \zeta_0 + \Delta\zeta.$$

Another transformation is made: $(x, \xi, \zeta) \xrightarrow[T_{S'}]{} (x, \xi_0, \zeta_0)$ so that the result of the transformation $T_{SS'} = T_S + T_{S'}$ is independent of α.

Note the following:

$$\frac{\partial(\xi_0, \zeta_0)}{\partial(y, z)} = J_{SS'} = R_0 \rho_0 u_{x0},$$

$$\frac{\partial(\xi_0, \zeta_0)}{\partial(z, x)} = R_0 \rho_0 u_{y1}, \quad \frac{\partial(\xi_0, \zeta_0)}{\partial(x, y)} = R_0 \rho_0 u_{z1},$$

$$\vec{u} \cdot \nabla_\alpha \xi_0 = -\vec{u} \cdot \nabla_\alpha (\Delta\xi) = O(\alpha^2), \quad \vec{u} \cdot \nabla_\alpha \zeta_0 = O(\alpha^2),$$

and $$(u_{x_0}\frac{\partial}{\partial x} + u_{y_1}\frac{\partial}{\partial y} + u_{z_1}\frac{\partial}{\partial z})R_0 = 0.$$

Equating terms of like order, the convective derivative, $\vec{u}\cdot\nabla_\alpha$, transforming as:

$$\vec{u}\cdot\nabla_\alpha \xrightarrow[T_{ss'}]{} \propto u_x\frac{\partial}{\partial x} + (\vec{u}\cdot\nabla_\alpha\xi_0)\frac{\partial}{\partial\xi_0} + (\vec{u}\cdot\nabla_\alpha\zeta_0)\frac{\partial}{\partial\zeta_0}$$

gives: $$(u_{x_0}\frac{\partial}{\partial x} + u_{y_1}\frac{\partial}{\partial y} + u_{z_1}\frac{\partial}{\partial z}) \xrightarrow[T_{ss'}]{} u_{x_0}\frac{\partial}{\partial x} \equiv O_0,$$

$$(u_{x_1}\frac{\partial}{\partial x} + u_{y_2}\frac{\partial}{\partial y} + u_{z_2}\frac{\partial}{\partial z}) \xrightarrow[T_{ss'}]{} u_{x_1}\frac{\partial}{\partial x} - (O_0\xi_1)\frac{\partial}{\partial\xi_0} + - (O_0\zeta_1)\frac{\partial}{\partial\zeta_0} \equiv O_1,$$

$$(u_{x_2}\frac{\partial}{\partial x} + u_{y_3}\frac{\partial}{\partial y} + u_{z_3}\frac{\partial}{\partial z}) \xrightarrow[T_{ss'}]{} u_{x_2}\frac{\partial}{\partial x} - (O_0\xi_2 + O_1\xi_1)\frac{\partial}{\partial\xi_0} + - (O_0\zeta_2 + O_1\zeta_1)\frac{\partial}{\partial\zeta_0} \equiv O_2,$$

etc.

Thus the zeroth order fluid equations for the core are:

$$\rho_0 u_{x_0}\frac{\partial u_{x_0}}{\partial x} + \frac{dp_0}{dx} = F_{x_0},$$

$$\rho_0 u_{x_0}\frac{\partial h_0}{\partial x} = u_{x_0}\frac{dp_0}{dx} + j_0^2/\sigma_0,$$

$$p_0(x) = \rho_0 T(h_0),$$

$$R_0 = R_0(\xi_0, \zeta_0),$$ a known function.

The functions ξ_0 and ζ_0 appear only as parameters in the above equations. The next set of equations is:

$$O_0 R_1 + O_1 R_0 = 0,$$

$$\rho_0 (O_0 u_{x_1} + O_1 u_{x_0}) + \rho_1 O_0 u_{x_0} + \frac{\partial p_1}{\partial x} = F_{x_1},$$

$$\rho_0 (O_0 h_1 + O_1 h_0) + \rho_1 O_0 h_0 = O_0 p_1 + O_1 p_0 + 2 \frac{\vec{j}_0 \cdot \vec{j}_1}{\sigma_0} + - j_0^2/\sigma_0 \left(\frac{\sigma_1}{\sigma_0}\right),$$

$$p_1 = \rho_1 T(h_0) + \rho_0 h_1 \frac{dT}{dh}(h_0),$$

$$\rho_0 O_0 \vec{u}_{T_1} + \nabla_T p_2 = \vec{F}_{T_1}$$

where $\nabla_T = (\nabla_T \xi_0) \frac{\partial}{\partial \xi_0} + (\nabla_T \zeta_0) \frac{\partial}{\partial \zeta_0}$,

$\xi_{0,y} = J_{ss'} \frac{\partial z}{\partial \zeta_0}$, etc.

Since O_1 operates on known functions, ξ_0 and ζ_0 are again parameters. Note that the above are linear with ξ_1 and ζ_1 unknown. The $\nabla_T p_2$ term can be eliminated by taking the curl of the corresponding equation. The result is a constraint on $\vec{F}_{T_1}$. The boundary and entrance conditions on the ξ_i and ζ_i are obtained from T_S :

$$\xi_0 = 0 \ @ \ z = -\beta f, \ \xi_0 = -1 \ @ \ z = \beta f,$$

$$\zeta_0 = 0 \ @ \ y = -f, \ \zeta_0 = 1 \ @ \ y = f,$$

$$\xi_0|_{x=0} = -\frac{1}{2}(1 + z/\beta), \ \zeta_0|_{x=0} = \frac{1}{2}(1+y),$$

$$\xi_i = 0 \ @ \ y = \pm f \quad (i>0),$$

$$\xi_i = 0 \ @ \ z = \pm \beta f \quad (i>0),$$

$$\xi_i|_{x=0} = \zeta_i|_{x=0} = 0 \quad (i>0).$$

The transformation $T_{55'}$ is given as follows:

$$Y = (2\xi_0 - 1) f(x) + C_{y_0}(x, \xi_0, \zeta_0),$$

$$Z = -\beta (2\xi_0 + 1) f(x) + C_{z_0}(x, \xi_0, \zeta_0)$$

where

$$C_{y_0} = 0 \text{ @ } \xi_0 = 0, 1; \; x = 0 \text{ and } C_{z_0} = 0 \text{ @ } \xi_0 = 0, -1; \; x = 0.$$

Comparing these expressions to those found for T_5, it is seen:

$$C_{y_i} = -2 f \xi_i \quad (i > 0) \qquad \text{and} \qquad C_{z_i} = 2\beta f \xi_i \quad (i > 0).$$

The Pfaffians for the transformation are:

$$dy = \frac{u_{y1}}{u_{x_0}} dx + \frac{\xi_{0,z}}{J_{55'}} d\xi_0 - \frac{\xi_{0,z}}{J_{55'}} d\zeta_0,$$

$$dz = \frac{u_{z1}}{u_{x_0}} dx - \frac{\xi_{0,y}}{J_{55'}} d\xi_0 + \frac{\xi_{0,y}}{J_{55'}} d\zeta_0.$$

Therefore,

$$\frac{\partial \vec{C}_{T_0}}{\partial x}\Big|_{x=0} = \frac{\vec{u}_{T_1}}{u_{x_0}}\Big|_{x=0} + f'(0) \begin{pmatrix} 1 - 2\xi_0 \\ \beta(1 + 2\xi_0) \end{pmatrix}.$$

This is simply the zeroth order part of the similar relation given on page 20. To get the higher order parts of this relation, the transformation T_{51} of the axial derivative is formed:

$$\frac{\partial}{\partial x} \xrightarrow[T_{51}]{} \frac{\partial}{\partial x} - \alpha \left(\xi_{1,x} \frac{\partial}{\partial \xi_0} + \zeta_{1,x} \frac{\partial}{\partial \zeta_0} \right) +$$

$$+ \alpha^2 \left[\xi_{1,x} \left(\xi_{1,\xi_0} \frac{\partial}{\partial \xi_0} + \zeta_{1,\xi_0} \frac{\partial}{\partial \zeta_0} \right) + \zeta_{1,x} \left(\xi_{1,\zeta_0} \frac{\partial}{\partial \xi_0} + \zeta_{1,\zeta_0} \frac{\partial}{\partial \zeta_0} \right) + \right.$$

$$\left. - \left(\xi_{2,x} \frac{\partial}{\partial \xi_0} + \zeta_{2,x} \frac{\partial}{\partial \zeta_0} \right) \right] + O(\alpha^3).$$

Application of this yields:

$$\xi_{1,x} = \frac{u_{x1}}{(u_{x_0})^2} \vec{u}_{T_1} \cdot \nabla_T \xi_0 - \frac{1}{u_{x_0}} \vec{u}_{T_2} \cdot \nabla_T \xi_0 ,$$

and

$$\zeta_{1,x} = \frac{u_{x1}}{(u_{x_0})^2} \vec{u}_{T_1} \cdot \nabla_T \zeta_0 - \frac{1}{u_{x_0}} \vec{u}_{T_2} \cdot \nabla_T \zeta_0 .$$

From these are obtained $\xi_{1,x}|_{x=0}$ and $\zeta_{1,x}|_{x=0}$ in terms of

$(\vec{u}_{T_2}/u_{x_0})|_{x=0}$ and $(u_{x_1}/u_{x_0})|_{x=0}$.

2. Boundary layer regions. The effect of the expansions in the parameter α on the boundary layer equations is now obtained. The expansions of the Jacobian and variable in the transformation to the stream coordinate in the electrode boundary layer region are:

$$J_{\xi E} = J_{\xi E_0} + \alpha J_{\xi E_1} + \cdots = \xi_{0,z\ core}|_{y=\pm f} + \alpha \xi_{1,z\ core}|_{y=\pm f} + \cdots ,$$

$$\xi_{core} = \xi_{0\ core} + \alpha \xi_{1\ core} + \cdots = \xi_{0\ core} + \Delta \xi_{core} .$$

The transformation $\xi_{core} \xrightarrow{T_{\xi'}} \xi_{0\ core}$ is made. An arbitrary smooth function $S(x, \eta, \xi_{core})$ is expanded in a Taylor series about $\xi_{0\ core}$: $S(x, \eta, \xi_{0\ core} + \Delta\xi_{core}) = S(x, \eta, \xi_{0\ core}) +$

$$+ (\Delta\xi_{core}) \frac{\partial}{\partial \xi_{core}} S(x, \eta, \xi_{0\ core}) + \frac{1}{2} (\Delta\xi_{core})^2 \frac{\partial^2 S}{\partial \xi_{core}^2} (x, \eta, \xi_{0\ core}) + \cdots .$$

Let this expansion be applied to each dependent variable. If there are no large cross-flows, then in the boundary layer region $\xi, \eta = O(\epsilon)$ and therefore $\vec{u} \cdot \nabla_\perp \xi = 0$ implies

$$\alpha \bar{u}_x \frac{\partial}{\partial x} \xi_{core} + \bar{u}_z \frac{\partial}{\partial z} \xi_{core} = 0 ,$$

or $\bar{u}_{z_0} J_{\xi E_0} = 0$, $\bar{u}_{z_0} = 0$, as expected, where

$$\bar{u}_x = \bar{u}_{x_0} + \alpha \bar{u}_{x_1} + \cdots ,$$

$$\bar{u}_y = \alpha \bar{u}_{y_1} + \cdots , \qquad \text{etc.}$$

Combining these expansions, the first set of equations for the electrode boundary layer is:

Continuity: $\frac{\partial}{\partial x} \rho_0 \bar{u}_{x_0} + \frac{\partial}{\partial \eta} \rho_0 \bar{u}_{y_1} = \rho_0 \bar{u}_{x_0} \frac{\partial}{\partial x} \ln J_{sE_0}$

Momentum: $\rho_0 \bar{u}_{x_0} \frac{\partial}{\partial x} \bar{u}_{x_0} + \rho_0 \bar{u}_{y_1} \frac{\partial}{\partial \eta} \bar{u}_{x_0} + \frac{dp_0}{dx} = F_{x_0} + \frac{\partial}{\partial \eta} \mu_{y_0} \frac{\partial \bar{u}_{x_0}}{\partial \eta}$

where $p_0(x) = p_{0\,core}$, also $p_1 = p_{1\,core}$,

$\frac{\partial p_1}{\partial z} = F_{z_0}$, $\therefore \frac{\partial}{\partial \eta} F_{z_0} = 0$

Energy: $\rho_0 \bar{u}_{x_0} \frac{\partial}{\partial x} h_0 + \rho_0 \bar{u}_{y_1} \frac{\partial}{\partial \eta} h_0 = \bar{u}_{x_0} \frac{dp_0}{dx} + j_0^2/\sigma_0 +$

$+ \mu_{y_0} \left(\frac{\partial \bar{u}_{x_0}}{\partial \eta}\right)^2 + \frac{1}{P_r} \frac{\partial}{\partial \eta} \mu_{y_0} \frac{\partial h_0}{\partial \eta} \pm G \frac{\partial q_{ey_0}}{\partial \eta}$

State: $p_0 = \rho_0 T(h_0)$

Since $\bar{u}_{x_0} \frac{\partial}{\partial x} \xi_{0\,core} + \bar{u}_{z_1} \frac{\partial}{\partial z} \xi_{0\,core} = 0$,

$\bar{u}_{z_1}$ is given simply by: $\bar{u}_{z_1} = - \bar{u}_{x_0} \frac{\partial}{\partial x} \xi_{0\,core} / J_{sE_0}$

or $\bar{u}_{z_1} = \bar{u}_{x_0} (u_{z_1}/u_{x_0})_{core}$.

The next set of equations is linear. Equations for the insulator boundary layer region are had in a similar manner. One result is: $\frac{\partial}{\partial \nu} F_{y_0} = 0$.

3. Maxwell's equations: field potentials. Next, Maxwell's equations are examined in the limit of small α. The electromagnetic fields are given by the potentials ϕ, ψ:

$$\vec{\mathcal{B}} = \nabla_\alpha \phi,$$

$$\vec{E} = \nabla_\alpha \psi + \vec{i}_x \, E_{x_0}(x)$$

where $\nabla_\alpha^2 \phi = 0,$

$$\phi = \phi_0 + \alpha \phi_1 + \cdots,$$

and $$\psi = \psi_0 + \alpha \psi_1 + \cdots.$$

Induction $\vec{\mathcal{B}}$ lies mainly in the z-direction; field drop-off at the entrance and exit results in fringing (E_x and $\mathcal{B}_x$ not small). The component $\mathcal{B}_{y_0} = \frac{\partial \phi_0}{\partial y}$ is taken equal to zero, that is, $\mathcal{B}_y \leq O(\alpha)$. Assuming that the tangential electric field is invariant across the electrode boundary layer $(\Delta > O(10^{-3}))$, then $E_z = \frac{\partial \psi}{\partial z} = 0$ at $y = \pm f$. The component $E_{z_0} = \frac{\partial \psi_0}{\partial z}$ is also taken to be zero; this boundary condition is then automatically satisfied to $O(\alpha)$ and the crossed fields are perpendicular to $O(\alpha)$.

The potential ϕ is separated into two parts: $\phi \equiv \phi_A(x, z; \alpha) + \phi_B(x, y, z)$ such that $\phi_A = \alpha^{-1} \mathrm{Re}\, F(x + i\alpha z; \alpha)$ where F is an analytic function and $\lim_{\alpha \to 0} \phi_{A, z} = O(1)$, $\lim_{\alpha \to 0} \nabla_T \phi_B = 0$, and $\nabla_\alpha^2 \phi_B = 0$. The potential ϕ_0 is 'contained' within ϕ_A and $\phi_B \sim \alpha$ for α small. The zeroth order induction is:

$$\mathcal{B}_{x_0} - i\, \mathcal{B}_{z_0} = \lim_{\alpha \to 0} F'(x + i\alpha z).$$

The function F is regarded as known, based on the physical situation of the problem at hand. If, in the physical situation, the induction at the entrance attains $O(1)$ in an axial length of $O(\alpha)$ (the shortest possible entrance length for the field), then the zeroth order field contains a Heaviside function. If, on the other hand, the induc-

tion varies weakly with X throughout the channel, a smooth zeroth order field results. The former is likely to represent most physical problems.

As an example, let $$\phi_A = \frac{1}{2\alpha} \int_0^a \frac{B(\bar{x}) \sin sz \, d\bar{x}}{\cos sz + \cosh s\left(\frac{x-\bar{x}}{\alpha}\right)} .$$

Consider the special case $B \equiv 1$ with

$$f_1(x,z) \equiv \sin^{-1}\left(\frac{1 + \cos sz \cosh sx/\alpha}{\cos sz + \cosh sx/\alpha}\right),$$

$$f_2(x,z) \equiv \sin^{-1}\left(\frac{1 + \cos sz \cosh s\left(\frac{a-x}{\alpha}\right)}{\cos sz + \cosh s\left(\frac{a-x}{\alpha}\right)}\right),$$

then $$2s\phi_A = \begin{cases} f_1 - f_2, & x < 0 \\ \pi - f_1 - f_2, & 0 < x < a \\ f_2 - f_1 & x > a \end{cases}$$

Taking derivatives:

$$\phi_{A,x} = \frac{1}{2\alpha}\left[\frac{\sin sz}{\cos sz + \cosh \frac{sx}{\alpha}} - \frac{\sin sz}{\cos sz + \cosh s\left(\frac{a-x}{\alpha}\right)}\right],$$

$$\phi_{A,z} = \frac{1}{2}\left[\frac{\sinh \frac{sx}{\alpha}}{\cos sz + \cosh \frac{sx}{\alpha}} + \frac{\sinh s\left(\frac{a-x}{\alpha}\right)}{\cos sz + \cosh s\left(\frac{a-x}{\alpha}\right)}\right].$$

The limit $\alpha \to 0$ is now taken, giving:

$$\lim_{\alpha \to 0} \frac{1}{2\alpha} \frac{\sin sz}{\cos sz + \cosh \frac{sx}{\alpha}} = z\,\delta(x)$$ where δ is the Dirac delta function. $\therefore\ \mathcal{B}_{x_0} = \alpha z [\delta(x) - \delta(a-x)]$,

and similarly, $\mathcal{B}_{z_0} = \frac{1}{2}$ @ $x = 0, a$.

For the case when $B(\bar{x}) \neq 1$, $\mathcal{B}_{x_0} = \alpha z\, B(x)[\delta(x) - \delta(a-x)]$

and $$\mathcal{B}_{z_0} = \begin{cases} 0, & x < 0 \quad \text{and} \quad x > a \\ B(x), & 0 < x < a \\ \frac{1}{2} B(0), & x = 0 \\ \frac{1}{2} B(a), & x = a \end{cases} .$$

It is to be noted that, although $\mathcal{B}_{x_0}$ is arbitrarily large at $x = 0, a$ the integrated effect of this singularity in the transverse momentum equations on the pressure (assuming smooth, continuous streamlines) is of $O(\alpha^2)$. Field drop-off in channels with small α is not very important.

4. Ohm's law. Finally, zeroth order equations for Ohm's law are formed in the α- expansion. If the Hall parameter is given by $\vec{\omega\tau} \equiv \frac{\sigma^+ \vec{\mathcal{B}}^+}{q^+} = \frac{\sigma \vec{\mathcal{B}}}{q}$ (see Appendix A), then $q^+ \approx e^+ n_e^+$. Since $\mathcal{B}_T^2 \neq 0$, components of Ohm's law can be taken along the $\vec{\mathcal{B}}$, $\vec{i}_x$, and $\vec{i}_x \times \vec{\mathcal{B}}_T$ directions:

$$\sigma \vec{\mathcal{B}} \cdot \vec{E} = \vec{j} \cdot \vec{\mathcal{B}},$$

$$\frac{F_x}{q} + \frac{j_x}{\sigma} = E_x + (\vec{i}_x, \vec{u}_T, \vec{\mathcal{B}}_T),$$

$$(\vec{i}_x, \vec{B}_T, \vec{E}_T) + \frac{F_x}{\sigma} + B_T^2 (u_x - \frac{j_x}{q}) = \frac{\sigma}{q} B_x^2 (\vec{i}_x, \vec{u}_T, \vec{B}_T) +$$

$$+ B_x (\vec{u}_T \cdot \vec{B}_T) - \frac{\sigma}{q} B_x (\vec{B}_T \cdot \vec{E}_T) - \sigma F_x \left(\frac{B_x}{q}\right)^2 .$$

Let $\vec{b} = \vec{b}_0 + \alpha \vec{b}_1 + \alpha^2 \vec{b}_2 + \cdots$.

Consider the case $\overline{\omega\tau} \leq O(1)$. In the sections of the channel where the fields vary smoothly:

$$B_{x_0} = B_{y_0} = 0, \quad \phi_0 = z B_{z_0}(x),$$

$$\vec{j}_{T_0} = (\nabla_T b_{x_0}) \times \vec{i}_x, \quad E_{y_0} = E_{y_0}(x,y), \quad E_{z_0} = 0.$$

Therefore $j_{z_0} = -\frac{\partial b_{x_0}}{\partial y} = 0, \; j_{y_0} = j_{y_0}(x,z) = \frac{\partial b_{x_0}}{\partial z},$

and $F_{x_0} = j_{y_0} B_{z_0}$.

The constraint $\nabla_T \times \vec{F}_{T_0} = 0$ implies $\frac{\partial j_{x_0}}{\partial z} = 0, \; j_{x_0} = j_{x_0}(x,y).$

Thus, Ohm's law in the zeroth order is given by:

$$\frac{F_{x_0}}{q_0} + \frac{j_{x_0}}{\sigma_0} = E_{x_0}(x),$$

$$\frac{j_{y_0}}{\sigma_0} + (u_{x_0} - \frac{j_{x_0}}{q_0}) B_{z_0}(x) = E_{y_0} .$$

If $\overline{\omega\tau} \leq O(\alpha)$, the limit $q_0 \to \infty$ is taken. Then $j_{x_0} = E_{x_0} = 0$ or $\frac{\partial \sigma_0}{\partial z} = 0$. This is not a likely situation.

If Heaviside functions occur in B_{z_0} (with corresponding Dirac delta functions in B_{x_0}), appropriate matching across the discontinuities must be done.

The assumption that the stream functions do not vary across the boundary layers led to the following restrictions on the magnetic body forces in the boundary layers:

$$\frac{\partial}{\partial \eta} F_{z_0} = \frac{\partial}{\partial \nu} F_{y_0} = 0.$$

The force $F_{z_0} = -j_{y_0} B_{x_0}$ and $\frac{\partial}{\partial \eta} j_{y_0} = \frac{\partial}{\partial \eta} B_{x_0} = 0$ from Maxwell's equations; hence the first restriction is satisfied. The force $F_{y_0} = -j_{x_0} B_{z_0}$; also $\frac{\partial}{\partial \nu} B_{z_0} = 0$. The restriction $\frac{\partial}{\partial \nu} j_{x_0} = 0$, $\overline{\omega\tau} \leq O(\alpha)$ means $E_{x_0} = 0$ at $z = \pm\beta f$ or $\frac{\partial}{\partial \nu} \sigma_0 = 0$. Therefore, at the channel entrance, large fringe electric fields produce large cross-flow velocities in the boundary layers unless the temperature is constant in the insulator layer. For $\overline{\omega\tau} = O(1)$ a similar situation can occur throughout the channel*. This effect will be discussed next.

Effect of an Axial Electric Field in the Boundary Layers: Large Cross-Flows

This section is devoted to the formulation of boundary layer equations when the condition of a large axial electric field or a large Hall parameter exists. Stream coordinates will not be used.

The insulator boundary layer is divided into two parts: an 'outer layer' in which the temperature and axial velocity are invariant and in which there is no large cross-flow, and an 'inner layer' where the temperature adjusts to the wall temperature in which a large cross-flow is present. The inner layer thickness is given by $\delta_{CF} = \alpha^{1/4} \epsilon$, i.e., it is of $O(\alpha^{1/4})$ of the boundary layer thickness.

---

* $j_{x_0} = \frac{\sigma_0}{1 + (\omega\tau_0)^2} \left[E_{x_0} - \omega\tau_0 \left(E_{y_0} - u_{x_0} B_{z_0} \right) \right]$ where

$\frac{\partial}{\partial \nu} E_{x_0} = \frac{\partial}{\partial \nu} E_{y_0} = 0$; thus, j_{x_0} varies with temperature and u_{x_0}.

For physical situations, $\alpha \approx 10^{-1}$ to 10^{-2} and $\alpha^{1/4} \approx \frac{1}{2}$ to $\frac{1}{3}$; the cross-flow exists in the lower half of the boundary layer. The outer variable is ν , the inner variable is $\nu' \equiv \alpha^{-1/4}\nu$. The inner dependent variables will be distinguished from the outer dependent variables by a prime ('). For the outer layer:

$$\tilde{u}_x = \tilde{u}_{x_0} + \alpha \tilde{u}_{x_1} + \alpha^2 \tilde{u}_{x_2} + \cdots$$

$$\tilde{u}_y = \alpha \tilde{u}_{y_1} + \alpha^2 \tilde{u}_{y_2} + \cdots$$

$$\tilde{u}_z = \alpha^{3/4} \tilde{u}_{z\,3/4} + \alpha^{5/4} \tilde{u}_{z\,5/4} + \cdots$$

$$p = p_0(x) + \alpha p_1 + \cdots$$

$$h = h_0 + \alpha h_1 + \cdots$$

$$\rho = \rho_0 + \alpha \rho_1 + \cdots$$

Terms of $O(\alpha^{3/4})$ give $\frac{\partial h_0}{\partial \nu} = \frac{\partial \tilde{u}_{x_0}}{\partial \nu} = \frac{\partial \tilde{u}_{z\,3/4}}{\partial \nu} = 0$.

Terms of $O(\alpha)$ give:

$$\frac{\partial \rho_0 \tilde{u}_{x_0}}{\partial x} + \frac{\partial \rho_0 \tilde{u}_{y_1}}{\partial y} = 0,$$

$$\rho_0 \tilde{u}_{x_0} \frac{\partial \tilde{u}_{x_0}}{\partial x} + \rho_0 \tilde{u}_{y_1} \frac{\partial \tilde{u}_{x_0}}{\partial y} + \frac{dp_0}{dx} = F_{x_0},$$

$$\frac{\partial p_1}{\partial y} = F_{y_0} = -j_{x_0} B_{z_0},$$

$$\rho_0 \tilde{u}_{x_0} \frac{\partial h_0}{\partial x} + \rho_0 \tilde{u}_{y_1} \frac{\partial h_0}{\partial y} = \tilde{u}_{x_0} \frac{dp_0}{dx} + j_0^2/\sigma_0.$$

Let the subscript "c" denote core values at $z = \pm \beta f$. Then, since $u_{z_{1c}} = \pm \beta f' u_{x_0 c}$ and $\frac{\partial}{\partial x}\Big)_{y,\nu} = \frac{\partial}{\partial x}\Big)_{y,z} \pm \beta f' \left(\frac{\partial}{\partial z}\right)_{x,y}$, the above

equations merely state $\tilde{u}_{x_0} = u_{x_{0c}}$, $\tilde{u}_{y_1} = u_{y_{1c}}$, $h_0 = h_{0c}$, $\rho_0 = \rho_{0c}$, $j_{x_0} = j_{x_{0c}}$, etc., and $\frac{\partial}{\partial \nu} \tilde{u}_{z\,3/4} = 0$, i.e., the outer layer is core flow. Cross-flow boundary layers are slightly thinner than layers without cross-flow; mass is effectively bled from the layer. Higher order terms (up to $O(\epsilon)$) give the same result: $\frac{\partial}{\partial \nu} \equiv 0$.

Next, the inner layer is considered. Transforming from ν to ν' : $\frac{\partial}{\partial \nu} \longrightarrow \alpha^{-1/4} \frac{\partial}{\partial \nu'}$. The following expansions are used:

$$\tilde{u}_x' = \tilde{u}_{x_0}' + \alpha^{1/2} \tilde{u}_{x\,1/2}' + \alpha \tilde{u}_{x_1}' + \cdots$$

$$\tilde{u}_y' = \alpha^{1/2} \tilde{u}_{y\,1/2}' + \alpha \tilde{u}_{y_1}' + \alpha^{3/2} \tilde{u}_{y\,3/2}' + \cdots$$

$$\tilde{u}_z' = \alpha^{3/4} \tilde{u}_{z\,3/4}' + \alpha^{5/4} \tilde{u}_{z\,5/4}' + \cdots$$

$$p = p_0(x) + \alpha p_1 + \cdots$$

$$h' = h_0' + \alpha^{1/2} h_{1/2}' + \alpha h_1' + \cdots$$

$$\rho' = \rho_0' + \alpha^{1/2} \rho_{1/2}' + \alpha \rho_1' + \cdots$$

The matching is obvious: $\lim_{\nu' \to \infty} \tilde{u}_{x_0}' = \lim_{\nu \to 0} \tilde{u}_{x_0}$, etc.; for the 'prime' variables of $O\left(\frac{n}{2}\right)$ where n is odd: $\lim_{\nu' \to \infty} \tilde{u}_{x\,1/2}' = 0$, etc. (these are the 'cross-flow variables'). The following sets of equations are formed:

From $O(\alpha^{1/2})$:

$$\frac{\partial}{\partial y} \rho_0' \tilde{u}_{y\,1/2}' + \frac{\partial}{\partial \nu'} \rho_0' \tilde{u}_{z\,3/4}' = 0,$$

$$\rho_0' \tilde{u}_{y\,1/2}' \frac{\partial \tilde{u}_{x_0}'}{\partial y} + \rho_0' \tilde{u}_{z\,3/4}' \frac{\partial \tilde{u}_{x_0}'}{\partial \nu'} = \frac{\partial}{\partial \nu'} \mu_{v_0}' \frac{\partial \tilde{u}_{x_0}'}{\partial \nu'},$$

$$\rho_0' \tilde{u}_{y\,1/2}' \frac{\partial h_0'}{\partial y} + \rho_0' \tilde{u}_{z\,3/4}' \frac{\partial h_0'}{\partial \nu'} = \frac{1}{P_r} \frac{\partial}{\partial \nu'} \mu_{v_0}' \frac{\partial h_0'}{\partial \nu'} + \mu_{v_0}' \left(\frac{\partial \tilde{u}_{x_0}'}{\partial \nu'} \right)^2.$$

From $O(\alpha)$:

$$\rho_0' \tilde{u}_{y1/2}' \frac{\partial \tilde{u}_{y1/2}'}{\partial y} + \rho_0' \tilde{u}_{z3/4}' \frac{\partial \tilde{u}_{y1/2}'}{\partial \nu'} + \left(\frac{\partial p_1}{\partial y} - F_{y_0}'\right) = \frac{\partial}{\partial \nu'} \mu_{\nu_0}' \frac{\partial \tilde{u}_{y1/2}'}{\partial \nu'}.$$

(This equation and the state equation complete a set of equations; the cross-flow velocity is of $O(\alpha^{1/2})$.)

$$\frac{\partial}{\partial x} \rho_0' \tilde{u}_{x_0}' + \frac{\partial}{\partial y}\left(\rho_0' \tilde{u}_{y_1}' + \rho_{1/2}' \tilde{u}_{y1/2}'\right) + \frac{\partial}{\partial \nu'}\left(\rho_0' \tilde{u}_{z5/4}' + \rho_{1/2}' \tilde{u}_{z3/4}'\right) = 0,$$

$$\rho_0' \tilde{u}_{x_0}' \frac{\partial \tilde{u}_{x_0}'}{\partial x} + \rho_0' \tilde{u}_{y_1}' \frac{\partial \tilde{u}_{x_0}'}{\partial y} + \rho_0' \tilde{u}_{z5/4}' \frac{\partial \tilde{u}_{x_0}'}{\partial \nu'} + \rho_0' \tilde{u}_{y1/2}' \frac{\partial \tilde{u}_{x1/2}'}{\partial y} +$$

$$+ \rho_0' \tilde{u}_{z3/4}' \frac{\partial \tilde{u}_{x1/2}'}{\partial \nu'} + \rho_{1/2}'\left(\tilde{u}_{y1/2}' \frac{\partial \tilde{u}_{x_0}'}{\partial y} + \tilde{u}_{z3/4}' \frac{\partial \tilde{u}_{x_0}'}{\partial \nu'}\right) + \frac{dp_0}{dx} =$$

$$= F_{x_0}' + \frac{\partial}{\partial \nu'} \mu_{\nu_0}' \frac{\partial \tilde{u}_{x1/2}'}{\partial \nu'} + \frac{\partial}{\partial \nu'} \mu_{\nu_{1/2}}' \frac{\partial \tilde{u}_{x_0}'}{\partial \nu'},$$

$$\rho_0' \tilde{u}_{x_0}' \frac{\partial h_0'}{\partial x} + \rho_0' \tilde{u}_{y_1}' \frac{\partial h_0'}{\partial y} + \rho_0' \tilde{u}_{z5/4}' \frac{\partial h_0'}{\partial \nu'} + \rho_0' \tilde{u}_{y1/2}' \frac{\partial h_{1/2}'}{\partial y} +$$

$$+ \rho_0' \tilde{u}_{z3/4}' \frac{\partial h_{1/2}'}{\partial \nu'} + \rho_{1/2}'\left(\tilde{u}_{y1/2}' \frac{\partial h_0'}{\partial y} + \tilde{u}_{z3/4}' \frac{\partial h_0'}{\partial \nu'}\right) = \tilde{u}_{x_0}' \frac{dp_0}{dx} +$$

$$+ j_0^2/\sigma_0 + \frac{\partial}{\partial \nu'} \mu_{\nu_0}' \frac{\partial h_{1/2}'}{\partial \nu'} + \frac{\partial}{\partial \nu'} \mu_{\nu_{1/2}}' \frac{\partial h_0'}{\partial \nu'}.$$

To complete the second set, the y-momentum equation from $O(\alpha^{3/2})$ is needed:

$$\rho_0' \tilde{u}_{x_0}' \frac{\partial \tilde{u}_{y1/2}'}{\partial x} + \rho_0' \tilde{u}_{y_1}' \frac{\partial \tilde{u}_{y1/2}'}{\partial y} + \rho_0' \tilde{u}_{z5/4}' \frac{\partial \tilde{u}_{y1/2}'}{\partial \nu'} + \rho_0' \tilde{u}_{y1/2}' \frac{\partial \tilde{u}_{y_1}'}{\partial y} +$$

$$+ \rho_0' \tilde{u}_{z3/4}' \frac{\partial \tilde{u}_{y_1}'}{\partial \nu'} + \rho_{1/2}'\left(\tilde{u}_{y1/2}' \frac{\partial \tilde{u}_{y1/2}'}{\partial y} + \tilde{u}_{z3/4}' \frac{\partial \tilde{u}_{y1/2}'}{\partial \nu'}\right) =$$

$$= \frac{\partial}{\partial \nu'} \mu_{\nu_0}' \frac{\partial \tilde{u}_{y_1}'}{\partial \nu'} + \frac{\partial}{\partial \nu'} \mu_{\nu_{1/2}}' \frac{\partial \tilde{u}_{y1/2}'}{\partial \nu'}.$$

It is to be noted that both sets are necessary for matching to the first set of equations for the outer layer (core). The sets are solved sequentially. Higher order equations will not be discussed. A similar procedure can be used for the electrode boundary layer.

Next, attention is given to the turning of a cross-flow at a corner. The flow deflection is accomplished by large pressure gradients; it is essentially nonmagnetic. If equations are written in terms of inner variables, $\nu' = \alpha^{-1/4}\nu$ and $\eta' = \alpha^{-1/4}\eta$ with $u_x \equiv \tilde{\tilde{u}}_x'$, $u_y \equiv \mp(\tilde{\tilde{u}}_y' - \alpha f' \tilde{\tilde{u}}_x')$, $u_z \equiv \mp(\tilde{\tilde{u}}_z' - \alpha\beta f' \tilde{\tilde{u}}_x')$; using the following expansions:

$$\tilde{\tilde{u}}_x' = \tilde{\tilde{u}}_{x0}' + \alpha^{1/2}\tilde{\tilde{u}}_{x1/2}' + \cdots$$

$$\tilde{\tilde{u}}_y' = \alpha^{1/2}\tilde{\tilde{u}}_{y1/2}' + \alpha\tilde{\tilde{u}}_{y1}' + \cdots$$

$$\tilde{\tilde{u}}_z' = \alpha^{1/2}\tilde{\tilde{u}}_{z1/2}' + \alpha\tilde{\tilde{u}}_{z1}' + \cdots$$

$$p' = p_0(x) + \alpha p_1' + \alpha^{3/2} p_{3/2}' + \cdots$$

$$h' = h_0' + \alpha^{1/2} h_{1/2}' + \cdots$$

$$\rho' = \rho_0' + \alpha^{1/2}\rho_{1/2}' + \cdots$$

there is obtained the following lowest order set of equations:

$$\frac{\partial}{\partial\eta'}\rho_0'\tilde{\tilde{u}}_{y1/2}' + \frac{\partial}{\partial\nu'}\rho_0'\tilde{\tilde{u}}_{z1/2}' = 0,$$

$$\rho_0'\tilde{\tilde{u}}_{y1/2}'\frac{\partial}{\partial\eta'}\tilde{\tilde{u}}_{y1/2}' + \rho_0'\tilde{\tilde{u}}_{z1/2}'\frac{\partial}{\partial\nu'}\tilde{\tilde{u}}_{y1/2}' + \frac{\partial p_1'}{\partial\eta'} = 0,$$

$$\rho_0'\tilde{\tilde{u}}_{y1/2}'\frac{\partial}{\partial\eta'}\tilde{\tilde{u}}_{z1/2}' + \rho_0'\tilde{\tilde{u}}_{z1/2}'\frac{\partial}{\partial\nu'}\tilde{\tilde{u}}_{z1/2}' + \frac{\partial p_1'}{\partial\nu'} = 0,$$

$$\left(\tilde{\tilde{u}}_{y1/2}'\frac{\partial}{\partial\eta'} + \tilde{\tilde{u}}_{z1/2}'\frac{\partial}{\partial\nu'}\right)\tilde{\tilde{u}}_{x0}' = \left(\tilde{\tilde{u}}_{y1/2}'\frac{\partial}{\partial\eta'} + \tilde{\tilde{u}}_{z1/2}'\frac{\partial}{\partial\nu'}\right)h_0' = 0,$$

$$p_o(x) = p_{oc} = \rho_o' T(h_o').$$

These equations are inviscid. Since the entrance flow to the corner has a boundary layer profile ($\tilde{u}_x' = 0$ @ $v' = 0$), it is obvious that separation occurs. This, of course, is not unexpected. The above equations can be valid only far away from the resulting separation streamline and circulation region. A solution to this problem does not seem to be feasible; no further examination of boundary layer regions will be carried out.

Formulation of Proper Entrance Conditions

The statement of the problem is now completed with the prescription of permissible entrance conditions. The entrance is taken at $X = 0$; this point is sufficiently upstream of the electrodes and pole pieces of the magnet so that the fields are small. Thus, it is assumed that the zeroth order flow is nearly nonmagnetic near the entrance. All dependent variables are assumed analytic in X and a Taylor series in X for each variable is used. A calorically perfect gas will be considered. The fluid equations in stream coordinates are:

$$\rho_o u_{x_o} \frac{\partial u_{x_o}}{\partial x} + \frac{dp_o}{dx} = 0$$

$$\rho_o \frac{\partial h_o}{\partial x} = \frac{dp_o}{dx}$$

$$p_o(x) = \frac{\gamma - 1}{\gamma} \rho_o h_o$$

The solution is:

$$h_o + \tfrac{1}{2} u_{x_o}^2 = \mathcal{H}(\xi_o, \zeta_o) = h_o(0) + \tfrac{1}{2}(u_{x_o}(0))^2,$$

$$u_{x_o} = u_{x_o}(0) \left\{ 1 + 2 \frac{h_o(0)}{(u_{x_o}(0))^2} \left[1 - \left(\frac{p_o}{p_o(0)} \right)^{\frac{\gamma-1}{\gamma}} \right] \right\}^{1/2},$$

$$h_o = h_o(0) \left(\frac{p_o}{p_o(0)} \right)^{\frac{\gamma-1}{\gamma}},$$

$$\rho_o = \rho_o(0) \left(\frac{p_o}{p_o(0)} \right)^{1/\gamma}.$$

Let $\mathcal{P} \equiv p_o(0)$, $\mathcal{M}(\xi_o, \zeta_o) \equiv M_o(0) = \dfrac{u_{x_o}(0)}{\sqrt{(\gamma-1) h_o(0)}}$.

The functions $\mathcal{P}$, $\mathcal{H}$, and $\mathcal{M}$ are known. The Mach number is given by:

$$M_o^2 = \mathcal{M}^2 \left(\frac{p_o}{\mathcal{P}} \right)^{\frac{1-\gamma}{\gamma}} + \frac{2}{\gamma-1} \left[\left(\frac{p_o}{\mathcal{P}} \right)^{\frac{1-\gamma}{\gamma}} - 1 \right].$$

$J_{ss'}$ is given by: $\dfrac{\partial(\xi_o, \zeta_o)}{\partial(y, z)} = \rho_o u_{x_o} R_o = \dfrac{1}{4\beta} \dfrac{\rho_o u_{x_o}}{\rho_o(0) u_{x_o}(0)}$

or $$J_{ss'} = \frac{1}{4\beta} \left(\frac{p_o}{\mathcal{P}} \right)^{1/\gamma} \left\{ 1 + \frac{2}{(\gamma-1)\mathcal{M}^2} \left[1 - \left(\frac{p_o}{\mathcal{P}} \right)^{\frac{\gamma-1}{\gamma}} \right] \right\}^{1/2}.$$

$J_{ss'}$ is also given by: $(J_{ss'})^{-1} = \dfrac{\partial(y, z)}{\partial(\xi_o, \zeta_o)}$

where

$$y = (2\zeta_o - 1) f(x) + X F_{1y}(\xi_o, \zeta_o) + \frac{X^2}{2!} F_{2y} + \cdots,$$

$$z = -\beta(2\xi_o + 1) f(x) + X F_{1z}(\xi_o, \zeta_o) + \frac{X^2}{2!} F_{2z} + \cdots,$$

$F_{iy} = 0$ @ $\xi_0 = 0, 1$; $F_{iz} = 0$ @ $\xi_0 = 0, -1$;

$f(x) = 1 + a_1 x + \frac{a_2}{2!} x^2 + \cdots$.

The pressure is expanded in a Taylor series:

$$\frac{p_0}{\rho} = 1 + b_1 x + \frac{b_2}{2!} x^2 + \cdots .$$

The transverse entrance velocities satisfy the relation:

$$\frac{\vec{u}_{T_1}(0)}{u_{x_0}(0)} = \vec{F}_{1T} - a_1 \begin{pmatrix} 1 - 2\xi_0 \\ \beta(1+2\xi_0) \end{pmatrix} .$$

Equating like powers of x in the two expressions for J_{ss1}:

$$4\beta \frac{b_1}{\gamma} \frac{1-\eta^2}{\eta^2} = 2\left(\beta \frac{\partial F_{1y}}{\partial \xi_0} - \frac{\partial F_{1z}}{\partial \xi_0}\right) + 8\beta a_1,$$

$$4\beta \frac{b_2}{\gamma} \frac{1-\eta^2}{\eta^2} + 4\beta \left(\frac{b_1}{\gamma}\right)^2 \left[3 \frac{1-\eta^2}{\eta^4} + 1 + \gamma\right] = 2 \frac{\partial (F_{1y}, F_{1z})}{\partial (\xi_0, \xi_0)} +$$

$$+ 4a_1 \left(\beta \frac{\partial F_{1y}}{\partial \xi_0} - \frac{\partial F_{1z}}{\partial \xi_0}\right) + 2\left(\beta \frac{\partial F_{2y}}{\partial \xi_0} - \frac{\partial F_{2z}}{\partial \xi_0}\right) + 8\beta (a_1^2 + a_2),$$

etc.

The first equation reduces to: $\frac{\partial F_{1y}}{\partial \xi_0} - \frac{1}{\beta} \frac{\partial F_{1z}}{\partial \xi_0} = 2 \frac{b_1}{\gamma} \frac{1-\eta^2}{\eta^2} - 4a_1$.

A continuous solution requires $2\gamma a_1 = b_1 \left[\int_0^1 \int_{-1}^0 \frac{d\xi_0 \, d\xi_0}{\eta^2} - 1\right]$;

this corresponds to the relation: $A(x) \equiv 4\beta f^2 = \iint dy \, dz =$

$$= \iint \frac{d\xi_0 \, d\xi_0}{J_{ss1}} = \frac{1}{p_0} \int_0^1 \int_{-1}^0 \frac{T(h_0)}{R_0 u_{x_0}} d\xi_0 \, d\xi_0 .$$

The pressure and channel area are related functions. $\vec{F}_{1T}$ is given by the potential $\mathcal{L}$:

$$F_{1y} = \frac{1}{\beta}\frac{\partial \mathcal{L}}{\partial \bar{\xi}_0} + \frac{2b_1}{\gamma}\int_0^{\bar{\xi}_0} \frac{d\bar{\xi}_0}{\eta^2(\bar{\xi}_0,\bar{\xi}_0)} - (4a_1 + 2\frac{b_1}{\gamma})\bar{\xi}_0,$$

$$F_{1z} = \frac{\partial \mathcal{L}}{\partial \bar{\xi}_0},$$

where $\mathcal{L}$ is arbitrary except that $\mathcal{L} = 0$ @ $\bar{\xi}_0 = 0, -1$, $\bar{\xi}_0 = 0$;

$$\mathcal{L}|_{\bar{\xi}_0=1} = \frac{2\beta}{\gamma} b_1 \left[\bar{\xi}_0(1 + 2\gamma\frac{a_1}{b_1}) + \int_{\bar{\xi}_0}^{0}\int_0^1 \frac{d\bar{\xi}_0 d\bar{\xi}_0}{\eta^2}\right].$$

The main conclusion to be drawn is that the transverse velocities at the entrance cannot be specified; the potential $\mathcal{L}$ must be specified instead. In considering the next terms in the series, a constraint given by the transverse momentum equations must be obeyed:

$$\nabla_T \times (\rho \vec{u}\cdot\nabla_\alpha \vec{u}_T) = 0.$$

Combining this constraint with the equation of second order terms of J_{ss}; there is obtained an elliptic partial differential equation for a potential related to $\vec{F}_{2T}$; it can be thought of as a 'streamline curvature potential'. Again, a continuous solution (equivalent to the requirement that no singularities or sources exist in the region) gives a relation between a_2 and b_2 – relating pressure change to area change.

II. NONEQUILIBRIUM FLOWS

Discussion of the Problem

In this section, flows with elevated electron temperatures are examined. Inlet Mach numbers cannot be expected to be very large considering the minimum temperature necessary for operation of a channel; only large power facilities could produce flows with $M^2 = O(10)$. As an example, if $H_o = 0.5m$, $p^+ = 1$ atm, $T^+ = 2000^\circ K$, and $M = 2$, the power input is of $O(10^5$ kw). Since large conductivities are possible, the interaction length for the supersonic section of such a channel would tend to be short and the methods used in this study would probably not apply. Slightly supersonic entrance conditions will invariably lead to a shock and subsonic flow thereafter; the larger the local interaction parameter or the smaller the inlet Mach number, the sooner this will occur. The tendency to these conditions being mutually exclusive, the length of the slightly supersonic section of the channel could be expected to be relatively short. Thus, it is not unrealistic to consider totally subsonic flow (for up to moderately large power outputs); this is done here. This assumption certainly produces analytical simplification, and yet effects of radiation and a large Hall parameter can be studied. As pointed out in Appendix A, a limitation imposed by ion slip means attention can be restricted to values of $\overline{\omega\tau}$ of $O(10)$ or less.

While radiation plays a negligible role in equilibrium flows at low electron temperatures, it is important in the examination of nonequilibrium flows[18, 21]. The model energy equation must be altered to include the radiation loss as a negative source term in its right

hand side. An electron energy equation (which also involves the radiation loss) must be used to calculate T_e^+ ; it may also be necessary to include an ion energy equation in order to specify T_i^+ (see Appendix A).

Ohm's Law

The zeroth order expressions from Ohm's law can be written as follows:

$$j_{x_0} = \frac{\sigma_0}{1+(\omega\tau_0)^2}\left[E_{x_0}(x) + \omega\tau_0\,(u_{x_0}B_{z_0} - E_{y_0})\right],$$

$$j_{y_0} = \frac{\sigma_0}{1+(\omega\tau_0)^2}\left[E_{y_0} - u_{x_0}B_{z_0} + \omega\tau_0\,E_{x_0}(x)\right].$$

The condition $|j_{x_0}| \leq O(|j_{y_0}|)$ implies $|E_{x_0}| \geq O(1)$. Take the limit $\omega\tau_0 \to \infty$; then $j_{y_0} \to \frac{\sigma_0}{\omega\tau_0}E_{x_0}$ where $\frac{\sigma_0}{\omega\tau_0} = \frac{q_0}{B_{z_0}}$ and $j_{y_0} = \frac{\partial b_{x_0}}{\partial \bar{z}}$. Allowing for arbitrary b_{x_0} and integrating:

$$b_{x_0} \longrightarrow \frac{E_{x_0}}{B_{z_0}}\int_{-\beta f}^{\bar{z}} q_0\, d\bar{z} + C_1(x,y)$$

Boundary conditions on j_{z_0} yield:

$$C_1 = 0, \quad \frac{E_{x_0}}{B_{z_0}}\int_{-\beta f}^{\beta f}\frac{\partial q_0}{\partial y}\,dz \longrightarrow 0 .$$

If it is required that $j_{z_0} = 0$, then $\frac{E_{x_0}}{B_{z_0}}\frac{\partial q_0}{\partial y} \to 0$, that is, the electron number density and electron temperature are required to be nearly uniform, or the axial electric field may not be large, or both. It is therefore concluded that inhomogeneities in the transverse direction do not permit buildup of large axial Hall fields. It is also

impossible to avoid axial Hall currents. Not only is it practically difficult to produce large Hall parameters (greater than $2, 3$), it is not especially desirable. If the Hall parameter is not too large, and if the electron temperature is fairly uniform, the magnitude of the Hall current can be kept to within reasonable bounds. Joule dissipation and radiative losses tend to make the temperature uniform; upon the effectiveness of these processes depends the value of the Hall parameter that can be achieved, keeping jx_0 small. This is one of the more important effects of transverse variations in the fluid properties.

Radiative Transfer*

In this section, an approximate method for the solution of the equation of radiative transfer is discussed. The following notations are employed:

I_ν - specific radiation intensity, the energy flux per unit area per unit time per unit frequency per unit solid angle,

$\vec{l}$ - vector of the direction cosines (referring to the above),

ν - frequency,

Ω - solid angle,

$\vec{q}_R$ - radiant energy flux vector,

j_ν - source function (per unit mass),

k_ν - a form of the absorption coefficient, the absorption cross-section per unit mass,

α_ν - another form of the same, the effective cross-section per unit volume,

* All quantities in this section are dimensional.

τ_ν – optical depth,

B_ν – Planck function,

σ_{SB} – Stefan-Boltzmann constant.

Consider radiation traveling along a path whose differential length is dr, then if $r=0$ is the source point, the optical depth at a point r is given by $\tau_\nu(r) = \int_0^r \alpha_\nu \, dr$. A large optical depth at point r implies most of the radiation flux has been absorbed, and conversely. These are the optically thick and thin limits, respectively; for these, the transport equation can be solved and the energy loss calculated without reference to the particular geometry of the situation. On the other hand, if $\tau_\nu = O(1)$, the geometry plays an important role in the solution. The solutions in the limit cases are given by Chapter XI of reference 22.

The equation of transfer is $\vec{\ell} \cdot \nabla I_\nu = \rho(j_\nu - k_{\nu_e} I_\nu)$. The left hand side is the convective derivative; the right hand side consists of source and sink terms. The effective absorption coefficient, $k_{\nu_e} \equiv k_\nu \left(1 - \exp\left(-\frac{h\nu}{kT_e}\right)\right)$; the added factor is a correction due to induced emission. It is assumed that the distribution of quantum states is given by the Boltzmann equilibrium distribution (Appendix A); hence the source function is given by Kirchhoff's law. Let $\alpha_\nu = \rho k_{\nu_e}$; then $\vec{\ell} \cdot \nabla I_\nu = \alpha_\nu (B_\nu - I_\nu)$.

The radiation flux vector is $\vec{q}_R = \int_0^\infty \int_0^{4\pi} \vec{\ell} \, I_\nu \, d\Omega \, d\nu$. The radiation loss, $Q_R = \nabla \cdot \vec{q}_R = \int_0^\infty \int_0^{4\pi} \alpha_\nu (B_\nu - I_\nu) \, d\Omega \, d\nu$. For the frequency range where the gas is thin, $I_\nu << B_\nu$ and $Q_R \doteq 4\pi \int_\nu \alpha_\nu B_\nu \, d\nu = 4\alpha_p \sigma_{SB} T_e^4$ where α_p is the Planck

mean absorption coefficient: $\alpha_p = \int_\nu \alpha_\nu B_\nu d\nu / \int_0^\infty B_\nu d\nu =$

$$= \frac{15}{\pi^4} \int_\nu \alpha_\nu \left(\frac{h\nu}{kTe}\right)^3 \left[\exp\left(\frac{h\nu}{kTe}\right) - 1\right]^{-1} d\left(\frac{h\nu}{kTe}\right).$$

For the thick case, $\vec{q}_R \doteq -\frac{16}{3} \frac{\sigma_{SB}}{\alpha_R} Te^3 \nabla Te$ where α_R is the Rosseland mean absorption coefficient:

$$\alpha_R^{-1} = \int_\nu \frac{1}{\alpha_\nu} \frac{dB_\nu}{dTe} d\nu \Big/ \int_0^\infty \frac{dB_\nu}{dTe} d\nu =$$

$$= \frac{15}{4\pi^4} \int_\nu \frac{1}{\alpha_\nu} \left(\frac{h\nu}{kTe}\right)^4 \left[\exp\left(\frac{h\nu}{kTe}\right)\right] \left[\exp\left(\frac{h\nu}{kTe}\right) - 1\right]^{-2} d\left(\frac{h\nu}{kTe}\right).$$

The approximation to be employed here is to assume

$$Q_R = 4\alpha_p \sigma_{SB} Te^4 - \frac{16}{3} \sigma_{SB} \nabla \cdot \frac{Te^3}{\alpha_R} \nabla Te,$$

a sum of terms corresponding to the two limit cases. There remains the task of deciding what ranges of frequency are to be used in defining α_p and α_R ; this provides an opportunity to include geometric effects in the above simplified model. It is first to be noted that α_p is linear in α_ν and that the entire radiation continuum is thin; thus $\alpha_p \equiv \alpha_{pc} + \alpha_{p\ell}$ where $\alpha_{pc} = \int_0^\infty \alpha_{\nu c} B_\nu d\nu / \int_0^\infty B_\nu d\nu$, $\alpha_{\nu c}$

is the continuum absorption coefficient, and $\alpha_{p\ell}$ refers to line radiation. Nearly all of the line radiation is contained in the resonance lines; only these are considered. The core of the resonance lines is quite thick; only in the very far wings do the lines become thin (this is true except at the very edge of the gas near the walls). Since the effect of Doppler broadening decays rapidly away from the line center, it is important mainly in the line core, while the wings are governed by the Lorentz (dispersion) profile. The line profile is

separated into two parts: the inner or core part, and the outer or wing part; the division defined by use of cut-off frequencies ν_c such that $\alpha_\nu(\nu_c) H_c = 1$ for some characteristic dimension H_c, α_ν having the dispersion form. The inner part is used to calculate α_R, the outer for $\alpha_{p\ell}$. The length H_c is defined as the reciprocal of the average reciprocal distances from the point in question to the walls (entrance and exit taken to be at infinity):*

$$H_c^{-1} = \frac{1}{6}\left[\frac{1}{H_0\frac{f}{2}-y} + \frac{1}{H_0\frac{f}{2}+y} + \frac{1}{W_0\frac{f}{2}-z} + \frac{1}{W_0\frac{f}{2}+z}\right].$$

It is sufficient to consider H_c as given on a streamline by letting

$$\vec{C}_T = 0: \quad H_c = 6\beta H_0 f(x)\left[\frac{\beta}{\xi_0(1-\xi_0)} - \frac{1}{\xi_0(1+\xi_0)}\right]^{-1}.$$

This is nearly true close to the walls where H_c varies strongly with position; away from the walls H_c is only a weak function of position. Consider the portion of the line profile defined by the frequency ranges such that $0.1 \le \alpha_\nu H_c \le 10.0$; this portion occupies a fraction of $O\left(\frac{w_\nu}{|\nu_0-\nu_c|}\right)$ (see Appendix C) of the total. Almost all of the radiant energy lies in the regimes of the two limit cases. The approximation can only be considered valid if the result, Q_R, is insensitive to the value of H_c; this suggests that this is so. As the walls are approached, the line becomes thin closer to the

---

* Close to the walls ($\zeta \to 0, 1$; $\xi \to 0, -1$), this definition must be modified to account for the boundary layer. It must also be modified in the zeroth order problem when a step in the induction occurs. See Appendix C. Note that $H_c \ge 1/(\alpha_\nu)_{max}$.

core*; the geometrical effect is qualitatively correct. The quantity α_R^{-1} is formed by summing integrals over line cores. Formulas for the absorption coefficients are given in Appendix B. The emissivity and reflectivity of the walls are neglected. The system of equations for nonequilibrium flows is now complete.

---

* The Doppler core is thick through most of the boundary layer up to a distance of $O(10^{-6}$ cm) from the wall.

III. FORMULATION OF A PROBLEM IN TWO INDEPENDENT VARIABLES, RESULTS AND CONCLUSIONS

Zeroth Order Core Flow in Two Independent Variables

For purposes of numerical computation, a simplified problem is taken with

$$\frac{\partial}{\partial z} = \frac{\partial}{\partial \bar{\xi}_0} = 0 \qquad \text{(except for } b_{x_0}\text{)},$$

$$b_{x_0} = z\, J(x),$$

$$R_0 = R_0(\bar{\xi}_0),$$

$$y = (z\,\bar{\xi}_0 - 1) f(x) + C_{y_0}(x, \bar{\xi}_0),$$

$$z = -\beta (z\,\bar{\xi}_0 + 1) f(x).$$

For this problem, the constraint $\nabla_T \times \vec{F}_{T_0} = 0$ is automatically satisfied and no potential $\mathcal{L}$ is to be specified. For the general problem, this constraint and the expression relating the Jacobian of the stream transformation to the fluid properties are used to calculate the transformation; the latter with the above conditions yields:

$$C_{y_0} = z\, f(x) \int_0^{\bar{\xi}_0} \left[\frac{T(h_0)}{A R_0 p_0 u_{x_0}} - 1 \right] d\bar{\xi}_0$$

and

$$p_0(x) = \frac{1}{A(x)} \int_0^1 \frac{T(h_0)}{R_0 u_{x_0}}\, d\bar{\xi}_0.$$

The Joule dissipation $j_0^2/\sigma_0 = \left[\frac{1 + (\omega\tau_0)^2}{\sigma_0} \right] J^2 + \sigma_0 E_{x_0}^2 - 2\,\omega\tau_0\, J E_{x_0}.$

The functions J and E_{x_o} need to be fixed. An average load parameter, given as a function of the axial distance, is used to define the transverse current:

$$J(x) = -\mathcal{B}_{z_o}(x)\,[1-K(x)] \int_0^1 \sigma_o\, u_{x_o}\, d\xi_o .$$

The axial Hall current is to be kept as small as possible; by requiring its average values to be zero, an expression for the axial electric field is found:

$$E_{x_o}(x) = -\mathcal{B}_{z_o}(x)\,[1-K(x)] \int_0^1 \omega\tau_o\, u_{x_o}\, d\xi_o .$$

The specific numerical techniques used on this problem are discussed in Appendix C. This problem is an inverse problem in the sense that the transverse current is specified and the voltages on the electrodes result from the calculation, rather than vice versa.

Results*

1. Accuracy of calculations. A one-dimensional flow whose analytical solution was known was used to check the accuracy of the integration and matrix inversion subroutines (Appendix C). The local truncation error was held to within 10^{-7} ; results had an uncertainty of $\leq 10^{-8}$ near the exit point.

The approximation of a finite number (N) of streamlines (Appendix C) was checked by two calculations. An equilibrium calculation for $N=16$, $\mathcal{B}_z = 0.6\ web/m^2$ and $K=0.6$ for $0.0\,m \leq X \leq 1.04\,m$,

---

* All numerical calculations were performed assuming an argon parent gas with potassium seed. The function $f(x)$ was taken as $1.0 + 5X$. The subscript 'o' is omitted, and the subscript 'in' refers to entrance conditions.

$\beta = 1.5$, $S = 0.3$, initial pressure $p_{in} = 4.0$ atm , $u_{x_{in}} =$ $= 1.8 + 0.65(1-S)$ $\frac{km}{sec}$, $h_{in} = 7 + 45(1-S)$ km^2/sec^2, and $\gamma_s = 0.01$. The result was used as a standard; another calculation with $N = 10$ was made. The deviation from the standard near the exit was of $O(.01\%)$. Similarly, calculations with $N = 8$ and 10 were made for $B_z = 0.7$ web/m^2, $S = 0.2$, $p_{in} = 3.0$ atm , $u_{x_{in}} = 1 + \sin^2(2\pi S)$ km/sec , $h_{in} = 5.5 + 2\sin(\pi S)$ km^2/sec^2 , with the other parameters being as above. Note that for this second comparison, the variation of the entrance conditions with S is more pronounced. The deviations were found to be of $O(1\%)$ (the largest being 4.6%). From these calculations it was concluded that use of the value $N = 10$ is sufficient and should result in an accuracy of $\leq O(.1\%)$.

Lastly, the effects of changing the parameters H_c, τ_{b1} , and τ_B (Appendix C) are given in Table 1, page 90. It is seen that the results of the calculations do not depend strongly on these parameters; hence, their use is acceptable. The value of τ_{b1} is the most critical and affects mostly the end streamlines $(S = 0, 1)$.

2. Typical results. Some results of numerical calculation are given on pages 91 through 105. The units for the fluid and electromagnetic properties are: velocity = km/sec, enthalpy = km^2/sec^2, pressure = atm, temperature = 10^3 °K, electrical conductivity = mho/cm, induction = web/m^2, current density = $abamp/cm^2$, electric field = kv/m, and potential drops = kv.

For Hall parameters of order unity, for both equilibrium and nonequilibrium flows, the electron temperature, Hall parameter, and conductivity tend to be uniform. One example of this is given by an

equilibrium calculation for $B_z = 0.8$ web/m and $K = 0.6$ ($0.02\ m \leq X \leq 1.02\ m$), $\beta = 1.5$, $S = 0.2$, $\gamma_s = 0.01$, $p_{in} = 3.0$ atm, $u_{x,in} = 1.5[1+1.5S(1-S)]$ km/sec, and $h_{in} = 5[1+2S(1-S)]$ km^2/sec^2. At $X = 0.04$ m, h ranges from 5.54 to 7.64, $\omega\tau = 3.83$ to 1.16, and $\sigma = 0.45$ to 2.82*. At $X = 0.72$ m, the local interaction parameter per unit length integrated to the point in question = 0.46, h ranges from 6.60 to 7.42, $\omega\tau = 2.09$ to 1.33, and $\sigma = 1.54$ to 2.80; the ratio of enthalpies dropped from 1.38 to 1.12, the Hall parameter ratio dropped from 3.30 to 1.57 and the conductivity ratio 6.27 to 1.82. Another equilibrium calculation is given by Graphs 1 to 3, pages 91 to 94; the same ratios drop 1.30 to 1.17, 2.92 to 1.77, and 4.42 to 2.21, respectively. If elevated electron temperatures are considered, then this effect can be much more pronounced, as Tables 2 to 12 show. In the case of a Hall parameter of $\frac{1}{2}$ or less, however, the ratios tend to remain constant. In one test calculation, the initial conditions were uniform except for a 33% 'spike' in h at one streamline; at the exit the ratio was 32%, the integrated interaction parameter was 0.63.

Finally, examine Tables 2 to 12, pages 95 to 105.** It is seen immediately that the ratio of maximum axial current to transverse current can actually be reduced by increasing the Hall parameter; the radiative transport acts to 'smooth out' profiles. Tables 5 to 7 and Table 9 show that there is an optimum value of the Hall parameter that gives this ratio it lowest value. In general, this optimum value is strongly dependent on other properties such as the load parameter, Mach number, and pressure, as is the value of the ratio obtained. A

* In the units listed above.

** For arbitrary X with certain properties specified.

lower ratio is obtained for the lower value of the load parameter. It is to be noted that the Hall parameter is not linearly related to the magnetic field strength, but rather varies more weakly with the field.

It may appear that a high ratio of axial current at an end streamline to transverse current (Table 7, entry 3, for example) is due to the value of τ_{b1} selected. To check on this, a computation was made for this particular situation with τ_{b1} changed from 2.0 to 6.0; the current ratio changed from 0.62 to 0.45. For such cases, the value of τ_{b1} is important; however, qualitatively the results are correct.

Comparing the entries in Table 10, entry 1 in Table 7 with Table 11, and entry 3 in Table 8 to Table 12, it appears that the current ratio increases as the Mach number decreases. This is not always so: if again the situation pertaining to entry 3, Table 7 is changed by lowering the velocity by a factor of 0.7, the current ratio drops from 0.62 to 0.55 while the maximum value of the Hall parameter increases from 2.06 to 2.46.

The current ratio maximum stayed constant ($\doteq$ 0.26) for the nonequilibrium flow depicted in the graphs; the Mach number varied more weakly than in the equilibrium flow. The voltage drop also remained constant at a value $\Delta\psi$ = .12 kv. within 2%.

Summary and Conclusions

Numerical computations have been carried out for subsonic MFD generator channels with a large length-to-height ratio and fine electrode segmentation. The working gas was taken as potassium

seeded argon. Variable transport properties and radiation effects were considered. It has been shown that transverse variations in fluid properties are very important in Faraday generators. Axial currents in nonequilibrium flows can be kept low if the right value of the Hall parameter can be obtained; this also depends critically on the Mach number and load parameter. Attainment of large Hall parameters and fields cannot be expected. It is better to employ load parameters near 1/2 rather than the use of higher values, say 3/4. On the whole, it seems desirable to avoid Mach numbers much less than one. The inclusion of radiative transfer is necessary in calculations for $\omega\tau = O(1)$.

The desirability of low load parameters and relatively high Mach numbers (high velocities) can be explained simply. The 'smoothing' effect of radiative transport is dependent on the attainment of high electron temperatures; this requires rather large dissipation. If the load parameter is relatively large or the velocity low, the effective electric field and resultant current density are low, yielding low dissipation.

The question of optimum flow conditions in a supersonic section of a generator channel is left open. It seems likely that there exists an optimum value of the Hall parameter as in the subsonic case.

The boundary layer regions in nonequilibrium generators are quite complicated; this is especially true at the electrode walls if they are cold. In general, boundary layer flows do not seem to be amenable to direct solution in cases of interest; perhaps integral

techniques could be used to obtain qualitative results. No attempts were made to make an analysis of these regions.

If one-dimensional analysis were to apply at all, it would have to be for equilibrium flows at a small value of $\omega\tau$. For these flows, the assumption that the velocity and temperature (enthalpy) profiles are similar to the entrance profiles may be better.

REFERENCES

1. Bendor, E., "One-Dimensional Flow in MHD Generators," AIAA J., 3, 1, 167-169 (Jan. 1965).

2. Karkosak, J. J. and Hoffman, M. A., "Electrode Drops and Current Distributions in a MGD Channel" AIAA J., 3, 6, 1198-1200 (June 1965).

3. Leonard, R. L. and Fay, J. A., "Experiments on a Quasi-Steady J×B Accelerator," AIAA J., 3, 1, 115-121 (Jan. 1965).

4. Talaat, M. E., "Nonequilibrium Ionization in Magnetoplasmadynamic Power Generator: Theory and Experiment," AIAA J., 3, 6, 1022-1027 (June 1965).

5. Sutton, G. W. and Robbins, F., "Preliminary Experiments on MHD Channel Flow with Slightly Ionized Gas," Symposium on Electromagnetics and Fluid Dynamics of Gaseous Plasmas, Poly Press of Polytechnic Institute of Brooklyn, 11th Microwave Research Institute Symposium Series, 307-321 (April 1961, pub. 1962).

6. Blackman, V. H., et al., "MHD Power Generator Studies in Rectangular Channels," Engineering Aspects of MHD, 2nd Symposium, Editors: Mannal and Mather, Columbia University Press, 180-210 (March 1961, pub. 1962).

7. Way, S., "Comparison of Theoretical and Experimental Results in an MHD Generator," ibid., 166-179.

8. Harris, L. P. and Moore, G. E., "Some Electrical Measurements on MHD Channels," Engineering Aspects of MHD, 3rd Symposium, Editors: Mather and Sutton, Gordon and Breach Science Publishers, 259-277 (March 1962, pub. 1964).

9. Brogan, T. R., et al., "A Review of Recent MHD Generator Work at the AVCO-Everett Research Laboratory," AVCO AMP 74, March 1962.

10. Louis, J. F., Gal, G., and Blackburn, P. R., "Detailed Theoretical and Experimental Study on a Large MHD Generator," AVCO RR 174, March 1964.

11. Wood, G. P., et al., "Experiments in Steady State Crossed-Field Acceleration of a Plasma," Phys. Fluids, 4, 652-653 (1961).

12. Oates, G. L., et al., "Loss Mechanisms of a Low Temperature Plasma Accelerator," BSRL Report D1-82-0124, July 1961.

13. Robbin, F. A., "Experimental Studies of Non-equilibrium Ionization in an MHD Generator," General Electric TIS Report R62SD13, Feb. 20, 1962.

14. Cole, J. D. and Caseau, P., "Some Problems in MHD Pipe Flow," Part IV, Final Report on the Magnetohydrodynamics of Power Generators, California Institute of Technology, AFOSR PR 64-553, 1965.

15. Hunt, J. R. C. and Stewartson, K., "MHD Flow in Rectangular Ducts, II," J. Fluid Mech., 23, pt. 3, 563-581 (Nov. 1965).

16. McCune, J. E., "Linear Theory of an MHD Oscillator," AVCO RR 198, Dec. 1964.

17. Sutton, G. W. and Witalis, E., "Linearized Analysis of MHD Generator Flow Stability," General Electric TIS Report R64SD5, Jan. 1964.

18. Kerrebrock, J. L., "MHD Generators with Nonequilibrium Ionization," AIAA J., 3, 4, 591-601 (April 1965).

19. Liubimov, G. A., "On the Viscous Boundary Layer on an Electrode in a Medium with Variable Electrical Conductivity," PMM, 28, 5, 845-851 (1964).

20. Hurwitz, H., Jr., Sutton, G. W., and Tamar, S., "Electron Heating in Magnetohydrodynamic Power Generator," ARS J., 32, 1237-1243 (Aug. 1962).

21. Lutz, M., "Radiant Energy Loss from a Cesium-Argon Plasma to an Infinite Plane Parallel Enclosure," AVCO RR 175, Sept. 1963.

22. Vincenti, W. and Kruger, C., Jr., Introduction to Physical Gas Dynamics, John Wiley and Sons, New York, 1965.

23. Herdan, R. and Liley, B. S., "Dynamical Equations and Transport Relationships for a Thermal Plasma," Rev. Mod. Phys., 32, 4, 731-741 (Oct. 1960).

24. Zhdanov, V. M., "Transport Phenomena in a Partly Ionized Gas," PMM, 26, 2, 280-288 (1962).

25. Cann, G. L., "Transport Properties of a Three-Component Non-equilibrium Plasma with Applications to MGD Accelerators," ARS Electric Propulsion Conference, Berkeley, Calif., March 1962, Paper 2396-62.

26. Chapman, S. and Cowling, T. G., The Mathematical Theory of Non-Uniform Gases, Cambridge University Press, 1960.

27. Cann, G. L., "Energy Transfer Processes in a Partially Ionized Gas," GALCIT Hypersonic Research Memo No. 61, June 15, 1961.

28. Russel, G. R., Byron, S., and Bortz, P. I., "Performance and Analysis of a Crossed-Field Accelerator," AIAA Electric Propulsion Conference, Colorado Springs, Colorado, March 1963, Paper 63-005.

29. Griem, H. R., Plasma Spectroscopy, McGraw-Hill Book Co., New York, 1964.

30. Wilson, R., "The Spectroscopy of Non-thermal Plasmas," JQSRT, 2, 477-490 (1962).

31. Byron, S., Bortz, P. I., and Russell, G. R., "Electron-Ion Reaction Rate Theory: Determination of the Properties of Non-Equilibrium Monatomic Plasmas in MHD Generators and Accelerators and in Shock Tubes," Proceedings of 4th Symposium on the Engineering Aspects of MHD, Berkeley, California, April 1963.

32. Burgess, A. and Seaton, M. J., "A General Formula for the Calculation of Atomic Photo-Ionization Cross Sections," Mon. Not. Royal Astron. Soc., 120, 121-151 (1958).

33. Biberman, L. M., Norman, G. E., and Ulyanov, K. N., "On the Calculation of Photoionization Absorption in Atomic Gases," Optics and Spect., 10, 5, 265-269 (May 1961).

34. Pomerantz, J., "The Influence of the Absorption of Radiation in Shock Tube Phenomena," JQSRT, 1, 185-248 (1961).

35. Herzberg, G., Atomic Spectra and Atomic Structure, Dover Publishers, New York, 1944.

36. Menzel, D. H. and Pekeris, C. L., "Absorption Coefficients and Hydrogen Line Intensities," Mon. Not. Royal Astron. Soc., 96, 77-111 (Nov. 1935).

APPENDIX A

Formulation of Model Equations*

The dynamical equations for the components of an ionized gas have been generated from the Boltzmann equations for the components by the 13-moment method[23, 24, 25]. In this section, these equations are developed into a flow model for use in channel flows**.

The following notations are used:

k - Boltzmann's constant

$\vec{w}_j$ - drift velocity of the j^{th} specie

I_s - ionization potential of the seed gas

Q_{elj} - exchange energy gained by the j^{th} specie by elastic collisions

e - electron charge (absolute value)

Q_{inelj} - exchange energy gained by inelastic collisions

Q_R - radiant energy loss of the gas

i_e - internal energy of the electrons

n_j - number density of the j^{th} specie

m_j - molecular mass of the j^{th} specie

subscripts "j, k" - denote a specie

subscript "e" - denotes electrons

subscript "i" - denotes ions

subscript "o" - denotes seed neutrals

subscript "p" - denotes parent gas (neutrals)

---

* All quantities are dimensional.

** It is to be noted that the references cited developed the equations for the components for limiting cases; these have been generalized in a consistent manner to include a more general case.

subscript "a" - denotes all neutrals

By definition:

$$\vec{u}_j \equiv \vec{u} + \vec{w}_j ,$$

$$\rho_a \equiv \rho_o + \rho_p ,$$

$$q_c \equiv e (n_i - n_e) ,$$

$$\vec{j} \equiv e (n_i \vec{w}_i - n_e \vec{w}_e) ,$$

$$\rho_a \vec{w}_a \equiv \rho_o \vec{w}_o + \rho_p \vec{w}_p .$$

Combining the continuity equations for the electrons and ions:

$$\nabla \cdot (\vec{j} + q_c \vec{u}) = 0$$

As shown on page 8, net charge effects are of $O(\frac{\epsilon}{Rm}) \leq O(10^{-6})$, therefore, this equation simplifies to $\nabla \cdot \vec{j} = 0$. This means also $n_i \doteq n_e$. Ohm's law results from combining the momentum equations for the electrons and ions:

$$\vec{j} + \vec{j} \times \vec{\omega_e \tau_o} - \delta_o (\vec{j} \times \vec{\omega_e \tau_o}) \times \vec{\omega_e \tau_o} - \Delta_o \bar{\bar{A}} \cdot \vec{j} = \sigma_o \{ \vec{E} +$$

$$+ \vec{u} \times \vec{B} + \frac{1}{e n_e} \nabla p_e - \alpha_T \frac{k}{e} \bar{\bar{A}} \cdot \nabla T_e + \frac{\delta_o}{(1-\bar{\alpha}) e n_e} [\bar{\alpha} \nabla p - \nabla (p_e + p_i) +$$

$$- \frac{m_e}{k T_e} \frac{\delta_{ea}}{\tau_{ea}} \vec{R}_e] \times \vec{\omega_e \tau_o} \} ,$$

where $\tau_{jk} = \frac{3}{16} \left[\frac{k}{2\pi} \left(\frac{T_j}{m_j} + \frac{T_k}{m_k} \right) \right]^{-1/2} (n_k q_{jk})^{-1}$

is the mean time between collisions of a particle of specie j with particles of specie k , and q_{jk} is a suitably averaged diffusion cross-section,

$$(\tau_o)^{-1} = (\tau_{ea})^{-1} + (\tau_{ei})^{-1} ,$$

$$\vec{\omega_e} = \frac{e}{m_e} \vec{B} ,$$

$\alpha_T \equiv \frac{5}{2} \nu_o \tau_e$ is a form of the thermal diffusion ratio,

$$\bar{\alpha} \equiv \rho_i/\rho ,$$

$$\Delta_0 \equiv \alpha_T \nu_0 \tau_e ,$$

$$\delta_0 \equiv \bar{\varepsilon}(1-\bar{\alpha})^2 \frac{\tau_{ea}}{\tau_0} = 2 \frac{\omega_i \tau_{ia}}{\omega_e \tau_0}$$, twice the ratio of the ion to electron Hall parameters, or the ion slip parameter,

$$(\tau_e)^{-1} = \frac{2}{5} \frac{A_{ee}^*}{\tau_{ee}} + \frac{5}{2}\left[(1 - \tfrac{12}{25} B_{ei}^*)/\tau_{ei} + (1 - \tfrac{12}{25} B_{ea}^*)/\tau_{ea} \right] ,$$

$$\nu_0 = \zeta_{ei}/\tau_{ei} + \zeta_{ea}/\tau_{ea} ,$$

$$\zeta_{jk} \equiv \frac{6}{5} C_{jk}^* - 1 ,$$

$A_{jk}^*, B_{jk}^*, C_{jk}^*$ are cross-section ratios (see references),

$$\bar{\varepsilon} = 2 \frac{n_e}{n_i} \frac{m_e}{m_i} \frac{\tau_{ia}}{\tau_{ea}} ,$$

$$\sigma_0 = \frac{e^2 n_e \tau_0}{m_e} ,$$

For an arbitrary vector $\vec{W}$:

$$\bar{\bar{A}} \cdot \vec{W} \equiv \frac{1}{1+(\omega_e \tau_e)^2}\left[\vec{W} + (\vec{\omega_e \tau_e} \cdot \vec{W})\, \vec{\omega_e \tau_e} + \vec{\omega_e \tau_e} \times \vec{W} \right] ,$$

$$\vec{R_e} = -\lambda_e \bar{\bar{A}} \cdot \vec{D_e} ,$$

$$\lambda_e = \frac{5}{2} \frac{p_e k \tau_e}{m_e} ,$$

$$\vec{D_e} = \nabla T_e - \alpha_T \frac{k T_e}{e \lambda_e} \vec{j} + \frac{2}{5} \frac{e}{k p_e} \bar{\bar{P}}_e \cdot \left(\vec{E} + \vec{u} \times \vec{B} - \frac{m_e}{e} \vec{g} \right) ,$$

$\bar{\bar{P}}_e$ is the electron stress tensor,

and $\vec{g}$ is the acceleration of gravity.

In the above equation, it is assumed $|\zeta_{ia}| << 1$. Even if this were not so, the additional terms that would be present can be neglected if $\bar{\alpha}\, \delta_0 (\omega_e \tau_0)^2 << 1$, which is the case here. The factor Δ_0 results from the second approximation to the diffusion coeffi-

cients; it reduces to Δ_{ei} as $\tau_{ea} \longrightarrow \infty$ (see references 25, 26). It has also been assumed that $T_e \frac{m_e}{m_i} \ll T_j \ll T_e \left(\frac{m_i}{m_e}\right)^{1/2}$. The cross-sectional ratios are:

$$A_{ee}^* = 1 - (2 \ln \Lambda_{ee})^{-1},$$

$$A_{ei}^* = 1 - (2 \ln \Lambda_{ei})^{-1},$$

$$B_{ei}^* = 1, \quad C_{ei}^* = \frac{1}{3}$$

where

$$\Lambda_{jk} = \frac{4\pi \varepsilon_o}{e^2} \lambda_D \mu_{jk} \left[3k \left(\frac{T_j}{m_j} + \frac{T_k}{m_k}\right)\right],$$

$$\mu_{jk} = \frac{m_j m_k}{m_j + m_k}, \qquad \text{the reduces mass,}$$

$$\lambda_D = \left[\frac{\varepsilon_o k T_i}{e^2 n_e (1 + T_i/T_e)}\right]^{1/2}, \text{ the Debye length,}$$

and by linear extrapolation from the tables given in reference 27, if the parent gas is A,

$$C_{ep}^* = 1.7 - 0.025 \, (T_e/10^3 \, ^\circ K),$$

$$B_{ep}^* = 2.083 \left[1 - 5_{ep}^{\,2} (1.4 + 0.075 \, (T_e/10^3 \, ^\circ K))\right].$$

(These values reflect the Ramsauer effect; otherwise the ratios are near unity.) Note that $\overline{\overline{P}}_e = \mathcal{G}(p_e \tau_e \nabla \vec{u} + e n_e \tau_e \vec{w}_e (\vec{E} + \vec{u} \times \vec{B} - \frac{m_e}{e} \vec{g})) + p_e \overline{\overline{I}}$, where $\mathcal{G}$ denotes an operator whose $|\mathcal{G}| = O(1)$,

$$\vec{w}_e = -\frac{1}{e n_e} \vec{j} + (1 - \bar{\alpha}) \vec{V}_i$$

where

$$\vec{V}_i \doteq \frac{\bar{\varepsilon}}{1+\bar{\varepsilon}} \left[\frac{1}{en_e} \vec{j} + \frac{1-\bar{\alpha}}{en_e} \vec{j} \times \omega_e \vec{\tau}_{ea} - S_{ea} \frac{\vec{R}_e}{p_e} \right] +$$

$$+ \frac{2\tau_{ia}}{(1+\bar{\varepsilon})\rho_i} \left[\bar{\alpha} \nabla p - \nabla (p_e + p_i) \right] \quad \text{for } |S_{ia}| \ll 1,$$

$$\vec{w}_i = (1-\bar{\alpha}) \vec{V}_i,$$

and $\vec{w}_p \doteq \vec{w}_a = -\bar{\alpha} \vec{V}_i$.

The equation for the electron energy is: $\frac{d}{dt}(n_e i_e) + n_e i_e \nabla \cdot \vec{u} +$

$$+ \nabla \cdot \vec{q}_e - p_e \vec{w}_e \cdot \vec{F}_e + \bar{\bar{P}}_e : \nabla \vec{u} = Q_{inel_e} - n_e \sum_k n_k \nu_{ek} (T_e - T_k)$$

where $\vec{q}_e = n_e (i_e + kT_e) \vec{w}_e + \vec{R}_e$

is the electron heat flux vector,

$$\vec{F}_e = \vec{g} - \frac{d\vec{u}}{dt} - \frac{e}{m_e} (\vec{E} + \vec{u} \times \vec{B}),$$

$$\nu_{ek} = 3k \frac{m_e}{m_k} (n_k \tau_{ek})^{-1},$$

$$i_e = \frac{3}{2} kT_e + e I_5.$$

Combining the equations for all species gives essentially the fluid equations given on pages 2 and 3. The density, heat flux, pressure, and stress tensor are summed over all components, the temperature averaged with number density weighting factors, and the velocities averaged with mass density weighting factors so that $\sum_k \rho_k \vec{w}_k = 0$. This will be discussed further later.

Next, the order of magnitude of terms in Ohm's law and the electron energy equation are compared in order to simplify these complicated expressions. The following are assumed:

$$q_{ep} \approx 10^{-16} \text{ cm}^2,$$

$$q_{ip} \approx 10^{-15} \text{ cm}^2,$$

$$q_{ei} \approx 10^{-12} \text{ cm}^2,$$

$$\bar{\alpha} \approx \frac{n_e}{n_a} \lesssim O(10^{-3}),$$

$$(\omega_e \tau_o)^2 \lesssim O(10^3),$$

$$\left(\frac{m_e}{m_k}\right)_{k \neq e} \lesssim O(10^{-4}),$$

$$m_i = m_o \approx m_p,$$

$$\frac{n_o + n_i}{n_p} \lesssim O(10^{-2}).$$

The discussion is restricted to use of a monatomic alkali seed gas in an inert parent gas; hence, inelastic energy exchange between electrons and seed neutrals is given by the radiant energy loss and change of electron number density[28]:

$$Q_{inel_e} = -Q_R - (i_e + kT_e)\frac{dn_e}{dt}.$$

Model Equations for Ohm's Law

The Hall parameter $\omega_e \tau_o \approx \omega_e \tau_e = O(\bar{\omega\tau})$. First, consider the magnitude of the third term on the L. H. S. (left hand side) of Ohm's law as compared to the first term, $\vec{j}$. The ratio of the terms $\approx \delta_o \bar{\omega\tau}^2 \approx 2\frac{m_e}{m_i}\frac{\tau_{ia}}{\tau_o}\bar{\omega\tau}^2$. The expression τ_{ia} can be replaced by τ_{ip}, τ_{ea} by τ_{ep}. The ratio $\frac{\tau_{ip}}{\tau_o} \lesssim \left(\frac{T_e}{T}\frac{m_p}{m_e}\right)^{1/2}$ assuming $T \approx T_i \approx T_o \approx T_p$. Therefore, $\delta_o \bar{\omega\tau}^2 \lesssim \bar{\omega\tau}^2\left(\frac{T_e}{T}\frac{m_e}{m_i}\right)^{1/2}$. If $\bar{\omega\tau} \leq O(1)$, then the ratio of the terms is $\lesssim O(10^{-2})$ and the third

term is $\lesssim O(\epsilon)$ and can be neglected. If $\bar{\omega\tau} \gtrsim O(10)$, the term should be kept in the model. For any $\bar{\omega\tau}$, $|\bar{\bar{A}}| \leq O(1)$. The ratio of the fourth term on the L. H. S. to the first term $\approx \Delta_o$. But $\Delta_o \approx (\nu_o \tau_o)^2$ and $\zeta_{ei} = -\frac{3}{5}$, $\zeta_{ep} \lesssim 1$. Substituting: $\nu_o \approx \frac{\zeta_{ep} - 10^4 \bar{\alpha}}{\tau_{ep}}$, $\frac{\tau_o}{\tau_{ep}} \approx (1+10^4\bar{\alpha})^{-1}$, or $\Delta_o \approx (\zeta_{ep} - 10^4\bar{\alpha})^2 (1+10^4\bar{\alpha})^{-2}$, $\Delta_o \leq O(1)$. In many circumstances, Δ_o may be small, but the fourth term and hence the entire L. H. S. of Ohm's law is kept. The R. H. S. (right hand side) may be simplified, however. Note that $p_i = n_i k T_i = n_e k T_i \lesssim p_e$ and $|\bar{\alpha} \nabla p| \approx \frac{n_e}{n_a} |\nabla (n_a k T_a)| \lesssim |\nabla p_e|$. It will be shown that the largest terms in $\vec{D}_e$ are $\approx \frac{k T_e}{e \lambda_e} \vec{j}$ if ∇T_e is not great. Thus, $|\vec{R}_e| \lesssim \frac{k T_e}{e} |\vec{j}|$ and $\frac{m_e}{k T_e} \left| \frac{\zeta_{ea}}{\tau_{ea}} \vec{R}_e \right| \lesssim \frac{m_e}{e} \left| \frac{\zeta_{ea}}{\tau_{ea}} \vec{j} \right|$. Also note $|\vec{j}| \lesssim \sigma_o u B$. Compare the pressure terms in the last expression on the R. H. S. to the $\frac{1}{e n_e} \nabla p_e$ term; the ratio is $\lesssim \delta_o \bar{\omega\tau}$. For $\bar{\omega\tau} \leq O(1)$ these pressure terms can be neglected as being $\leq O(\epsilon)$; in any case, under the assumptions used, the ratio $< O(1)$. Compare the term involving $\vec{R}_e$ in the last expression with $\vec{u} \times \vec{B}$; the ratio is $\lesssim \delta_o \bar{\omega\tau} \zeta_{ea} \frac{\tau_o}{\tau_{ea}} \lesssim \delta_o \bar{\omega\tau}$ and the same conclusion can be drawn. The expression $|-\alpha_T \frac{k}{e} \bar{\bar{A}} \cdot \nabla T_e| \lesssim \frac{k}{e} |\nabla T_e|$. In turn, $\frac{k}{e} |\nabla T_e| \approx \frac{1}{e n_e} |\nabla p_e|$. Since the load parameter is near unity, $|\vec{E}| \approx |\vec{u} \times \vec{B}|$. The remaining comparison is that of $\frac{1}{e n_e} |\nabla p_e|$ to $|\vec{u} \times \vec{B}|$ or $\frac{k}{e} |\nabla T_e|$ to $|\vec{u} \times \vec{B}|$. Assuming the scales of the electron and ordinary temperature gradients are nearly the same, $\frac{k}{e} |\nabla T_e| \approx \frac{1}{e n_a} \frac{T_e}{T} |\nabla p|$ and $|\nabla p| \approx \sigma_o u B^2$. The ratio of these terms is thus $\bar{\alpha}\, \bar{\omega\tau}\, T_e/T$ as $\sigma_o B = e n_e \omega_e \tau_o$. This ratio at most is $O(10^{-1})$; under most conditions it will be $\leq O(10^{-2})$.

Now the model equation can be formulated. For an equilibrium situation, $\overline{\omega\tau} \leq O(1)$, an adequate model good to at least $O(\epsilon)$ is:

$$\vec{j} + \vec{j} \times \vec{\omega_e \tau_o} - \Delta_o \bar{\bar{A}} \cdot \vec{j} = \sigma_o (\vec{E} + \vec{u} \times \vec{B}).$$

Since $\vec{j}$ is perpendicular to $\vec{B}$ to $O(\alpha)$, and since a simple model is desirable, the second term in the operator $\bar{\bar{A}}$ will be neglected. The final result is:

$$\vec{j} + \vec{j} \times \vec{\omega\tau} = \sigma (\vec{E} + \vec{u} \times \vec{B}),$$

where $\vec{\omega} \equiv \vec{\omega_e}$,

$$\tau = \tau_o \left[1 + (\omega_e \tau_e)^2 + \frac{\tau_e}{\tau_o} \Delta_o\right] \left[1 + (\omega_e \tau_e)^2 - \Delta_o\right]^{-1},$$

and $$\sigma = \sigma_o \left[1 + (\omega_e \tau_e)^2 - \Delta_o\right]^{-1} \left[1 + (\omega_e \tau_e)^2\right].$$

For $\overline{\omega\tau} > O(1)$, the basic equation simplifies to:

$$\vec{j} + \vec{j} \times \vec{\omega_e \tau_o} - \delta_o (\vec{j} \times \vec{\omega_e \tau_o}) \times \vec{\omega_e \tau_o} - \Delta_o \bar{\bar{A}} \cdot \vec{j} =$$

$$= \sigma_o (\vec{E} + \vec{u} \times \vec{B}) - \delta_1 (\bar{\bar{A}} \cdot \vec{j}) \times \vec{\omega_e \tau_o},$$

where $\delta_1 = 2 \alpha_T \delta_{ea} \frac{m_e}{m_i} \frac{\tau_{ia}}{\tau_{ea}} < O\left(\sqrt{\frac{m_e}{m_i}}\right)$.

Comparing the L. H. S. of the above equation to the R. H. S., the term involving δ_1 can be neglected. It is to be noted that if large gradients of the electron temperature exist, say, near the electrode surface, a more complete model should be employed. The L. H. S. can be written:

$$\vec{j}\left[1+\delta_0(\omega_e\tau_0)^2-\frac{\Delta_0}{1+(\omega_e\tau_e)^2}\right]+\vec{j}\times\vec{\omega_e\tau_0}\left[1+\frac{\tau_e}{\tau_0}\frac{\Delta_0}{1+(\omega_e\tau_e)^2}\right]+$$

$$-(\vec{j}\cdot\vec{\omega_e\tau_0})\,\vec{\omega_e\tau_0}\left[\delta_0+\left(\frac{\tau_e}{\tau_0}\right)^2\frac{\Delta_0}{1+(\omega_e\tau_e)^2}\right].$$

The ratio of the third expression to the first is of $O(\alpha)$, to the second of $O(\alpha/\overline{\omega\tau})$. It is neglected. The model equation is:

$$\vec{j}+\vec{j}\times\vec{\omega\tau}=\sigma\,(\vec{E}+\vec{u}\times\vec{B})$$

where $\vec{\omega}\equiv\vec{\omega_e}$,

$$\tau=\tau_0\left[1+\delta_0(\omega_e\tau_0)^2\right]^{-1},$$

and

$$\sigma=\sigma_0\left[1+\delta_0(\omega_e\tau_0)^2\right]^{-1}.$$

This model is qualitatively the same as the previous one, and thus a single model equation describes Ohm's law. The restrictions as to its validity are to be carefully noted and comparison made with final results. The parameter δ_0 accounts for ion slip, α_T -thermal diffusion, and Δ_0 - the second approximation. The general forms for τ and σ in the model equation for any $\overline{\omega\tau}$ are:

$$\tau=\tau_0\left[1+\frac{2}{5}\frac{\alpha_T^2}{1+(\omega_e\tau_e)^2}\right]\left[1+\delta_0(\omega_e\tau_0)^2-\frac{\Delta_0}{1+(\omega_e\tau_e)^2}\right]^{-1},$$

$$\sigma=\sigma_0\left[1+\delta_0(\omega_e\tau_0)^2-\frac{\Delta_0}{1+(\omega_e\tau_e)^2}\right]^{-1}.$$

Model Equation for Electron Energy

For the purpose of this discussion, $B\approx 1$ web./m.^{2}, $\omega_e\approx 10^{11}$/sec., and $u\gtrsim 10^2$ m./sec. The ratio of the first term in $\vec{F}_e$ to the last is $|\vec{g}|/u\omega_e\lesssim 10^{-12}$; the ratio of the second to the

last is $u/L\omega_e \lesssim 10^{-7}$ as $\left|\frac{d\vec{u}}{dt}\right| \approx \frac{u^2}{L}$. Thus, $\vec{F}_e \doteq -\frac{e}{m_e}(\vec{E}+\vec{u}\times\vec{B})$. The viscous part of $|\overline{\overline{P}}_e|$, $|\mathring{\overline{\overline{P}}}_e| \approx \tau_e |p_e \nabla\vec{u} - \vec{j}(\vec{E}+\vec{u}\times\vec{B})| \approx \tau_e (p_e|\nabla\vec{u}| - \sigma u^2 B^2) \approx \tau_e (p_e \frac{u}{L} - \rho\frac{u^3}{L})$ as $\frac{\sigma L B^2}{\rho u} \gtrsim 1$. But $\rho u^2 \approx M^2 p$; therefore, the mechanical term in $|\mathring{\overline{\overline{P}}}_e|$ is of $O(M^{-2}\frac{p_e}{p}) = O(\alpha)$ smaller than the electromagnetic part, giving $|\mathring{\overline{\overline{P}}}_e| \approx n_e m_e u^2 \omega\tau^2 \approx p_e \omega_e^2$. Since $n_e m_e u^2 \omega\tau^2/p_e \approx \frac{T}{T_e} M^2 \omega\tau^2 \frac{m_e}{m_a} \leq O(10^{-1})$,

$\overline{\overline{P}}_e \doteq p_e \overline{\overline{I}}$. The terms in $\vec{R}_e$ are now compared:

$$|\vec{R}_e| \approx \lambda_e |\nabla T_e| + |\alpha_T| \frac{k T_e}{e}|\vec{j}| + \frac{2}{5}\frac{e\lambda_e}{k} u B,$$

where $\frac{kT_e}{e}|\vec{j}| \approx u p_e \omega\tau \approx \frac{2}{5}\frac{e\lambda_e}{k} u B$. The ratio of the first term to the others $\approx \frac{T_e}{T}\alpha\omega\tau \leq O(10^{-1})$ for $|\nabla T_e| \approx T_e \frac{|\nabla p|}{p}$, $|\nabla p| \approx \sigma_0 u B^2$. This term is small unless large electron temperature gradients and Hall parameter exist. It is assumed

$$\vec{R}_e \doteq \frac{k T_e}{e}\overline{\overline{A}}\cdot\left[\alpha_T \vec{j} - \frac{\tau_e}{\tau_0}\sigma_0 (\vec{E}+\vec{u}\times\vec{B})\right].$$

It will be shown later that $\vec{R}_e$ is of small importance. Next, the expression for $\vec{V}_i$ is simplified. First, $\xi_{ea}\frac{\vec{R}_e}{p_e} \lesssim \frac{1}{en_e}\vec{j}$ and $\bar{\varepsilon}\omega_e\tau_{ea} \approx \delta_0\omega\tau \approx \omega_i\tau_{ia}$. Thus,

$$|\vec{V}_i| \approx \frac{\bar{\varepsilon}}{en_e}|\vec{j}| + \delta_0\omega\tau\frac{1}{en_e}|\vec{j}| + \tau_{ia}\frac{|\nabla p|}{\rho}.$$

The terms proportional to $\vec{j}$ and $\vec{R}_e$ are negligible compared to $\frac{1}{en_e}|\vec{j}|$; the terms involving pressure gradients are of $O(\alpha)$ compared to the other terms. Since interest is in $\vec{\omega}_e$ and not $\vec{V}_i$ directly, it is sufficient to say $\vec{V}_i \doteq \frac{2}{en_e}\vec{j}\times\vec{\omega}_i\vec{\tau}_{ia}$ and $\vec{\omega}_e \doteq -\frac{1}{en_e}(\vec{j} - \delta_0\vec{j}\times\vec{\omega}_e\vec{\tau}_0)$.

The simplified expressions for $\vec{F}_e$, $\overline{\overline{P}}_e$, $\vec{R}_e$, and $\vec{\omega}_e$ can now be substituted into the energy equation. Note that $\frac{kT_e}{eI_s} = O(10^{-1})$.

The expression $\overline{\overline{P}}_e : \nabla\vec{u} \doteq p_e \nabla\cdot\vec{u}$; $\frac{d}{dt} = \vec{u}\cdot\nabla$. The energy equation now is:

$$(\vec{j} - \delta_0 \vec{j}\times\vec{\omega_e\tau_0})\cdot(\vec{E}+\vec{u}\times\vec{B}) \doteq \nabla\cdot\vec{q_e} + Q_R +$$

$$+ n_e \sum_k \frac{m_e}{m_k} 3k \frac{T_e - T_k}{\tau_{ek}} + \vec{u}\cdot\nabla(n_e i_e) + (i_e + kT_e)\nabla\cdot(n_e\vec{u}).$$

The L. H. S. $\approx j^2/\sigma \approx \vec{u}\cdot\nabla p$. The last two terms on the R. H. S. $\approx \alpha\left(\frac{eI_s}{kT_e}\right) \approx O(\epsilon)$ compared to the L. H. S. and can be neglected. The heat flux term is of $O\left(\frac{kT_e}{eLuB}\right) \approx O(\epsilon)$ compared to the L. H. S. ; it may also be neglected. Perhaps in the electrode boundary layer the flux terms should be considered. Combining with the model Ohm's law and neglecting $(\vec{j}\cdot\vec{\omega_e\tau_0})^2$ compared to $j^2(\omega_e\tau_0)^2$ (the ratio = $O(\alpha^2)$):

$$j^2/\sigma\,[1+\delta_0(\omega_e\tau_0)^2]^{-1} \doteq Q_R + n_e \sum_k \frac{m_e}{m_k} \frac{3k(T_e - T_k)}{\tau_{ek}}.$$

The above model equation is accurate to near $O(\epsilon)$ except in regions of very large electron temperature gradients. Assuming that $T_k \approx T$ and $m_k \approx m_a$ and neglecting the radiation term, an approximate upper bound on the electron heating for large $\overline{\omega\tau}$ is obtained:

$$\left(\frac{T_e}{T} - 1\right) \approx (1-K)^2 M^2 \omega\tau^2 \approx (1-K)^2 M^2 \overline{\omega\tau}^2 [1+\delta_0\overline{\omega\tau}^2]^{-2}.$$

Since the parameter δ_0 does not vary significantly, the effect of ion slip is to limit the electron temperature elevation for large $\overline{\omega\tau}$. For M fixed, the maximum of the R. H. S. is for $\overline{\omega\tau}^2 = \delta_0^{-1} \approx 10^2$ or 10^3 ; hence, the restriction given on page 64. It is unlikely that such a large, or larger, value of the Hall parameter can be obtained in a

physical situation due to operating restrictions of high pressure and limited field strength.

Comments on the Combined Fluid Equations

As noted in the previous section, $\overline{\overline{P_e}} \doteq p_e \overline{\overline{I}}$. The ion stress will be of the same form; the ratio of these stresses to the atom stress is of $O(\alpha)$; hence, the pressure and viscous stress tensor for the fluid is essentially that for the atoms alone. The same applies to the density and temperature. The effects of the seed neutrals are of $O(\rho_o/\rho_p) \lesssim 10^{-2}$ and thus the fluid equations are nearly the equations for the parent gas alone with added electromagnetic terms -- the multicomponent gas equations degenerate into single fluid equations. The model equations for Ohm's law and the electron energy (i.e., T_e) serve as constitutive relations.

Next, examination is given to the problem of calculating T_i , T_o , T_p , α , and the seed ratio.

Calculation of Temperature and Number Densities

The elastic energy exchange of species j is approximately given by:

$$Q_{el_j} \doteq - n_j \sum_k \frac{m_j m_k}{(m_j + m_k)^2} \frac{3k(T_j - T_k)}{\tau_{jk}} .$$

Here, the effects of drift velocities have been ignored; this is a good approximation if $|\vec{w_k}| << \left(\frac{3kT_k}{m_k}\right)^{1/2}$.

This criterion for ions gives $1 >> \frac{1}{3} M^2 \delta_o^2 \overline{\omega\tau}^4$; for electrons,

$1 >> \frac{1}{3} M^2 \frac{T}{T_e} \frac{m_e}{m_a} \overline{\omega\tau}^2$; and for atoms, $1 >> \frac{1}{3} M^2 \delta_0^2 \alpha^2 \overline{\omega\tau}^4$

The last two are easily met, but for large $\overline{\omega\tau}$ the effect of ion slip should be included. This correction is not unduly important, however, and the above expression is used, but for ordering only. In any case, it is to be noted that the above equation is valid only for monatomic species and that the collision integral has been evaluated only approximately except for the case of species of equal mass interacting under a Maxwellian potential. Then the above expression is exact if T_j is replaced by $T_j + \frac{m_j w_j^2}{3k}$, and similarly for T_k [26].

The momentum exchange is given approximately by:

$$\vec{L}_{el_j} \doteq - n_j \sum_k \frac{\mu_{jk}}{\tau_{jk}} (\vec{w}_j - \vec{w}_k).$$

Consider the cases $j \neq e$. Besides the term Q_{el_j}, the other significant terms in the energy equations are $\approx p_j \nabla \cdot \vec{u} \approx$ $\approx n_j k T_j \nabla \cdot \vec{u}$ for the atoms, and a like term plus the term $\rho_i \vec{w}_i \cdot \frac{e}{m_i} (\vec{E} + \vec{u} \times \vec{B}) \approx \delta_0 \overline{\omega\tau}^2 j^2/\sigma \approx \delta_0 \overline{\omega\tau}^2 p \nabla \cdot \vec{u}$ for the ions. The latter mentioned term is important only if $\delta_0 \overline{\omega\tau}^2 p/p_i \approx \delta_0 \overline{\omega\tau}^2/\alpha \gtrsim O(1)$. The ratio of Q_{el_j} to these terms must be less than or equal to $O(1)$; this criterion gives limits on possible temperature differences. The comparison is made assuming $T_j \approx 10^3$ °K to 10^4 °K, $\nabla \cdot \vec{u} \approx$ 10^3/sec., cross-sections δ_{jk} are equivalent to those given on page 64, and the number densities are in the following ranges: $n_e \approx 10^{12}$/cc to 10^{15}/cc, $n_o \approx 10^{14}$/cc to 10^{16}/cc, $n_p \approx 10^{18}$/cc. The results

are $T_o = T_p \equiv T$ to $O(10^{-4})$, $T_i \doteq T$ if $n_e >> 10^{13}$/cc or $\alpha >> 10^{-5} \delta_o \overline{\omega\tau}^2$, and $T_e \doteq T_i$ if $n_e \alpha >> 10^{11} \delta_o \overline{\omega\tau}^2$/cc. It can be said that $T_i \doteq T$ if $\overline{\omega\tau}$ is not too large, but as $\overline{\omega\tau} \to \delta_o^{-1/2}$ this can be only so for a restricted range of the ionization ratio of $O(10^{-4})$ ($\overline{\omega\tau}$ and T_e cannot be large for larger values of n_i). If necessary, the ion energy equation can be included in the model; here, it is assumed $T_i = T$.

A comparison is now made to estimate the relative values of $\vec{\omega}_o$ and $\vec{\omega}_p$. For neutrals, the momentum equations of the species[24] give the criterion $|\vec{L}_{elj}| \lesssim |\nabla p_j|$; this must hold for every k. Consider $j = o$, $k = p$, then $|\vec{\omega}_o - \vec{\omega}_p| \lesssim 10^{-8} |\nabla \frac{kT}{m_a}| \approx$ 1 cm./sec. The maximum flow time $\approx 1 m./10^2 \frac{m.}{sec.} \approx 10^{-2}$ sec., giving a maximum diffusion distance of seed neutrals in the parent gas of about 10^{-2} cm. This can be neglected; the only possible cause of a change of the seed ratio on a streamline is consequently due to $\vec{V}_i$. For $\overline{\omega\tau} \leq O(1)$, this can also be ignored. For large $\overline{\omega\tau}$, the transverse diffusion velocity $\approx \bar{\varepsilon}\, \overline{\omega\tau}\, u^*$. But since large $\overline{\omega\tau}$ can occur only at low to moderate electron and ion number densities, i.e., at a relatively low degree of ionization, again diffusion effects are small and the seed ratio can be regarded as a constant on a streamline.

Since only the two temperatures T and T_e are required, then n_e and the excited state populations given as functions of the seed ratio, p, T, and T_e closes the system of equations. If the electron quantum states are in equilibrium with each other at the electron temperature, then n_e is given by the Saha equation and the

population of levels by the Boltzmann distribution.

The free electrons will have a Maxwellian velocity distribution for $\alpha \gtrsim 10^{-6}$; it is assumed this holds[18]. Since the collisional excitation and de-excitation cross-sections for the upper energy levels of an atom are large, they are usually in equilibrium with the free electrons. For an optically thin gas, singly ionized, a level with principal quantum number N is in L. T. E. (local thermodynamic equilibrium) with higher levels if $n_e \gtrsim 7\times10^{18} N^{-17/2} \left(\frac{kT_e}{I_H}\right)^{1/2}/cc$

where $I_H = 13.6$ ev. (see reference 29, Ch. 6, p. 148). This gives $N_{min} \approx 17 - \log n_e$ with n_e in per cc. The lower levels may have an equilibrium population without L. T. E. if the corresponding absorption lines are optically thick; resonance lines are thick at the core if

$$n_o H_o \gtrsim 4\times10^{9} (kT/m_o I_H)^{1/2}/(f_o \lambda_o)$$

where f_o is the absorption oscillator strength, λ_o is the wavelength in cm, H_o is in cm, and n_o is in per cc. (See reference 29, Ch. 6, p. 152.) This means $n_o \gtrsim 10^{12}$/cc for H_o = 10 cm; this criterion is easily satisfied. For a thin plasma, the thermal energy level* limit reaches the ground state if

$$n_e \gtrsim 6\times10^{17} (I_S/I_H)^3 (kT_e/I_H)^{1/2}/cc$$

($\approx 10^{14}$/cc for alkali seed[30]). Since the resonance lines (principal series, $^2P_{3/2,1/2} - {}^2S_{1/2}$) are optically thick and transitions (first of the sharp and diffuse series) involving the first excited state ($^2P_{3/2,1/2}$) have large absorption oscillator strengths, the above

* A thermal level is one in which the radiative depopulation rate is much smaller than the collisional depopulation rate.

mentioned limits on n_e are too stringent and can be relaxed by one or two orders of magnitude. Here, it is assumed that the electron states are in equilibrium with each other. A further discussion on this point is given by Kerrebrock[18].

The continuum radiation is thin as seen from the following criteria given by Wilson[30]:

1) Photo-ionization absorption is negligible if $H_o n_o \lesssim 10^{16} I_s g N^{(1)}/O_e$ where H_o is in cm., n_o in per cc, I_s in ev, g is the Gaunt factor ≈ 0.8, $N^{(1)}$ * is the quantum number of the ground state, and O_e is the number of optical electrons.

2) Free-free transition absorption is negligible if $H_o n_e^2 \lesssim 4 \times 10^{37} (kT_e)^{7/2}$ where kT_e is in ev, H_o in cm, and n_e in per cc.

3) Electron scattering effects (based on the Thomson coefficient) are negligible if $H_o n_e \lesssim 1.5 \times 10^{24}$ where H_o is in cm and n_e in per cc.

All three conditions are satisfied. Essentially the same conclusions on the optical depths of the various transitions are given in reference 31.

The electron number density is given by Saha's equation:

$$n_e^2 = \frac{2 b_i}{b_o} n_o (2\pi m_e kT_e/h^2)^{3/2} \exp\left(-(I_s - \Delta I)/kT_e\right),$$

where the b_j are partition functions, h is Planck's constant, and

---

* Superscript numbers refer to term energy levels: (1) for the ground state, (2) for the first excited state, etc. See, for example, Herzberg, reference 35, p. 72, for KI.

ΔI is the lowering of the ionization potential due to the presence of neighboring particles. Let the seed ratio be $\gamma_s \equiv \frac{n_o + n_i}{n_p} = \frac{n_o + n_e}{n_p}$ where $n_p = \frac{p}{(1+\gamma_s) kT}$. Then $\bar{\alpha} = \frac{n_e}{n_p} \left(\frac{m_o}{m_p + \gamma_s m_o} \right)$. Let the degree of ionization $n_e/(\gamma_s n_p) = d$; then

$$d^2/(1-d) = \frac{2 b_i}{b_o} \frac{(1+\gamma_s) kT}{\gamma_s p} (2\pi m_e kT_e/h^2)^{3/2} \exp\left(-(I_s - \Delta I)/kT_e\right).$$

The lowering of the ionization potential is given by[29]

$$\Delta I = e^2/(4\pi \epsilon_o \lambda_D).$$

Since the excitation energy of the first excited state of the ion, $E_i^{(2)} = O(10\ ev)$, the ion partition function approximately equals the degeneracy of the ion ground state ^1S_o : $b_i \doteq g_i^{(1)} = (2L_i^{(1)}+1)(2S_i^{(1)}+1) = 1$, where $L_i^{(1)}$ and $S_i^{(1)}$ are the total angular momentum and spin quantum numbers. In calculating the atomic partition function, it is assumed that the levels for $n \geq n'$ are nearly continuous and the excitation energies $E_o^{(n)}$ are known for all configurations with angular momentum quantum numbers $0 \leq l_o^{(n)} \leq n'-2$, $n < n'$. Then[29]

$$b_o \equiv \sum_{n=1}^{n_{max}} g_o^{(n)} \exp\left(-E_o^{(n)}/kT_e\right) \doteq$$

$$\sum_{n=1}^{n'-1} g_o^{(n)} \exp\left(-E_o^{(n)}/kT_e\right) + \frac{2}{3} g_i^{(1)} \left(\frac{I_H}{\Delta I}\right)^{3/2} \exp\left(-(I_s - \Delta I)/kT_e\right).$$

The atomic alkali ground state is $^2S_{1/2}$, giving $g_o^{(1)} = 2 \approx b_o$.

APPENDIX B*

Absorption Coefficients

1. Resonance Lines. The profile of an alkali resonance absorption line is the result of six mechanisms: Stark broadening, natural broadening, Doppler broadening, resonance broadening, Van der Waals broadening, and Zeeman splitting. Of the diverse broadening mechanisms, all but the Doppler effect give a dispersion profile; their net effect is had by simply adding the half-widths of each.** The resultant overall Lorentz profile is enfolded with the Gaussian Doppler profile by a convolution integral of the two profiles; this procedure must be done for each Zeeman component in each direction (aligned and perpendicular to the induction). It is to be noted that although the oscillator strengths of the various components are anisotropic, the net oscillator strength is isotropic, i.e., the total absorption is the same for every direction. This applies separately to the $^2P_{3/2} - {}^2S_{1/2}$ and $^2P_{1/2} - {}^2S_{1/2}$ transitions. The amount of Zeeman splitting is of the order of the electron cyclotron frequency: $\omega_e \approx 10^{11}$/sec. for $B \approx$ 1 web./m.^{2}. Since the line frequency $\approx 10^{15}$/sec., this gives Zeeman splitting of $O(1A^\circ)$. Broadening gives a half-width of $O(10^{-2}A^\circ)$ to $O(10^{-1}A^\circ)$. The Zeeman components can be considered as independent lines. Since interest here is in an integrated net absorption coefficient and since the radiative transport is given only approximately, the effect of Zeeman splitting is ignored.

* All quantities are dimensional.

** This is equivalent to adding collision frequencies based on optical cross-sections.

The expressions for the various half half-widths are taken from Griem, reference 29, Ch. 4.

Stark broadening results from the fluctuating electric microfields produced by ions and electrons. Broadening calculations are usually made by the use of one of two limit cases: the static limit or the impact limit. Consider a characteristic collision time for the perturber: an impact distance divided by the average perturber velocity. If this time is much larger than the radiative lifetime*, the perturber may be regarded as stationary; this is the static limit. If the converse is true, then the perturber interrupts the wave train; this is the impact limit. The impact limit gives the Lorentz profile. Under the conditions in a MFD generator plasma, the impact approximation holds for the electrons, while neither limit holds for the ions. However, calculations show that the ionic Stark broadening is at least an order of magnitude below that of the electron impact broadening, which in turn is relatively small except for the larger electron number densities. At these densities, T_e tends to T and radiative effects become less important. The ion effects can be ignored. Let dimensionless, reduced electron temperature and number density be defined by the following:

$$\bar{T}_e \equiv T_e/(10^3\,^\circ K), \quad \bar{n}_e \equiv n_e/(10^{16}/cc) .$$

If w_λ denotes the half half-width in A^o, then Table 4-5 of reference 29 listing the Stark profile factors is approximated within

---

* If another perturber is acting in the impact limit, this time should be considered as the reciprocal of the impact half-width in frequency units, i.e., the time between 'optical impact collisions.'

about 2 per cent ($2.5 \leq \bar{T}_e \leq 10$) by the following expressions:

for LiI, $w_\lambda \doteq 6.08 \times 10^{-3} \bar{n}_e \bar{T}_e^{0.30}$,

for NaI, $w_\lambda \doteq 6.93 \times 10^{-3} \bar{n}_e \bar{T}_e^{0.30}$,

for KI, $w_\lambda \doteq 2.18 \times 10^{-2} \bar{n}_e \bar{T}_e^{0.30}$,

and for CsI, $w_\lambda \doteq 5.00 \times 10^{-2} \bar{n}_e \bar{T}_e^{0.345}$.

If induced transitions are ignored, the full half-width for natural broadening in angular frequency units is given by the Einstein spontaneous emission coefficient. In this approximation, the half half-widths in A^o units for LiI, $w_\lambda \doteq 4.5 \times 10^{-5}$; for NaI, $w_\lambda \doteq 5.5 \times 10^{-5}$; for KI, $w_\lambda \doteq 5.9 \times 10^{-5}$; and for CsI, $w_\lambda \doteq 7.2 \times 10^{-5}$. It can be seen that natural broadening can be neglected.

If λ_o denotes the wavelength in A^o of the resonance line, then w_λ in A^o for the Doppler effect is $\left(\frac{2kT \ln 2}{m_o c^2} \right) \lambda_o$.

Let f denote the absorption oscillator strength of the resonance line and ω_o the angular frequency of the line: $\omega_o \lambda_o = 2\pi c$. The half half-width in angular frequency units, w , for resonance broadening is given by:

$$w = 3\pi \left(g_o^{(1)} / g_o^{(2)} \right)^{1/2} n_o \left(\frac{e^2 f}{4\pi \varepsilon_o m_e \omega_o} \right)$$

in the impact approximation. It is valid if

$$n_o << \frac{1}{2\pi}\left(\frac{2}{3}\right)^{3/2}\left(g_o^{(2)}/g_o^{(1)}\right)^{3/4}\left(\frac{4\pi\varepsilon_o m_e \omega_o v_o}{e^2 f}\right)^{3/2}$$

where $v_o = 4\left(\frac{kT}{\pi m_o}\right)^{1/2}$. This is easily satisfied.

The mean square radius of the first excited level of the emitter in units of Bohr radii,

$$\overline{\left(R_o^{(2)}\right)^2} \doteq \frac{1}{2}\frac{I_H}{I_s - E_o^{(2)}}\left[5\frac{I_H}{I_s - E_o^{(2)}} + 1 - 3\ell_o^{(2)}\left(\ell_o^{(2)}+1\right)\right].$$

The Van der Waals impact half half-width in angular frequency units is given by:

$$w = \pi n_p v_{op}^{3/5}\left(\frac{9\pi\hbar^5\,\overline{\left(R_o^{(2)}\right)^2}}{16 m_e^3\left(E_p^{(2)}\right)^2}\right)^{2/5}$$

where $v_{op} = \left(\frac{8kT}{\pi\mu_{op}}\right)^{1/2}$. A line shift equal to $-\frac{2}{3}w$ is also had; this need not be considered. If an impact parameter b_{min} is defined by

$$b_{min} = \left(\frac{9\pi\hbar^5\,\overline{\left(R_o^{(2)}\right)^2}}{16 m_e^3 v_{op}\left(E_p^{(2)}\right)^2}\right)^{1/5},$$

the impact approximation requires $n_p << \left(\pi b_{min}^3\right)^{-1}$. This is easily satisfied. It is also required that the emitter-perturber collision be elastic; this is so if $\hbar v_{op}/b_{min} << E_p^{(2)}$. This is also easily satisfied. Typically, $b_{min} \approx O(10A^o)$. This means the impact parameter is hardly any greater than the sum of the atomic radii of the interacting atoms. In the theoretical discussion leading to the above formula, the interaction potential was approximated by

the first term of a multipole expansion of the same. The small impact parameter indicates higher order terms should probably be considered (see Griem). The above expression is deemed adequate for the purpose of this study.

2. Continuum radiation. In order to determine the continuum absorption coefficient, the oscillator strengths as a function of frequency for free-bound and free-free transitions must be calculated; this in turn requires knowledge of the atomic radial wave functions. For atoms with LS coupling, the quantum defect method of Seaton and Burgess[32, 33] seems to give good results. However, it has been shown by Lutz[21] that the total continuum radiation is a fraction of the line radiation. Use of hydrogenic wave functions with effective quantum numbers is adopted here; the error in the use of this simplification should be small. For lighter elements it will tend to overestimate the radiation loss; on the other hand, neglect of line radiation from the higher excited levels will tend to compensate for this error. For heavier elements it may tend to have the opposite effect, but still this method gives results good to within a factor of two[33].

As before, it is assumed that for $n \gtrsim n'$, the atomic energy levels are nearly continuous. The effective quantum number for a level n is defined as $N_o^{(n)} \equiv \left(hR/(I_s - E_o^{(n)})\right)^{1/2}$,

where R is the Rydberg constant, $R = 3.29 \times 10^{15}/sec$. Let $N_o' \equiv N_o^{(n')}$, $\nu' \equiv \frac{(I_s - E_o^{(n')})}{h} = R(N_o')^2$. The absorption coefficient, $\alpha_\nu(\nu)$, is given by[34]:

(ν is circular frequency)

$$\text{for } \nu > \nu', \quad \alpha_\nu(\nu) = (4\pi B_\nu)^{-1} \left(\frac{2b_i}{b_0}\right) \theta^3 \frac{16}{3\sqrt{3}} n_0 k T_e \cdot$$

$$\cdot e^{-h\nu/kT_e} \exp\left(-(I_\infty - \Delta I)/kT_e\right) \left\{ \frac{2hR}{kT_e} \sum_{n^*}^{n'-1} \frac{g_{fb}}{(N_0^{(n)})^3} \exp\left(\frac{hR}{kT_e (N_0^{(n)})^2}\right) + \right.$$

$$\left. + \bar{g}'_{fb} \left[\exp\left(\frac{hR}{kT_e (N_0')^2}\right) - 1\right] + \bar{g}_{ff} \right\},$$

where $\theta =$ fine structure constant, $\frac{1}{137}$; n^* is the number of the highest level to which transition can occur, i.e., $N_0^{(n^*)} \geq (R/\nu)^{1/2}$, and g_{fb} , $\bar{g}'_{fb}$, $\bar{g}_{ff}$ are various Gaunt factors.

The Gaunt factors are[36]:

$$g_{fb} \doteq 1 - 0.1728 (N_0^{(n)})^{-2/3} - 0.0496 (N_0^{(n)})^{-4/3} \quad \text{if } N_0^{(n)} = O(1),$$

$$g_{fb} \doteq 1 - 0.1728 \left(\frac{\nu}{R}\right)^{1/3} \left[\frac{2R}{\nu (N_0^{(n)})^2} - 1\right] \quad \text{if } N_0^{(n)} \gg 1,$$

$$\bar{g}'_{fb} \doteq 1 + 0.1728 \left(\frac{\nu}{R}\right)^{1/3} \left\{1 + \frac{2kT_e}{h\nu}\left[1 - \frac{h\nu'}{kT_e}\left(1 - e^{-h\nu'/kT_e}\right)^{-1}\right]\right\},$$

and

$$\bar{g}_{ff} \doteq 1 + 0.1728 \left(\frac{\nu}{R}\right)^{1/3} \left(1 + \frac{2kT_e}{h\nu}\right).$$

If $\nu \leq \nu'$ $(n^* \geq n')$, then the sum term in α_ν disappears and the second term in the brackets becomes $\bar{g}_{fb} \left(e^{h\nu/kT_e} - 1\right)$ where $\bar{g}_{fb} \equiv \bar{g}'_{fb}\big|_{\nu'=\nu}$. As $\frac{h\nu}{kT_e} \longrightarrow 0$, $\bar{g}_{fb} \longrightarrow 1 + 0.0864 \left(\frac{\nu}{R}\right)^{1/3}$. The average Gaunt factor for free-free transitions, $\bar{g}_{ff}$, gives the effect of Bremsstrahlung.

APPENDIX C*

Numerical Procedure

1. Approximations in the formulation of the continuum radiation loss. The continuum absorption coefficient times the Planck function is integrated over all frequencies; the seed is taken to be KI with $n' = 4$, $\nu' = 2.06 \times 10^{15}$ /sec . The result is:

$$\int_0^\infty \alpha_{\nu c} B_\nu \, d\nu \doteq \frac{1}{4\pi} \left(\frac{2b_i}{b_0}\right) \theta^3 \frac{16}{3\sqrt{3}} n_0 k T_e \exp\left(-(I_s - \Delta I)/kT_e\right) \cdot$$

$$\cdot \nu' \left\{ 9.11 + 1.41 \left(\frac{kT_e}{h\nu'}\right) + 0.0686 \left(\frac{kT_e}{h\nu'}\right)^{4/3} \left[G\left(\frac{h\nu'}{kT_e}; \frac{1}{3}\right) + \right.\right.$$

$$\left.\left. + 2\left(1 - \frac{h\nu'}{kT_e}\right) G\left(\frac{h\nu'}{kT_e}; -\frac{2}{3}\right) \right] \right\}$$

where

$$G(n; m) \equiv e^n \int_n^\infty x^m e^{-x} \, dx .$$

Necessary accuracy (to within 7 per cent) is achieved by replacing the expression in the braces by the factor 10; the continuum radiation loss as used in the numerical calculations is:

$$Q_{Rc} = 10 \left(\frac{2b_i}{b_0}\right) \theta^3 \frac{16}{3\sqrt{3}} n_0 k T_e \nu' \exp\left(-(I_s - \Delta I)/kT_e\right).$$

2. Approximations in the formulation of the mean absorption coefficients. The dispersion profile is of the form:

$$\alpha_\nu = \frac{e^2}{4\pi \varepsilon_0 m_e c} n_0 f \left(1 - e^{-h\nu_0/kT_e}\right) \frac{w_\nu}{(\nu - \nu_0)^2 + w_\nu^2} \equiv \overline{\alpha_\nu} \frac{\nu_0 w_\nu}{(\nu - \nu_0)^2 + w_\nu^2}$$

---

* All quantities are dimensional.

where $\nu_0 \equiv \frac{\omega_0}{2\pi}$, $w_\nu \equiv \frac{w}{2\pi}$. The cut-off frequencies are given by: $\nu_c - \nu_0 = \pm (\bar{\alpha}_\nu H_c \nu_0 w_\nu - w_\nu^2)^{1/2} \doteq \pm (\bar{\alpha}_\nu H_c \nu_0 w_\nu)^{1/2}$. A non-dimensional parameter is now defined: $\xi \equiv h\nu / kT_e$ with $\xi_0 = \frac{h\nu_0}{kT_e}$, $\xi_w = h w_\nu / kT_e$, and $\xi_c = \frac{h}{kT_e} (\bar{\alpha}_\nu H_c \nu_0 w_\nu)^{1/2}$. Then

$$\alpha_{pl} = \frac{15}{\pi^4} \bar{\alpha}_\nu \xi_0 \xi_w \left(\int_0^{\xi_0 - \xi_c} \frac{(e^\xi - 1)^{-1} \xi^3 \, d\xi}{(\xi - \xi_0)^2 + \xi_w^2} + \right.$$

$$\left. + \int_{\xi_0 + \xi_c}^{\infty} \frac{(e^\xi - 1)^{-1} \xi^3 \, d\xi}{(\xi - \xi_0)^2 + \xi_w^2} \right),$$

and

$$\alpha_R^{-1} = \frac{15}{4\pi^4} (\bar{\alpha}_\nu \xi_0 \xi_w)^{-1} \int_{\xi_0 - \xi_c}^{\xi_0 + \xi_c} [(\xi - \xi_0)^2 + \xi_w^2] \xi^4 e^\xi (e^\xi - 1)^{-2} \, d\xi.$$

Note that $\xi_0 >> \xi_c >> \xi_w$. Hand calculations employing certain asymptotic representations for parts of the integrals in the expression for α_{pl} were made for the ranges of parameters $3 \le \xi_0 \le 7$, $10^{-2} \le \xi_c \le 1$, $\xi_w << \xi_c$. For these ranges, the results can be expressed approximately by:

$$\alpha_{pl} \doteq \frac{15}{\pi^4} \bar{\alpha}_\nu \xi_0 \xi_w \left\{ \xi_c^{-1} [2.59 + .01(\xi_0 - 3) + .062(\xi_0 - 9)(\xi_0 - 3)^2] \cdot \right.$$

$$\left. \cdot [1.0 + .22(\xi_0 - 6)(\xi_c - 0.1)] \right\}.$$

If $\xi_c < 10^{-2}$, the above formula with $\xi_c = .01$ expresses part of the sum of integrals; for the part corresponding to integrations from $\xi_0 - .01$ to $\xi_0 - \xi_c$ and $\xi_0 + \xi_c$ to $\xi_0 + .01$, the following is added to the expression in the braces:

$$\frac{2\xi_0^3}{e^{\xi_0} - 1} \frac{1}{\xi_w} \left[\tan^{-1}\left(\frac{.01}{\xi_w}\right) - \tan^{-1}\left(\frac{\xi_c}{\xi_w}\right) \right],$$

(the integrations being performed with the numerator of the integrand evaluated at $\xi = \xi_o$).

The integral in the expression for α_R^{-1} was evaluated using the approximation $e^{\xi_o} e^{-\xi}(e^{\xi}-1) = e^{\xi_o} - e^{-(\xi-\xi_o)} \doteq e^{\xi_o}-1$ (the error is roughly $O(\xi_c\,\%)$). The result was expanded in powers of ξ_c ; it was found that the first two terms of the expansion gave sufficient numerical accuracy for $\xi_c \leq 1$. Thus,

$$\alpha_R^{-1} \doteq \frac{15}{4\pi^4}(\bar{\alpha}_v \xi_o \xi_w)^{-1} e^{\xi_o}(e^{\xi_o}-1)^{-2}\left[\frac{2}{3}\xi_o^4 \xi_c^3 + \frac{1}{5}\xi_o^2(\xi_o-2)(\xi_o-6)\xi_c^5\right].$$

3. Use of a finite number of streamlines. For computational purposes, the flow field is approximated by a finite number of streamlines. Let this number be N , with $\xi_i \equiv \frac{i-1}{N-1}$ for $i = 1, N$. The variation of an arbitrary fluid property, F , with the transverse variable is assumed to be given by a finite Fourier series in the following manner:

$$F(\xi) \doteq F_1 + (F_N - F_1)\xi + \sum_{n=1}^{N-2} a_n(x) \sin n\pi\xi,$$

where $F_i(x) \equiv F(\xi_i)$.

If $C_m \equiv F_{m+1} - F_1 - \frac{m}{N-1}(F_N - F_1)$ for $m = 1, N-2$;

$$C_m = \sum_{n=1}^{N-2} a_n \sin\left(\frac{n m \pi}{N-1}\right) \equiv \sum_{n=1}^{N-2} a_n B_{mn}.$$

Inverting:

$$a_n = \sum_{n=1}^{N-2} B_{nm}^{-1} C_m.$$

The average value of F at a given axial position,

$$\bar{F} \equiv \int_0^1 F\, d\xi \doteq \tfrac{1}{2}(F_1 + F_N) + \sum_m b_m C_m ,$$

where $$b_m \equiv \sum_{n\ odd} \frac{2}{n\pi} B_{nm}^{-1} ,$$

and $$\int_0^\xi F(\bar{\xi})\, d\bar{\xi} \doteq F_1 \xi + \tfrac{1}{2}(F_N - F_1)\xi^2 + \sum_m C_m f_m(\xi) ,$$

where $$f_m \equiv \sum_n \frac{B_{nm}^{-1}(1 - \cos n\pi\xi)}{n\pi} .$$

The method of averaging can be written in the following way:

let $$L_1 \equiv \sum_{m=1}^{N-2} b_m , \quad L_2 \equiv \frac{1}{N-1} \sum_{m=1}^{N-2} m\, b_m ;$$

$$M_1 \equiv \tfrac{1}{2} - L_1 + L_2 , \quad M_N \equiv \tfrac{1}{2} - L_2 , \quad M_i \equiv b_{i-1} \quad (i = 2, N-1);$$

then $$\bar{F} \doteq \sum_{n=1}^{N} M_n F_n .$$

Since averaging corresponds to an integration, the error in assuming a finite Fourier series tends to be reduced. The weighting factors, M_i, give roughly equal weight to the interior streamlines and half as large a weight to the two 'end' streamlines ($\xi_i = 0, 1$). The method can be checked numerically by picking different values of

N for a given problem and noting differences in the outcomes.

For a calorically perfect gas, $T(h) = \frac{\gamma-1}{\gamma} h$, this procedure gives for the pressure:

$$p(x) = \frac{1}{A} \int_0^1 \frac{T\, d\mathcal{S}}{R\, u_x} \doteq \frac{\gamma-1}{\gamma A} \sum_n \frac{M_n h_n}{R_n u_{x_n}} .$$

(Zeroth order terms are had by placing a subscript "o" on each variable.) The pressure gradient is thus:

$$\frac{dp}{dx} \doteq \sum_n E_n \frac{dh_n}{dx} - \sum_n H_n \frac{du_{x_n}}{dx} + Q ,$$

where

$$E_n \equiv \frac{\gamma-1}{\gamma A} \frac{M_n}{R_n u_{x_n}} ,$$

$$H_n \equiv \frac{\gamma-1}{\gamma A} \frac{M_n h_n}{R_n (u_{x_n})^2} ,$$

and

$$Q \equiv \frac{\gamma-1}{\gamma A^2} \frac{dA}{dx} \sum_n \frac{M_n h_n}{R_n u_{x_n}} .$$

Applying this relation to the zeroth order core equations:

$$\frac{\gamma p_o}{\gamma-1} \frac{u_{x_{on}}}{h_{on}} \frac{du_{x_{on}}}{dx} + \sum_j E_{oj} \frac{dh_{oj}}{dx} - \sum_j H_{oj} \frac{du_{x_{oj}}}{dx} = J B_{z_o} + Q_o ,$$

$$\frac{\gamma p_o}{\gamma-1} \frac{u_{x_{on}}}{h_{on}} \frac{dh_{on}}{dx} - u_{x_{on}} \sum_j E_{oj} \frac{dh_{oj}}{dx} + u_{x_{on}} \sum_j H_{oj} \frac{du_{x_{oj}}}{dx} = D_{on} - Q_o u_{x_{on}} ,$$

where

$$D_{on} \equiv (j_o^2/\sigma_o)_n .$$

Defining the vectors $\vec{V}$ and $\vec{W}$:

$$\vec{V} \equiv \left[u_{x_{o1}}, u_{x_{o2}}, \cdots, u_{x_{oN}}; h_{o1}, \cdots, h_{oN} \right] ,$$

$$\vec{W} \equiv \left[J B_{z_0} + Q_0, \cdots, J B_{z_0} + Q_0 ; D_{01} - Q_0 u_{x_{01}}, \cdots, D_{0N} - Q_0 u_{x_{0N}} \right],$$

and the matrix $[R]$:

$$R_{jk} \equiv \frac{\gamma p_0}{\gamma - 1} \frac{u_{x_{0k}}}{h_{0k}} \delta_{jk} - H_{0k} \quad \text{for } j = 1, N \text{ and } k = 1, N;$$

$$\equiv E_{0_{k-N}} \quad \text{for } j = 1, N \text{ and } k = N+1, 2N;$$

$$\equiv u_{x_{0_{j-N}}} H_{0k} \quad \text{for } j = N+1, 2N \text{ and } k = 1, N;$$

$$\equiv \frac{\gamma p_0}{\gamma - 1} \frac{u_{x_{0k-N}}}{h_{0k-N}} \delta_{jk} - u_{x_{0_{j-N}}} E_{0_{k-N}} \quad \text{for } j = N+1, 2N \text{ and } k = N+1, 2N.$$

The fluid equations are given by the matrix equation $[R] \cdot \frac{d\vec{V}}{dx} = \vec{W}$,

or $$\frac{d\vec{V}}{dx} = [R]^{-1} \cdot \vec{W}.$$

This equation is first order and quasi-linear, yielding an initial value problem. The averaging procedure is applied to calculate p_0 , J , and E_{x_0} .

4. Inclusion of the electron energy equation. For nonequilibrium flows, the electron energy equation must be included in the above scheme. In the limit $\alpha \longrightarrow 0$, the axial derivatives in the radiative diffusion term drop, leaving only the transverse derivatives. After a transformation $y \longrightarrow \zeta_0$, the equation can be written in finite difference form with mesh points corresponding to the chosen set of streamlines. At each derivative evaluation taken from the given matrix equation during computation, the electron energy equation must be solved by iteration for the vector electron temperature

distribution, the functions J and E_{x_0} being redefined at each iterative step.

It can be shown that the ratio of the radiative diffusion term to the other term arising from the line radiation (corresponding to the optically thin limit) $\approx \left(\frac{2H_c}{H_0}\right)^2$. At the end streamlines, $\frac{2H_c}{H_0} = O(\epsilon)$; hence the diffusion term can be neglected and the resulting algebraic equations solved for T_e. These values serve as boundary values for the interior finite difference equation.

At the points $\xi_0 = 0,1$, the value of H_c must be defined differently than that given on page 47; let $H_c = 6\times10^{-3}\tau_{b1}$ m where the boundary layer thickness is $\tau_{b1} \times 10^{-3}$ m. The quantity τ_{b1} is known only within an order of magnitude; numerical calculations show that the results are quite insensitive to its precise value.

Similarly, at the singular points where the induction changes from a null value to a value of $O(1)$, the gas may make a transition from an equilibrium situation to a non-equilibrium situation and H_c must be redefined. The inverse distance $\frac{1}{6}\left(\frac{2}{H_0\tau_B}\right)$ is added to the definition of H_c^{-1}; the thickness of the transition is taken as $\frac{1}{2}H_0\tau_B$. Again, results are insensitive to the precise value of τ_B. For $\frac{\partial}{\partial\xi_0} = 0$, the value $\xi_0 = -\frac{1}{2}$ is used in H_c; as noted on page 47, H_c is a weak function of the stream variables away from the walls and the use of this value is a fairly good approximation for most of the fluid core.

5. Numerical method. Numerical computations were carried out on an IBM 7094 digital computer at the C. I. T. Booth Computer

Center. Library subroutines available at the Center were used for matrix inversion and for integration of the matrix equation. Matrix inversions were done in double precision. The differential equation integration subroutine uses the method of Runge-Kutta-Gill for its starting procedures, Adams-Moulton predictor-corrector formulae otherwise. The subroutine features an automatic control of truncation error; the starting procedure is used whenever the error control changes the step size. Round-off errors are controlled by use of double precision in parts of the subroutine.

TABLE 1. Effects of Values of H_c , τ_{bl} , and τ_B on Fluid Properties.

Deviations based on a distribution 'norm' calculated using H = 0.2 m , τ_{bl} = 1.0, τ_B = 1.0. For all cases: B_z = 0.7 , K = 0.6 , p = 3.0 , γ_s = 0.01, β = 1.5 , $u_x = 1 + \sin^2(2\pi s)$, $h = 5.5 + 2.0 \sin \pi s$.*

Case No.	H (m.)	τ_{bl}	τ_B	$\Delta_{max} T_e$ (%)	$\Delta_{max} n_e$ (%)	$\Delta_{max} \sigma$ (%)	$\Delta_{max} \omega\tau$ (%)
1	0.2	5.0	1.0	0.39	4.55	2.23	-1.95
2	0.2	1.0	4.0	0.07	0.15	0.23	2.14
3	0.8	1.0	1.0	0.19	1.94	1.02	1.38
4	0.2	1.0	0.5	-0.03	-0.12	-0.20	2.18
5	0.1	1.0	1.0	-0.19	-1.58	-0.88	2.78
6	0.2	0.3	1.0	-0.70	-6.37	-3.18	2.96

* See next page for units.

GRAPHS 1 TO 3*

Transverse variations of fluid properties for successive axial positions. Comparison of equilibrium and nonequilibrium calculations.

The calculations were performed for the following conditions: $H_o = 0.2$ m, $T_{el} = 2.0$, $T_B = 1.0$, $B_z = 0.7$ web/m^2, $K = 0.6$, $\beta = 1.5$, wall slope = 0.2, $p_{in} = 3.0$, $\gamma_s = 0.01$, $u_{x_{in}} = 1 + \sin^2(2\pi 5)$, $h_{in} = 5.5 + 2.0 \sin(\pi 5)$.**

Dotted lines indicate the equilibrium calculation, solid lines the nonequilibrium calculation.

Note the following values:**

	X = 0.1e	X = 0.1n	X = 0.5e	X = 0.5n	X = 1.0e	X = 1.0n
J =	-0.791	-1.339	-0.784	-1.201	-0.736	-1.088
E_x =	-0.612	-0.358	-0.508	-0.358	-0.476	-0.373
p =	2.995	2.959	2.959	2.752	2.814	2.447
$\overline{M^2}$ =	0.501	0.505	0.419	0.448	0.368	0.416
I.P. =	0.054	0.093	0.300	0.487	0.655	1.024

(e → equilibrium, n → nonequilibrium, I.P. is the local interaction parameter per unit length integrated to the point in question.)

---

* Subscript 'o' is omitted. Subscript 'in' refers to entrance conditions.

** The pressure, velocity, enthalpy, current, and electric field are in nondimensional form. Reference values are $p^* = 1$ atm, $u^* = 10^3$ m/sec, $h^* = 10^6$ m^2/sec^2, $j^* = 10^5$ amp/m^2, and $E^* = 10^3$ v/m.

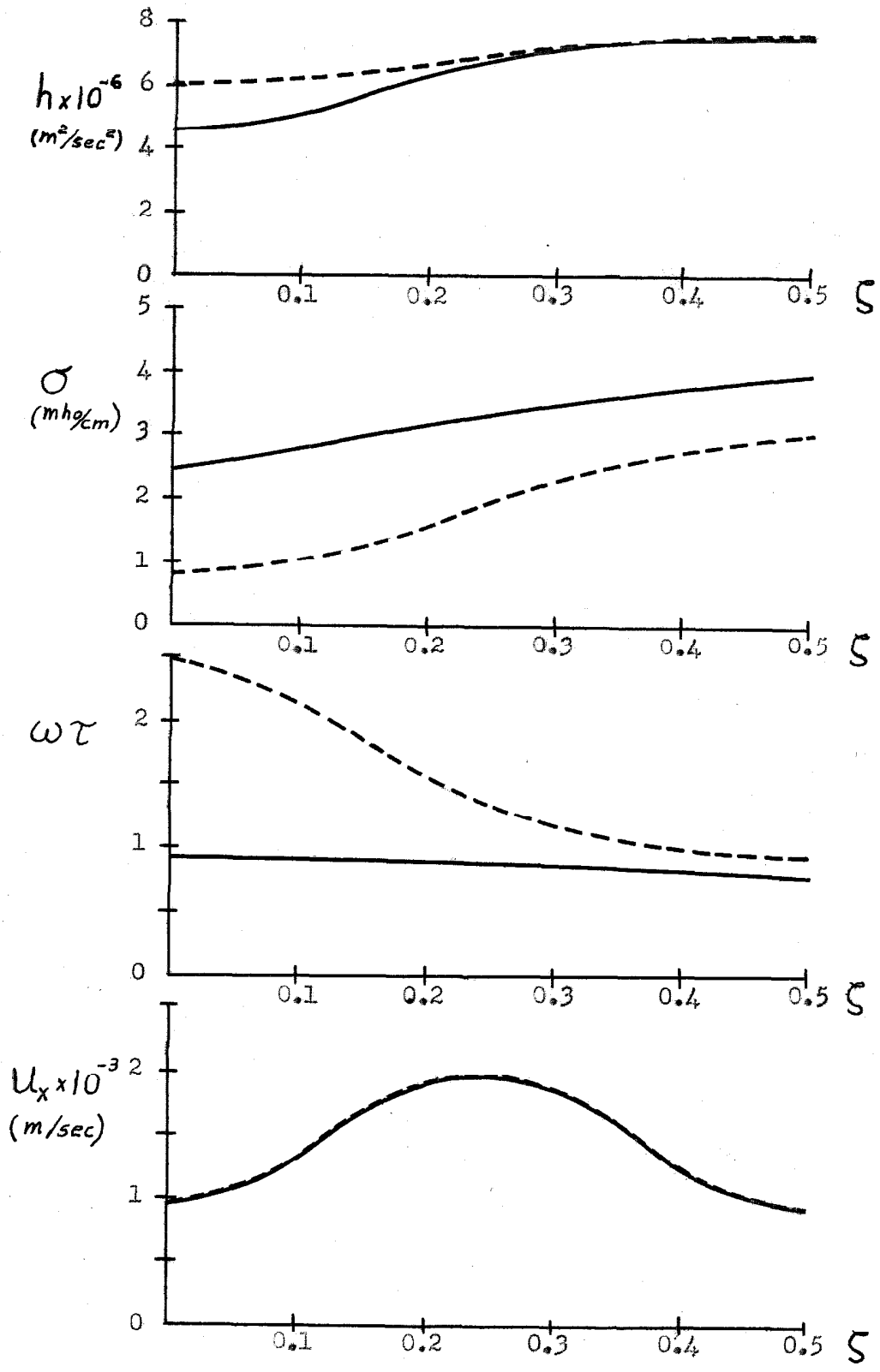

Graph 1. Axial Position: $x = 0.1$ m.

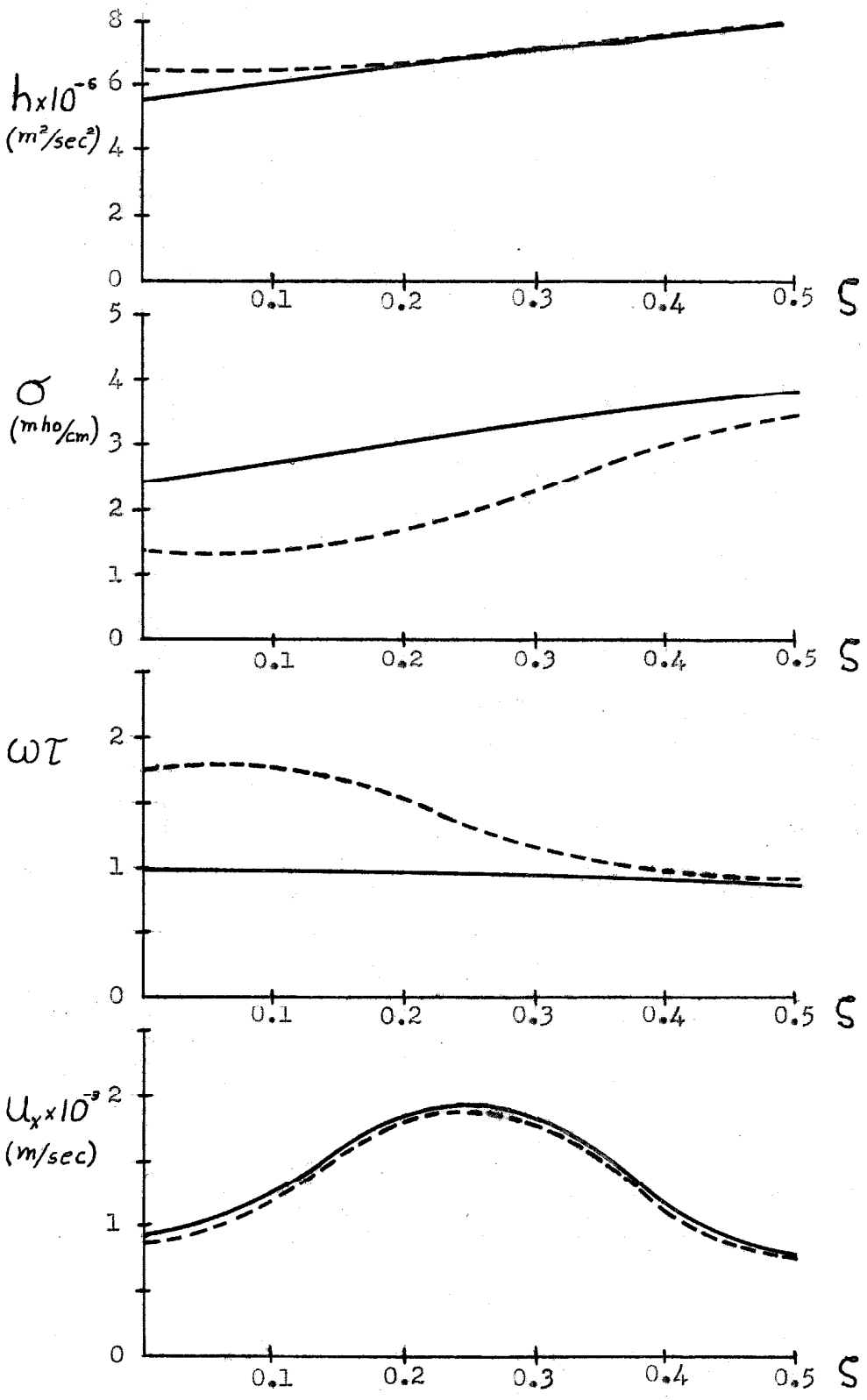

Graph 2. Axial Position: $x = 0.5$ m.

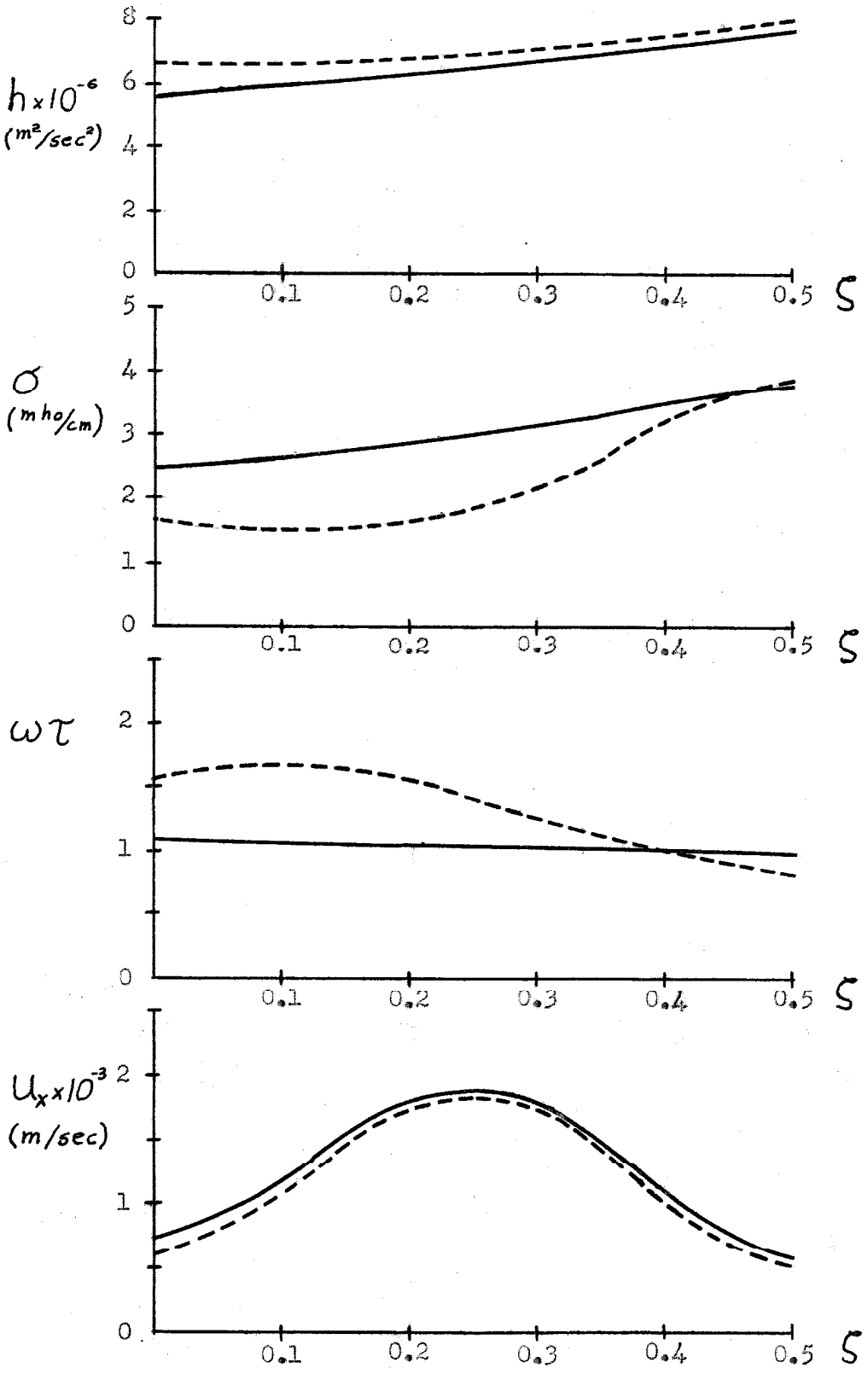

Graph 3. Axial Position: $x = 1.0$ m.

TABLES 2 TO 12

Transverse variations in fluid properties for an arbitrary axial position with specified pressure, velocity, enthalpy, seed ratio, induction, and load parameter in a nonequilibrium situation.

Calculations were performed for $H = 0.2$ m, $\beta = 1.5$, and $T_{b1} = 2.0$. Units are the same as those used for the graphs; see the preceding pages. $T^* = 10^3\ ^oK$. $\Delta\psi$ is the transverse voltage drop across the channel in kv. Truncation error was held to 10^{-4}.

TABLE 2

$K = 0.6$, $p = 5.0$, $\gamma_s = 0.006$, $u_x = 1.5 + 0.5 \sin \pi\xi$, $h = 5.5 + 1.5 \sin \pi\xi$

Property	$\xi = 0, 1$	$\xi = 1/9, 8/9$	$\xi = 2/9, 7/9$	$\xi = 1/3, 2/3$	$\xi = 4/9, 5/9$
(1)	$B_z = 0.8$, $J = -1.5284$, $E_x = -0.4460$, $\Delta\psi = 0.1709$, $\lvert j_x/J \rvert \leq 0.18$				
$\omega\tau$	0.8062	0.7864	0.7706	0.7548	0.7447
σ	2.1467	2.3750	2.5884	2.7773	2.8926
T_e	2.9567	3.0133	3.0632	3.1056	3.1308
j_x	0.2746	0.1426	0.0232	-0.0851	-0.1520
E_y	0.3849	0.6461	0.8597	1.0192	1.1047
(2)	$B_z = 1.0$, $J = -2.2029$, $E_x = -0.6199$, $\Delta\psi = 0.2142$, $\lvert j_x/J \rvert \leq 0.17$				
$\omega\tau$	0.8743	0.8648	0.8560	0.8453	0.8379
σ	2.5331	2.7702	2.9921	3.1845	3.3002
T_e	3.0586	3.1114	3.1586	3.1981	3.2214
j_x	0.3556	0.1879	0.0310	-0.1118	-0.2000
E_y	0.5075	0.8171	1.0763	1.2709	1.3757
(3)	$B_z = 1.2$, $J = -2.9758$, $E_x = -0.8112$, $\Delta\psi = 0.2576$, $\lvert j_x/J \rvert \leq 0.16$				
$\omega\tau$	0.9412	0.9366	0.9326	0.9256	0.9199
σ	2.8891	3.1440	2.3752	3.5715	3.6886
T_e	3.1442	3.1969	3.2426	3.2804	3.3026
j_x	0.4574	0.2369	0.0373	-0.1427	-0.2545
E_y	0.6210	0.9881	1.2937	1.5234	1.6476
(4)	$B_z = 1.6$, $J = -4.7824$, $E_x = -1.2388$, $\Delta\psi = 0.3463$, $\lvert j_x/J \rvert \leq 0.15$				
$\omega\tau$	0.9399	1.0701	1.0759	1.0889	1.0609
σ	4.1990	3.8077	4.0334	4.1511	4.4057
T_e	3.4130	3.3364	3.3772	3.3977	3.4435
j_x	-0.7070	0.4007	0.1486	0.0649	-0.3844
E_y	1.4193	1.3050	1.6889	1.9237	2.1949

TABLE 3

$K = 0.6,\ p = 5.0,\ \gamma_s = 0.009,\ u_x = 1.5 + 0.5 \sin \pi\varsigma,\ h = 5.5 + 1.5 \sin \pi\varsigma$

Property	$\varsigma = 0, 1$	$\varsigma = 1/9, 8/9$	$\varsigma = 2/9, 7/9$	$\varsigma = 1/3, 2/3$	$\varsigma = 4/9, 5/9$
(1)	$B_z = 0.7,\ J = -1.2705,\ E_x = -0.3504,\ \Delta\psi = 0.1490,\ \lvert j_x/J \rvert \leq 0.20$				
$\omega\tau$	0.7427	0.7136	0.6923	0.6725	0.6603
σ	1.9802	2.2244	2.4512	2.6566	2.7841
T_e	2.8527	2.9144	2.9677	3.0136	3.0411
j_x	0.2498	0.1273	0.0208	-0.0763	-0.1366
E_y	0.3147	0.5577	0.7508	0.8942	0.9707
(2)	$B_z = 1.0,\ J = -2.2563,\ E_x = -0.5976,\ \Delta\psi = 0.2140,\ \lvert j_x/J \rvert \leq 0.17$				
$\omega\tau$	0.8471	0.8357	0.8256	0.8136	0.8054
σ	2.5704	2.8237	3.0610	3.2693	3.3957
T_e	3.0053	3.0590	3.1068	3.1473	3.1712
j_x	0.3754	0.1983	0.0336	-0.1178	-0.2120
E_y	0.4986	0.8133	1.0752	1.2722	1.3782
(3)	$B_z = 1.3,\ J = -3.4632,\ E_x = -0.8833,\ \Delta\psi = 0.2787,\ \lvert j_x/J \rvert \leq 0.17$				
$\omega\tau$	0.9505	0.9422	0.9391	0.9270	0.9244
σ	3.0778	3.3707	3.6166	3.8567	3.9658
T_e	3.1195	3.1756	3.2205	3.2633	3.2822
j_x	0.5732	0.2858	0.0577	-0.1962	-0.3016
E_y	0.6478	1.0650	1.3952	1.6621	1.7872
(4)	$B_z = 1.6,\ J = -4.8635,\ E_x = -1.2002,\ \Delta\psi = 0.3459,\ \lvert j_x/J \rvert \leq 0.08$				
$\omega\tau$	0.9497	1.0374	1.0414	1.0453	1.0263
σ	4.0320	3.8700	4.1079	4.2764	4.4909
T_e	3.3056	3.2737	3.3143	3.3425	3.3785
j_x	-0.2205	0.4008	0.1348	-0.0486	-0.3984
E_y	1.2457	1.3095	1.6961	1.9674	2.1959

TABLE 4

$K = 0.6,\ p = 3.0,\ \gamma_s = 0.006,\ u_x = 1.5 + 0.5 \sin \pi\xi,\ h = 5.5 + 1.5 \sin \pi\xi$

Property	$\xi = 0, 1$	$\xi = 1/9, 8/9$	$\xi = 2/9, 7/9$	$\xi = 1/3, 2/3$	$\xi = 4/9, 5/9$
(1)	$B_z = 0.7,\ J = -1.6123,\ E_x = -0.4414,\ \Delta\psi = 0.1499,\ \lvert j_x/J \rvert \le 0.16$				
$\omega\tau$	0.8854	0.8782	0.8711	0.8612	0.8539
σ	2.6483	2.8971	3.1279	3.3282	3.4488
T_e	3.0408	3.0936	3.1404	3.1800	3.2033
j_x	0.2587	0.1372	0.0239	-0.0806	-0.1455
E_y	0.3547	0.5716	0.7529	0.8895	0.9621
(2)	$B_z = 1.0,\ J = -2.8694,\ E_x = -0.7494,\ \Delta\psi = 0.2149,\ \lvert j_x/J \rvert \le 0.15$				
$\omega\tau$	1.0339	1.0336	1.0336	1.0292	1.2048
σ	3.3852	3.6668	3.9119	4.1166	4.2374
T_e	3.2062	3.2593	3.3040	3.3406	3.3620
j_x	0.4296	0.2178	0.0342	-0.1319	-0.2350
E_y	0.5211	0.8271	1.0788	1.2690	1.3721
(3)	$B_z = 1.3,\ J = -4.3871,\ E_x = -1.0978,\ \Delta\psi = 0.2800,\ \lvert j_x/J \rvert \le 0.12$				
$\omega\tau$	1.1472	1.1614	1.1623	1.1642	1.1600
σ	4.0967	4.3481	4.6187	4.8074	4.9364
T_e	3.3501	3.3942	3.4411	3.4734	3.4953
j_x	0.5354	0.3221	0.0290	-0.1699	-0.3299
E_y	0.7292	1.0773	1.4107	1.6415	1.7789
(4)	$B_z = 1.6,\ J = -6.1381,\ E_x = -1.4757,\ \Delta\psi = 0.3448,\ \lvert j_x/J \rvert \le 0.12$				
$\omega\tau$	1.2523	1.2676	1.2681	1.2702	1.2708
σ	4.7001	4.9691	5.2615	5.4605	5.5671
T_e	3.4653	3.5114	3.5610	3.5944	3.6123
j_x	0.7513	0.4477	0.0193	-0.2609	-0.4145
E_y	0.8939	1.3241	1.7430	2.0294	2.1799

TABLE 5

$K = 0.8,\ p = 4.0,\ \gamma_s = 0.009,\ u_x = 1.5 + 0.5 \sin \pi s,\ h = 5.5 + 1.5 \sin \pi s$

Property	$s = 0, 1$	$s = 1/9, 8/9$	$s = 2/9, 7/9$	$s = 1/3, 2/3$	$s = 4/9, 5/9$
(1)	$B_z = 0.7,\ J = -0.4898,\ E_x = -0.2634,\ \Delta\psi = 0.1981,\ \lvert j_x/J \rvert \le 0.47$				
$\omega\tau$	1.2185	1.1162	1.0453	0.9820	0.9445
σ	1.4050	1.6468	1.8696	2.0882	2.2318
T_e	2.6545	2.7305	2.7943	2.8529	2.8895
j_x	0.2268	0.1129	0.0195	-0.0691	-0.1253
E_y	0.5047	0.7957	1.0021	1.1510	1.2282
(2)	$B_z = 1.0,\ J = -0.8414,\ E_x = -0.4533,\ \Delta\psi = 0.2846,\ \lvert j_x/J \rvert \le 0.39$				
$\omega\tau$	1.3656	1.3085	1.2602	1.2099	1.1771
σ	1.8183	2.0438	2.2601	2.4702	2.6083
T_e	2.7880	2.8478	2.9018	2.9520	2.9837
j_x	0.3247	0.1745	0.0358	-0.1017	-0.1919
E_y	0.7934	1.1476	1.4292	1.6422	1.7564
(3)	$B_z = 1.3,\ J = -1.2625,\ E_x = -0.6722,\ \Delta\psi = 0.3711,\ \lvert j_x/J \rvert \le 0.35$				
$\omega\tau$	1.5066	1.4714	1.4360	1.3943	1.3651
σ	2.1818	2.4043	2.6196	2.8254	2.9603
T_e	2.8899	2.9429	2..921	3.0375	3.0665
j_x	0.4355	0.2415	0.0521	-0.1389	-0.2664
E_y	1.0706	1.4994	1.8573	2.1346	2.2865
(4)	$B_z = 1.6,\ J = -1.7459,\ E_x = -0.9135,\ \Delta\psi = 0.4575,\ \lvert j_x/J \rvert \le 0.32$				
$\omega\tau$	1.6339	1.6115	1.5842	1.5483	1.5218
σ	2.5135	2.7358	2.9513	3.1542	3.2866
T_e	2.9774	3.0242	3.0706	3.1131	3.1402
j_x	0.5564	0.3142	0.0698	-0.1782	-0.3454
E_y	1.3437	1.8504	2.2852	2.6268	2.8166

TABLE 6

$K = 0.6,\ p = 3.0,\ \gamma_s = 0.009,\ u_x = 1.5 + 0.5 \sin \pi s,\ h = 5.5 + 1.5 \sin \pi s$

Property	$s = 0, 1$	$s = 1/9, 8/9$	$s = 2/9, 7/9$	$s = 1/3, 2/3$	$s = 4/9, 5/9$
(1)	$B_z = 1.0,\ J = -2.9147,\ E_x = -0.7267,\ \Delta\psi = 0.2146,\ \lvert j_x/J \rvert \le 0.16$				
$\omega\tau$	1.0074	1.0051	1.0029	0.9963	0.9906
σ	3.4165	3.7108	3.9700	4.1892	4.3198
T_e	3.1440	3.1967	3.2416	3.2788	3.3006
j_x	0.4535	0.2331	0.0383	-0.1402	-0.2518
E_y	0.5131	0.8224	1.0775	1.2706	1.3754
(2)	$B_z = 1.3,\ J = -4.4040,\ E_x = -1.0722,\ \Delta\psi = 0.2797,\ \lvert j_x/J \rvert \le 0.12$				
$\omega\tau$	1.1186	1.1316	1.1581	1.1286	1.1257
σ	4.1271	4.3824	4.5093	4.8726	4.9942
T_e	3.2806	3.3231	3.3437	3.4029	3.4224
j_x	0.5010	0.2849	0.2653	-0.2541	-0.3974
E_y	0.7471	1.0938	1.3230	1.6679	1.7979
(3)	$B_z = 1.6,\ J = -6.2606,\ E_x = -1.4230,\ \Delta\psi = 0.3440,\ \lvert j_x/J \rvert \le 0.16$				
$\omega\tau$	1.2248	1.2318	1.2068	1.2210	1.2285
σ	4.7085	5.0179	5.4667	5.5888	5.6491
T_e	3.3862	3.4363	3.5068	3.5264	3.5362
j_x	0.9676	0.5714	-0.2358	-0.3087	-0.3471
E_y	0.8187	1.2857	1.8184	2.0401	2.1551

TABLE 7

$K = 0.75,\ p = 4.0,\ \gamma_s = 0.009,\ u_x = 1.5 + 0.5 \sin \pi\zeta,\ h = 5.5 + 1.5 \sin \pi\zeta$

Property	$\zeta = 0, 1$	$\zeta = 1/9, 8/9$	$\zeta = 2/9, 7/9$	$\zeta = 1/3, 2/3$	$\zeta = 4/9, 5/9$
(1)	$B_z = 2.0,\ J = -3.5334,\ E_x = -1.4184,\ \Delta\psi = 0.5374,\ \lvert j_x/J \rvert \leq 0.25$				
$\omega\tau$	1.5893	1.5823	1.5652	1.5511	1.5342
σ	3.3470	3.6005	3.8547	4.0498	4.1885
T_e	3.1635	3.2128	3.2609	3.2970	3.3221
j_x	0.8684	0.4842	0.0630	-0.2633	-0.5197
E_y	1.5319	2.1479	2.7006	3.0944	3.3316
(2)	$B_z = 2.5,\ J = -5.0143,\ E_x = -1.9508,\ \Delta\psi = 0.6624,\ \lvert j_x/J \rvert \leq 0.37$				
$\omega\tau$	1.8040	1.7829	1.7118	1.6577	1.6892
σ	3.6820	3.9751	4.4014	4.7552	4.7193
T_e	3.2366	3.2929	3.3714	3.4335	3.4281
j_x	1.8631	1.1853	-0.0030	-0.9642	-0.7363
E_y	1.4775	2.3845	3.4154	4.1142	4.1820
(3)	$B_z = 3.0,\ J = -6.6628,\ E_x = -2.5127,\ \Delta\psi = 0.7914,\ \lvert j_x/J \rvert \leq 0.62$				
$\omega\tau$	2.0615	1.8564	1.8126	1.8149	1.8185
σ	3.8120	4.5940	4.9648	5.1166	5.1854
T_e	3.2686	3.4146	3.4804	3.5079	3.5205
j_x	4.1569	0.8254	-0.3935	-0.7645	-0.9128
E_y	0.5041	3.2292	4.2676	4.7681	5.0124

TABLE 8

$K = 0.75,\ p = 2.5,\ \gamma_s = 0.009,\ u_x = 1.5 + 0.5 \sin \pi\xi,\ h = 5.5 + 1.5 \sin \pi\xi$

Property	$\xi = 0, 1$	$\xi = 1/9, 8/9$	$\xi = 2/9, 7/9$	$\xi = 1/3, 2/3$	$\xi = 4/9, 5/9$
(1)	$B_z = 2.0,\ J = -4.2387,\ E_x = -1.6424,\ \Delta\psi = 0.5364,\ \lvert j_x/J \rvert \le 0.36$				
$\omega\tau$	1.8938	1.8107	1.8086	1.8025	1.7788
σ	3.9586	4.4315	4.6409	4.8062	4.9688
T_e	3.2607	3.3489	3.3881	3.4186	3.4471
j_x	1.5257	0.3969	0.0405	-0.2533	-0.6209
E_y	1.1993	2.2233	2.7123	3.0791	3.3540
(2)	$B_z = 2.5,\ J = -6.1004,\ E_x = -2.1769,\ \Delta\psi = 0.6768,\ \lvert j_x/J \rvert \le 0.32$				
$\omega\tau$	1.7146	1.9610	1.8968	1.9393	1.9205
σ	5.6936	4.9873	5.4276	5.4101	5.5584
T_e	3.5693	3.4636	3.5408	3.5423	3.5683
j_x	-1.9346	1.1059	-0.2444	0.0535	-0.3842
E_y	3.2612	2.5195	3.5149	3.6858	4.0162
(3)	$B_z = 3.0,\ J = -7.8033,\ E_x = -2.8246,\ \Delta\psi = 0.8104,\ \lvert j_x/J \rvert \le 0.13$				
$\omega\tau$	2.0562	2.0873	2.0799	2.0685	2.0548
σ	5.3237	5.4583	5.6811	5.8634	5.9904
T_e	3.5315	3.5616	3.6047	3.6393	3.6622
j_x	1.0082	0.8708	0.1837	-0.4201	-0.8861
E_y	2.6448	3.2504	4.0234	4.6164	4.9785

TABLE 9

$K = 0.6,\ p = 4.0,\ \gamma_s = 0.009,\ u_x = 1.5 + 0.5 \sin \pi\xi,\ h = 5.5 + 1.5 \sin \pi\xi$

Property	$\xi = 0, 1$	$\xi = 1/9, 8/9$	$\xi = 2/9, 7/9$	$\xi = 1/3, 2/3$	$\xi = 4/9, 5/9$
(1)	$B_z = 2.0,\ J = -7.8189,\ E_x = -1.7895,\ \Delta\psi = 0.4284,\ \lvert j_x/J \rvert \le 0.26$				
$\omega\tau$	1.2779	1.2184	1.2270	1.2293	1.2316
σ	4.4508	5.1222	5.3773	5.5827	5.6818
T_e	3.3682	3.4775	3.5177	3.5498	3.5652
j_x	2.0268	0.3604	-0.0288	-0.3782	-0.5376
E_y	0.6614	1.7298	2.1953	2.5488	2.7252
(2)	$B_z = 2.5,\ J = -11.134,\ E_x = -2.4596,\ \Delta\psi = 0.5400,\ \lvert j_x/J \rvert \le 0.10$				
$\omega\tau$	1.3281	1.3453	1.3570	1.3614	1.3546
σ	5.5532	5.8365	6.0832	6.2813	6.4464
T_e	3.5542	3.5991	3.6381	3.6691	3.6941
j_x	1.1279	0.6228	0.1462	-0.2916	-0.7742
E_y	1.4753	2.1264	2.6906	3.1232	3.4166
(3)	$B_z = 3.0,\ J = -15.709,\ E_x = -3.0594,\ \Delta\psi = 0.6394,\ \lvert j_x/J \rvert \le 0.19$				
$\omega\tau$	1.4128	1.4210	1.4042	1.3479	1.4339
σ	6.3312	6.6896	7.1596	7.8764	7.3023
T_e	3.6801	3.7358	3.8056	3.9054	3.8316
j_x	2.8236	1.8571	0.1548	-2.9236	0.1873
E_y	1.3887	2.2702	3.2397	4.3049	3.7897

TABLE 10

$K = 0.6,\ p = 4.0,\ \gamma_s = 0.009,\ B_z = 2.5$

Property	$\xi = 0, 1$	$\xi = 1/9, 8/9$	$\xi = 2/9, 7/9$	$\xi = 1/3, 2/3$	$\xi = 4/9, 5/9$
(1)	$u_x = u_1,\ J = -11.134,\ E_x = -2.4596,\ \Delta\psi = 0.5400,\ \lvert j_x/J \rvert \leq 0.10$				
$\omega\tau$	1.3282	1.3453	1.3570	1.3614	1.3546
σ	5.5528	5.8365	6.0832	6.2812	6.4464
T_e	3.5541	3.5991	3.6381	3.6691	3.6941
j_x	1.1297	0.6227	0.1461	-0.2918	-0.7743
E_y	1.4747	2.1264	2.6907	3.1233	3.4166
(2)	$u_x = u_2,\ J = -6.1737,\ E_x = -2.0308,\ \Delta\psi = 0.3719,\ \lvert j_x/J \rvert \leq 0.29$				
$\omega\tau$	1.6479	1.6065	1.5730	1.5881	1.5961
σ	4.1257	4.5496	4.9298	5.0420	5.0978
T_e	3.3202	3.3958	3.4611	3.4809	3.4908
j_x	1.7952	0.6783	-0.3003	-0.4352	-0.4990
E_y	0.4115	1.3278	2.0309	2.2954	2.4319

$u_1 \equiv 1.5 + 0.5 \sin \pi\xi$

$u_2 \equiv 1.05 + 0.35 \sin \pi\xi$

$h \equiv 5.5 + 1.5 \sin \pi\xi$

TABLE 11

$K = 0.75,\ p = 4.0,\ \gamma_s = 0.009,\ u_x = 1.05 + 0.35 \sin \pi\xi,\ h = 5.5 + 1.5 \sin \pi\xi$

Property	$\xi = 0, 1$	$\xi = 1/9, 8/9$	$\xi = 2/9, 7/9$	$\xi = 1/3, 2/3$	$\xi = 4/9, 5/9$
(1)	$B_z = 2.0,\ J = -1.9998,\ E_x = -1.1821,\ \Delta\psi = 0.3717,\ \lvert j_x/J \rvert \leq 0.35$				
$\omega\tau$	1.9246	1.9049	1.8758	1.8335	1.8003
σ	2.6728	2.8848	3.0919	3.2907	3.4248
T_e	3.0148	3.0614	3.1059	3.1478	3.1754
j_x	0.6893	0.3994	0.0964	-0.2231	-0.4481
E_y	0.8555	1.3824	1.8447	2.2228	2.4410

TABLE 12

$K = 0.75,\ p = 2.5,\ \gamma_s = 0.009,\ u_x = 1.05 + 0.35 \sin \pi\xi,\ h = 5.5 + 1.5 \sin \pi\xi$

Property	$\xi = 0, 1$	$\xi = 1/9, 8/9$	$\xi = 2/9, 7/9$	$\xi = 1/3, 2/3$	$\xi = 4/9, 5/9$
(1)	$B_z = 3.0,\ J = -4.4616,\ E_x = -2.3248,\ \Delta\psi = 0.5492,\ \lvert j_x/J \rvert \leq 0.42$				
$\omega\tau$	2.2625	2.5965	2.4806	2.3060	2.4187
σ	4.7117	4.1840	4.5485	5.0793	4.8431
T_e	3.4281	3.3362	3.4108	3.5104	3.4713
j_x	-0.8598	1.8573	0.4928	-1.5202	-0.4682
E_y	2.6160	1.2902	2.5753	3.8711	3.4967